



This is to certify that the

dissertation entitled

NONLINEAR RANDOM VIBRATION OF
COMPOSITE LAMINATED PLATES

presented by

Mohamad Khaled Naja

has been accepted towards fulfillment
of the requirements for

Doctor of Philosophy degree in Civil Engineering

Ronald Harichandran

Major professor

Date 11/18/93

**LIBRARY
Michigan State
University**

**PLACE IN RETURN BOX to remove this checkout from your record.
TO AVOID FINES return on or before date due.**

DATE DUE	DATE DUE	DATE DUE
_____	_____	_____
_____	_____	_____
_____	_____	_____
_____	_____	_____
_____	_____	_____
_____	_____	_____
_____	_____	_____

**NONLINEAR RANDOM VIBRATION OF COMPOSITE
LAMINATED PLATES**

By

Mohamad Khaled Naja

A DISSERTATION

**Submitted to
Michigan State University**

**in partial fulfillment of the requirements
for the degree of**

DOCTOR OF PHILOSOPHY

Department of Civil and Environmental Engineering

1993

ABSTRACT

NONLINEAR RANDOM VIBRATION OF COMPOSITE LAMINATED PLATES

By

Mohamad Khaled Naja

Structural components in space vehicles, aircraft, automobiles, submarines, etc., that are made of filamentary composite laminae are usually subjected to stochastic loads. Composite laminae have strongly anisotropic properties and display significantly nonlinear elastic behavior when loaded in shear or along directions different from those of the filaments. While such components have been used for over a decade, their design has predominantly been performed using deterministic methods. In this study, the method of equivalent linearization is used in conjunction with the finite element method to perform nonlinear random vibration analysis of laminated composite plates. An approximate, but sufficiently accurate, series representation of the nonlinear shear stress-strain law is used to facilitate the formulation. Classical laminate theory that accounts for the coupling between extensional and bending responses is used, but higher-order shear deformation effects are not considered in the course of this study. Four-noded elements with five degrees-of-freedom per node are used to discretize the plate. The displacement, strain and stress responses are computed at different excitation load levels. The results indicate that the effect of nonlinearity on the responses for any given load level depends on the ply-arrangement, and as expected becomes more significant for higher loads.

ACKNOWLEDGMENTS

The author wishes to express his deep indebtedness to Dr. Ronald S. Harichandran for his guidance, encouragement, support, and valuable input, without which this work would not have been possible.

Grateful acknowledgments are due to Professors R. Wen of the Department of Civil and Environmental Engineering, N. J. Altiero of the Department of Materials Science and Mechanics and G. Ludden of the Mathematics Department, for serving on the author's doctoral committee. Gratitude is also due to the Mathematics Department for their continuous financial supports during the period of this study.

Thanks are also due to the director of the Minority Business Program Dr. E. Betts and his assistant Ms. L. Gross for their support and encouragement.

In addition, the author would like to express his sincere appreciation and thanks to his parents in Lebanon, especially his mother Myassar for her prayers and encouragement, and the sacrifices that she has suffered, during the long course of this study.

This work was funded by the State of Michigan Research Excellence Fund administered by the Composite Materials and Structures Center at Michigan State University.

Finally, the author would like to thank his students at Michigan State University and at Davenport College for their patience and understanding.

TABLES OF CONTENTS

1. Introduction	1
1.1 General.....	1
1.2 Objectives	2
1.3 Literature Review	2
1.3.1 Physical Nonlinearity.....	2
1.3.2 Shear Deformations	9
1.3.3 Stochastic Dynamic Analysis	10
2. Finite Element Formulation	19
2.1 General.....	19
2.2 Constitutive Equations.....	20
2.3 Finite Element Formulation using Classical Plate Theory	25
2.3.1 In-plane formulation	25
2.3.2 Out-of-plane formulation.....	28
2.3.3 Formulation of the linear elemental stiffness matrix	31
2.3.4 Formulation of the elemental consistent mass matrix	34
2.3.5 Numerical integration	35
3. Equivalent Linearization	36
3.1 Introduction.....	36
3.2 Formulation.....	37
3.3 Derivation of the Nonlinear Elemental Stiffness Matrices	40
3.4 Random Vibration Analysis.....	48
3.5 Computation of Strains and Stresses	49
3.6 Laminate Strength Analysis.....	51
4. Optimizing Computational Effort	53
4.1 Introduction.....	53
4.2 FORTRAN Implementation	53
4.3 Optimization Techniques.....	56
4.3.1 Optimizing α and β	57
4.3.2 Covariance optimization	59
4.3.3 The indexing scheme	61
4.3.4 Elimination of zero-valued computations.....	66
4.3.5 Unrolling of DO-loops.....	69
5. Numerical Results	72
5.1 General.....	72
5.2 In-Plane Loading.....	72
5.2.1 Extensional loading.....	72

5.2.2 Shear loading	86
5.3 Out-Of-Plane Loading	95
6. Conclusions and Recommendations	109
6.1 Conclusions.....	109
6.2 Recommendations for future work	110

LIST OF TABLES

TABLE 4.1.	Number of terms in each group	64
TABLE 4.2.	Comparison of total times.	71
TABLE 5.1.	First five natural frequencies from linear (first iteration) and nonlinear (last iteration) analysis for load level $S_0 = 12000 \text{ lb}^2 \text{ sec}$	74
TABLE 5.2.	Number of iterations required for convergence	74
TABLE 5.3.	First five natural frequencies from linear (first iteration) and nonlinear (last iteration) analysis for load level $S_0 = 12000 \text{ lb}^2 \cdot \text{sec}$	78
TABLE 5.4.	Number of iterations required for convergence.....	79
TABLE 5.5.	First five natural frequencies from linear (first iteration) and nonlinear (last iteration) analysis for load level $S_0 = 12000 \text{ lb}^2 \text{ sec}$	83
TABLE 5.6.	Number of iterations required for convergence	83
TABLE 5.7.	First five natural frequencies from linear (first iteration) and nonlinear (last iteration) analysis for load level $S_0 = 4000 \text{ lb}^2 \text{ sec}$	87
TABLE 5.8.	Number of iterations required for convergence.....	87
TABLE 5.9.	First five natural frequencies from linear (first iteration) and nonlinear (last iteration) analysis for load level $S_0 = 30000 \text{ lb}^2 \text{ sec}$	91
TABLE 5.10.	Number of iterations required for convergence	92
TABLE 5.11.	First five natural frequencies from linear (first iteration) and nonlinear (last iteration) analysis for load level $S_0 = 80 \text{ lb}^2 \text{ sec}$	96
TABLE 5.12.	Number of iterations required for convergence.....	96
TABLE 5.13.	First five natural frequencies from linear (first iteration) and nonlinear (last iteration) analysis for load level $S_0 = 80 \text{ lb}^2 \text{ sec}$	100
TABLE 5.14.	Number of iterations required for convergence	100
TABLE 5.15.	First five natural frequencies from linear (first iteration) and nonlinear (last iteration) analysis for load level $S_0 = 80 \text{ lb}^2 \text{ sec}$	104
TABLE 5.16.	Number of iterations required for convergence.....	104
TABLE 5.17.	The significance of nonlinearity on the responses of various loading conditions	108

LIST OF FIGURES

Figure 1.1.	Typical stress-strain curve behavior of fiber-reinforced composite material	3
Figure 2.2.	Fit of approximate stress-strain law for shear.....	23
Figure 2.5.	Layer nomenclature for laminate	32
Figure 4.2.	Direct implementation of	58
Figure 4.3.	Number of Permutations (Np) vs. Combinations (Nc).	60
Figure 4.4.	Derivation of reverse Pascal triangle.....	62
Figure 4.5.	Combinations for which F is computed.....	65
Figure 4.6.	Pascal triangle and RPT table	66
Figure 4.7.	RPT offset array needed for indexing.....	67
Figure 4.8.	Segment of code for computing	68
Figure 4.9.	Code segment illustrating unrolling of Do-loops	69
Figure 4.10.	Do-Loop Unrolling vs. Straight Implementation.....	70
Figure 5.1.	One-ply plate loaded in tension	73
Figure 5.2.	Variation of absolute r.m.s. shear strain at the center of element 2 with excitation load level.....	75
Figure 5.3.	Variation of normalized r.m.s. displacement at free corner nodes with excitation load.....	76
Figure 5.4.	Variation of normalized r.m.s. strains at the center of element 2 with excitation load level.....	76
Figure 5.5.	Variation of normalized r.m.s. stresses at the center of element 2 with excitation load level.....	77
Figure 5.6.	Two-ply laminated plate loaded in tension.....	78
Figure 5.7.	Variation of absolute r.m.s. shear strain at the center of element 2 with excitation load level.....	80
Figure 5.8.	Variation of normalized r.m.s. displacement at free corner nodes with excitation load level.....	80
Figure 5.9.	Variation of normalized r.m.s. strains at the center of element 2 with excitation load level.....	81
Figure 5.10.	Variation of normalized r.m.s. stresses at the center of element 2 with excitation load level.....	81
Figure 5.11.	Three-ply laminated plate loaded in tension.....	82
Figure 5.12.	Variation of normalized r.m.s. stresses at the center of element 2 with excitation load level.....	84
Figure 5.13.	Variation of normalized r.m.s. strains at the center of element 2 with excitation load level.....	84
Figure 5.14.	Twisting due to extensional loading for [30°], [30°/-30°] and [30°/0°/-30°] at $S_0 = 8000$	85
Figure 5.15.	One-ply plate loaded in shear	86

Figure 5.16. Variation of absolute r.m.s shear strain at the center of element 2 with excitation load level.....	88
Figure 5.17. Variation of normalized r.m.s. displacement at free corner nodes with excitation level.....	89
Figure 5.18. Variation of normalized r.m.s. strains at the center of element 2 with excitation load level.....	89
Figure 5.19. Variation of normalized r.m.s. stresses at the center of element 2 with excitation load level.....	90
Figure 5.20. Tree-ply laminated plate loaded in shear.....	91
Figure 5.21. Variation of absolute r.m.s. shear strain at the center of element 2 with excitation load level.....	92
Figure 5.22. Variation of normalized r.m.s. displacement at free corner nodes with excitation load level.....	93
Figure 5.23. Variation of normalized r.m.s. strains at the center of element 2 with excitation load level.....	94
Figure 5.24. Variation of normalized r.m.s. stresses at the center of element 2 with excitation load level.....	94
Figure 5.25. One-ply plate with fiber orientation α	95
Figure 5.26. Variation of absolute r.m.s. shear strain at the center of element 2 with excitation load level.....	97
Figure 5.27. Variation of normalized r.m.s. displacement at free corner node with excitation load level.....	97
Figure 5.28. Variation of normalized r.m.s. strains at the center of element 2 with excitation load level.....	98
Figure 5.29. Variation of normalized r.m.s. stresses at the center of element 2 with excitation load level.....	98
Figure 5.30. Two-ply plate with fiber orientation α	99
Figure 5.31. Variation of absolute r.m.s. shear strain at the center of element 2 with excitation load level.....	101
Figure 5.32. Variation of normalized r.m.s. displacement at free corner node with excitation load level.....	101
Figure 5.33. Variation of normalized r.m.s. strains at the center of element 2 with excitation load level.....	102
Figure 5.34. Variation of normalized r.m.s. stresses at the center of element 2 with excitation load level.....	102
Figure 5.35. One-ply plate with fiber orientation α	103
Figure 5.36. Variation of absolute r.m.s. strain at the center of element 2 with excitation load level.....	105
Figure 5.37. Variation of normalized r.m.s. displacement at free corner node with excitation load level.....	106
Figure 5.38. Variation of normalized r.m.s. strains at the center of element 2 with excitation load level.....	106

Figure 5.39. Variation of normalized r.m.s. stresses at the center of element 2
with excitation load level.....107

1. Introduction

1.1 General

During the last two decades, research and development of laminated composite structures has grown at an extremely rapid pace. It is becoming apparent and that more and more composite materials will be used in the design of structures, especially for applications in which the strength to weight ratio is of primary importance. Due to their high strength to weight and stiffness to weight ratios, advanced composite laminates made a direct impact in the aerospace industry over the last two decades, and are now slowly being introduced in automobile, ship building and other industries. For the most part deterministic dynamic analysis has been used in the analysis and design of composite components. However, recent advances in random vibration analysis allows more realistic techniques to be used since most composite components are exposed to stochastic dynamic loads. Space vehicle components made for NASA and the Air Force are now required to be designed for random loads. Major finite element program developers have begun to respond to these needs and have recently incorporated linear random vibration capabilities in their codes. However, very little work has been done on the random vibration analysis of elements made of composites which exhibit strongly anisotropic and moderately nonlinear behavior. There is an important need to address this deficiency, to develop suitable techniques for the random vibration analysis of composite components and to incorporate these techniques into general purpose finite element codes so that they may be widely used in analysis and design.

One of the most important differences that filamentary composite laminates have over the traditional materials (such as aluminum and steel) used in aircraft, ships, etc., is their anisotropic behavior. Another important feature is that the stress-strain relations exhibit significant nonlinearities even for modest loads, when the loading is not parallel to the filaments or when the loading involves shear (Hahn and Tsai 1973, Hahn 1973). For the

accurate analysis of such structures which exhibit nonlinear behavior arising due to geometry and/or material properties. It is necessary to include the nonlinearity in the analysis.

In this study a procedure for the computation of the nonlinear random vibration response of laminated anisotropic plates modeled using finite elements is developed using the method of statistical linearization. Geometrical nonlinearity occurs due to structural configuration or large displacement. Only physical nonlinearity is included in this present study.

This chapter describes the objectives of the present study, and presents a brief literature review of related studies.

1.2 Objectives

The main objective of the present work is to develop a procedure for the nonlinear elastic random vibration analysis of laminated composite plates. The exact solution of the nonlinear stochastic differential equations governing the dynamic response of systems is possible only for very simple systems (see literature review). For more complex systems, approximate methods must be used. Due to practical reasons it is crucial that the method be capable of dealing with structures modeled using finite elements, and the method of equivalent linearization is suited for this purpose. The excitation is assumed to be Gaussian.

Furthermore, it is hoped that the material presented will stimulate and enhance further research on the random response of other laminated composite systems. The computer code written as part of this work can be easily generalized to analyze laminated shells, and can be modified to include higher order shear deformation.

1.3 Literature Review

1.3.1 Physical Nonlinearity

The linear elastic theory of fiber-reinforced composite materials is well developed (see, for example, Jones). However, most composite materials exhibit mildly nonlinear

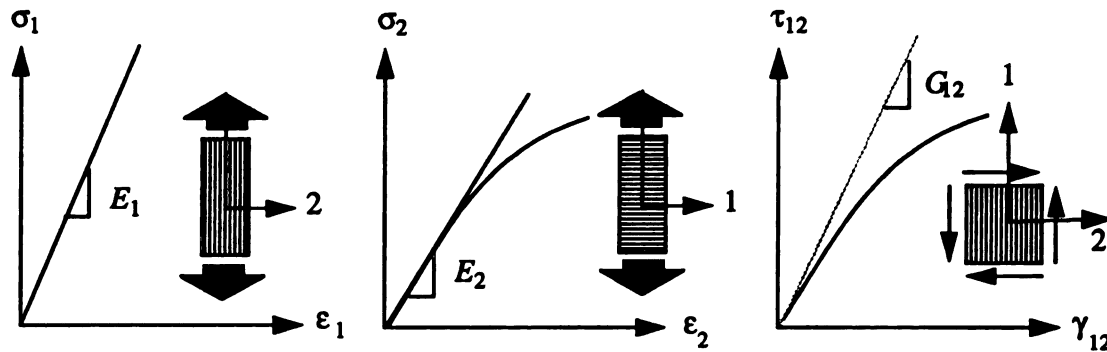


Figure 1.1 Typical stress-strain curve behavior of fiber-reinforced composite material

stress-strain behavior in at least one principal material direction. The stress-strain curve in the fiber direction of unidirectionally reinforced lamina is linear even at high stress level. However, the stress-strain response for loading transverse to the fibers is often somewhat nonlinear. Moreover, the shear response is quite nonlinear.

The degree of nonlinearity varies from composite to composite and is due mainly to the nonlinear matrix material, which significantly affects the transverse modulus E_2 and the shear modulus G_{12} of the composite. The effect of the nonlinear matrix material on the longitudinal modulus E_1 and Poisson's ratio ν_{12} is shown with micromechanics analysis to be negligible for normal combination of fibers and matrix materials. Specific examples of fiber-reinforced composite materials with nonlinear stress-strain behavior include boron/epoxy with slight E_2 nonlinearity but a strong G_{12} nonlinearity. On the other hand, metal-matrix composites such as boron/aluminum have strong E_2 and G_{12} nonlinearities. Three-dimensionally fiber-reinforced composites such as carbon/carbon have nonlinearities in all principal material directions. The nonlinearities for all these materials are more apparent with increasing temperature and moisture content. Thus, analysis of composites should include the effect of nonlinear stress-strain behavior.

Various investigators have attempted to include material nonlinearities in the analysis of composite materials.

Petit and Waddoups (1969) employed a piecewise linear method. According to this method, incremental stress-strain relations are first obtained at each state of strain and then the over-all behavior of the laminate is calculated by integrating the incremental stresses. The first increment in the laminate strains is calculated with the assumption that the laminate behaves linearly over the applied stress increment, i.e.,

$$[\Delta\varepsilon]_{n+1} = [A]_n [\Delta\sigma]_{n+1} \quad (1.1)$$

The increment in the laminate strains, $\Delta\varepsilon$, is added to the previous strains to determine the current total laminate strain

$$[\varepsilon]_{n+1} = [\varepsilon]_n + [\Delta\varepsilon]_{n+1} \quad (1.2)$$

The individual lamina strains may be computed using rotational transformations. Accounting for the orientation of the fibers in each lamina, the lamina constitutive equations are expressed as follows:

$$\begin{bmatrix} \sigma_1 \\ \sigma_2 \\ \tau_{12} \end{bmatrix}_n = \begin{bmatrix} Q_{11} & Q_{12} & 0 \\ Q_{12} & Q_{22} & 0 \\ 0 & 0 & Q_{66} \end{bmatrix}_n \begin{bmatrix} \varepsilon_1 \\ \varepsilon_2 \\ \gamma_{12} \end{bmatrix}_n \quad (1.3)$$

the stiffness matrix for (n+1) th stress increment can then be calculated.

Hahn and Tsai (1973) derived a stress-strain relation which is linear in uniaxial loading in the longitudinal and transverse directions, but nonlinear in shear. Their theory was based on the strain energy density function which includes a fourth order term:

$$\bar{W}^* = \frac{1}{2} S_{11} \sigma_1^2 + \frac{1}{2} S_{22} \sigma_2^2 + S_{12} \sigma_1 \sigma_2 + \frac{1}{2} S_{66} \tau_{12}^2 + \frac{1}{4} S_{66}^* \tau_{12}^4 \quad (1.4)$$

where \bar{W}^* is the complementary energy density function. They have explicitly shown that only one fourth order constant is needed to account for the nonlinear shear behavior of an off-axis composite lamina. In their study, Kirchoff's hypothesis that each lamina in the laminate is in the same state of membrane strain as that of the laminate was used. The stress-strain relation which takes account of frequently observed nonlinear behavior in in-plane shear is

$$\begin{Bmatrix} \varepsilon_1 \\ \varepsilon_2 \\ \gamma_{12} \end{Bmatrix} = \begin{bmatrix} S_{11} & S_{12} & 0 \\ S_{12} & S_{22} & 0 \\ 0 & 0 & S_{66} \end{bmatrix} \begin{Bmatrix} \sigma_1 \\ \sigma_2 \\ \tau_{12} \end{Bmatrix} + S_{66}^* \tau_{12}^2 \begin{Bmatrix} 0 \\ 0 \\ \tau_{12} \end{Bmatrix} \quad (1.5)$$

Their predictions of strain response under uniaxial off-axis loading agree fairly well with measurements by Cole and Pipes as well as the theory and experiments concerning the off-axis behavior.

Hashin, Bagchi, and Rosen (1974) implemented the Ramberg-Osgood stress-strain relations to represent the nonlinear response of the lamina subjected to transverse and shear loads. The behavior in the direction of fibers was assumed to be linear. The Ramberg-Osgood model is quite flexible and able to represent varying degrees of nonlinearities as well as hysteresis.

Sandhu (1976) used an approximation of stress-strain behavior under biaxial normal stress states to predict equivalent multiaxial strain increments. The incremental constitutive relationship used is defined under the following assumptions:

1. The increment of strain depends upon the strain state and the increment of stress.
2. The increment of strain is proportional to the increment of stress.

using these assumptions, the incremental constitutive law can be written as

$$d\varepsilon_{ij} = S_{ijrs}(\varepsilon_{ij}) d\sigma_{rs} \quad (i, j, r, s = 1, 2, 3) \quad (1.6)$$

where $d\epsilon_{ij}$, $d\sigma_{rs}$ are strain and stress increments and S_{ijrs} is a function of strains ϵ_{ij} . Under generalized plane stress, the above equation reduces to:

$$d\epsilon_i = S_{ij}(\epsilon_i) d\sigma_j \quad (1.7)$$

assuming that the lamina remains orthotropic at all load levels (this assumption was justified experimentally) the above equation can be written as

$$[d\sigma]_k = [C]_k [d\epsilon]_k \quad (1.8)$$

This model is similar to the one used by Petit-Waddoups (1969) since both methods use lamination theory to generate the laminate compliance which is used to compute laminate strain increments under applied stress increment. These laminate strain increments are added to those obtained previously to determine current strains. In the Petit-Waddoups technique these strains are used to compute the laminate compliance for the next load increment. This technique is essentially a predictor type. In Sandhu's analysis, the strains are used to determine the average laminate compliance for the same load increment, and a new set of laminate strains are obtained. This procedure is repeated until the difference between two consecutive sets of laminate strains is less than a prescribed tolerance. The results of this approach are in good agreement with Cole and Pipes' data and those of Hahn and Tsai as well.

Jones and Nelson (1976) developed an orthotropic material model in which the non-linear mechanical properties are functions of the strain energy density,

$$MP_i = A_i \left[1 - B_i \left(\frac{U}{U_{0i}} \right)^{C_i} \right] \quad (1.9)$$

where MP_i is the mechanical property (e.g. modulus of elasticity) for the i th stress- strain curve, and for lamina under plane stress U is given by

$$U = (\sigma_1 \epsilon_1 + \sigma_2 \epsilon_2 + \tau_{12} \gamma_{12}) / 2 \quad (1.10)$$

where A_i , B_i and C_i are the initial slope, initial curvature, and change of curvature of the i th stress-strain curve. The quantity U_0 is used to nondimensionalize the strain energy portion of the mechanical property equation. The Jones-Nelson model is used in an iterative procedure which converges to the state of stress and strain corresponding to an equivalent linear elastic body.

The mechanical properties in this model cannot be defined for strain energies greater than or equal to a specific value of strain energy \bar{U} (value of strain energy where the approximate mechanical property curve crosses the U axis). The value of \bar{U} at which the mechanical property becomes negative is $\bar{U} = B^{-1/C}$. Thus, \bar{U} is largest for stress-strain curves with low initial curvature and low rate of change of curvature. Accordingly, the Jones-Nelson model cannot be used as extrapolation for energies as large as \bar{U} but must be restricted to energies less than or equal to $\tilde{U} = \frac{1}{2}\tilde{\sigma}\tilde{\epsilon}$ ($\tilde{\sigma}$ is the maximum stress). This range is not sufficient to treat practical problems. Hence, modifications of this model are essential.

Jones and Morgan (1977) have extended the Jones-Nelson model to include treatment of more pronounced nonlinearities. Their approach is based on the concept that the stress-strain curve be connected to a straight line with equation $\sigma = m\epsilon + \sigma_0$ instead of merely specifying the slope m . This approach is useful in fitting the stress-strain curves while simultaneously considering the statistical nature of failure data which can be described with such a line. A disadvantage of this approach is that the fit of the actual stress-strain data is not as good as with other approaches. Their computed strains agree with strains measured by Cole and Pipes about as well as the theories mentioned previously.

Amijima and Adachi (1978) presented a simplified method of predicting the nonlinear stress-strain curves for an unidirectionally orthotropic lamina, and symmetric biaxial laminates. The analytical procedure is based on linear elastic analysis with the application of classical laminated plate theory (L.P.T) to the small stress increments of the stress-strain

curve. Because it is assumed that only the nonlinear component of the principal in plane shear response governs the nonlinearity of the unidirectional lamina stress-strain curves, the following relation between $\Delta\gamma_{12}$ and $\Delta\sigma_x$ was used

$$\begin{aligned} & (\Delta\sigma_x) [\cos 2\theta \{1 - (\bar{Q}_{11})_n ((\bar{S}_{11})_n - (\bar{S}_{12})_n)\}] \\ & + [\sin 2\theta (\bar{Q}_{16})_n ((\bar{S}_{11})_n - (\bar{S}_{12})_n)] = (\bar{Q}_{16})_n (\Delta\gamma_{12}) \end{aligned} \quad (1.11)$$

The n th stress increment, $(\Delta\sigma_x)_n$, in the loading direction corresponding to the n th increment of the in-plane shear strain component, $(\Delta\gamma_{12})_n$, is calculated from the above equation. The complete nonlinear stress-strain curve was predicted for various laminations. The nonlinear stress-strain curves for various cases could be estimated and the results have considerably good agreement with experimental ones.

Chou and Takahashi (1987) used the stepwise incremental analysis proposed by Petit and Waddoups (1969) to predict the non-linear stress/strain responses of flexible fiber composites. The uniaxial tensile stress/strain relations were obtained for several types of composites containing glass or kevlar fibers in an elastometric polymer. Their theoretical procedure considered the fiber geometric nonlinearity as well as the material nonlinearity.

Chou and Lou (1988) developed a constitutive model based upon the Eulerian description to account for material nonlinearity for flexible fibers. They used a complementary energy function to derive the following material nonlinear stress-strain relation

$$\{e_i\} = [S_{ij}] \{\sigma_j\} \quad (1.12)$$

where

$$\begin{aligned} S_{11} &= S_{11} + S_{111}\sigma_1 + S_{1111}\sigma_1^2 & S_{12} &= S_{12} = S_{21} \\ S_{22} &= S_{22} + S_{222}\sigma_2 + S_{2222}\sigma_2^2 & S_{16} &= S_{166}\sigma_6, \quad S_{16} = 2S_{166}\sigma_6 \\ S_{66} &= S_{66} + S_{6666}\sigma_6^2 & S_{26} &= S_{62} = 2S_{2266}\sigma_2\sigma_6 \end{aligned}$$

the terms S_{11} , S_{22} , S_{12} and S_{66} are needed for linear deformations; the terms S_{111} , S_{222} are needed for representing the bimodulus behavior in the axial and the transverse direction respectively; the terms S_{1111} , S_{2222} and S_{6666} are the nonlinear terms. Although this model resembles Hahn & Tsai's model, the former has the capability of treating complicated problems with more than one nonlinearity in the material property.

1.3.2 Shear Deformations

Classical plate theory can yield significant error for moderately thick composite laminas because transverse shear deformation is neglected. It is well known that transverse shear deformation is significant for thick plates, and this is especially true for composites since the shear moduli of polymer matrices are significantly lower than the extensional moduli. While a first-order shear theory (Reissner 1945, Mindlin 1951) is adequate for plates made of conventional materials, a higher-order shear theory is usually required for composite laminates (Reddy 1990, Noor and Burton 1989). Higher-order shear theories are usually adequate only for global modeling (i.e., prediction of displacements, natural frequencies and buckling loads), and are not sufficiently accurate for stress field computations. Local layer-wise models that represent each layer as a homogeneous anisotropic continuum are usually required for accurate stress computations, but these often greatly increase the size of the problem.

Numerous higher-order shear theories have been proposed (e.g., Nelson 1974, Whitney and Sun 1974, Lo 1977, Reddy 1984, and many others). All of them use through-the-thickness displacement assumptions of the form (Reddy 1987)

$$\begin{Bmatrix} u(x_1, x_2, x_3) \\ v(x_1, x_2, x_3) \\ w(x_1, x_2, x_3) \end{Bmatrix} = \begin{Bmatrix} u_0(x_1, x_2) \\ v_0(x_1, x_2) \\ w_0(x_1, x_2) \end{Bmatrix} + \begin{Bmatrix} U(x_1, x_2, x_3) \\ V(x_1, x_2, x_3) \\ W(x_1, x_2, x_3) \end{Bmatrix} \quad (1.13)$$

Where u_0 , and v_0 , and w_0 are the displacement components of the reference plane $x_3 = 0$, and U , V , and W are functions of x_3 which vanish at $x_3 = 0$. The different theories can be identified by the assumed functional dependence of U , V , and W on x_3 .

1.3.3 Stochastic Dynamic Analysis

General theory

The general problem of random excitation of physical systems was first investigated theoretically by Einstein (1905) and was generalized and extended by Smoluchowski (1916) in context of the theory of Brownian motion. In 1931, Kolmogorov derived a precise mathematical formulation of the equations governing the probability densities satisfied by such processes. Contributions of major importance were also made by Fokker, Planck, Burger, Furth, Ornstein, Uhlenbeck, Kramers and others. A number of important papers from this era have been collected in the book by Wax (1954).

Stochastically excited linear systems have been studied in great detail and several analytical techniques exist for treating both stationary and nonstationary problems. Unfortunately, many structures of engineering interest cannot be considered linear and the techniques for analyzing nonlinear systems are not nearly so well developed. Some simple nonlinear systems can be analyzed exactly by means of the Fokker-Planck equation. However, for most nonlinear systems exact solutions are not available. A number of approximate techniques have been applied successfully to simple one DOF systems, but much less has been done in the analysis of dynamical systems with more than one DOF. Several potentially useful techniques for the analysis of such systems have been developed, but most of these techniques are either very difficult to apply or their application is restricted to only a small class of problems. The statistical linearization technique shows considerable promise in this regard for it is not limited by the restrictions commonly imposed on the other approaches. In addition, this approach can be made quite direct and relatively easy to apply.

The earliest work on the problem of random excitation of nonlinear system was that of Andronov (1933), who used the Kolmogorov-Fokker-Planck equations (Kolmogorov, 1931) to study the motions of general dynamic system subject to random disturbances. Kramers (1940) used this technique to study chemical reaction rates. Caughey and Dienes (1961), Lyon (1961), Klein (1964), and Herbert (1965) have used the Fokker-Planck equation to study the response of nonlinear dynamical systems to white noise excitation. Barrett (1961), Merklinger (1963) and Stratonovich (1963) have applied the technique to solve nonlinear control problems.

In almost all these investigations only first order statistical properties were obtained. While first order statistics are important parameters in the description of random processes, there are numerous applications where additional statistical information is required. For example, the spectral density of a random process requires a knowledge of the second order statistics of the process. A number of approximate techniques have been developed to obtain second order statistics for the response of nonlinear systems to random excitation. Booton (1954) and Caughey (1959) independently developed the method of equivalent linearization, which is simply the statistical extension of the well known equivalent linearization technique of Krylov and Bogolinbov (1937). Crandall (1961) developed a perturbational method based on classical perturbation theory. Payne (1967), Wong (1964), and Atkinson (1970) have developed approximate techniques based on eigenfunction expansions and variational techniques.

Many problems in mechanics and related fields, involving the response of dynamical systems to stochastic excitation can be modeled as systems of first order differential equations of the form

$$\frac{dx}{dt} = a(t, x) + \sum_{k=1}^m b_k(t, x) \frac{d}{dt} w_k(t) \quad (1.14)$$

where $x, a, b_k, k = 1, 2, \dots, m$ are m vectors and the $w_k(t)$ for $k = 1, 2, \dots, n$ are independent processes of Brownian motion.

In nonlinear stochastic differential equations the structure of the transition probability density function is usually much more complex than that of linear systems, and cannot be obtained in a direct fashion. The most common method of obtaining the transition probability density function for nonlinear stochastic differential equations is through the use of the Kolmogorov-Fokker-Planck equations:

$$\frac{\partial q}{\partial t} + \alpha_x q = 0 \quad (1.15)$$

where α_x is expressed in the following way

$$\alpha_x = \frac{\partial}{\partial x_i} (A_j \cdot q) - \frac{1}{2} \frac{\partial^2}{\partial x_j \partial x_k} (B_{jk} \cdot q) \quad (1.16)$$

q must satisfy the initial condition $q(x, t_0 | x_0, t_0) = \delta(x - x_0)$

Exact solutions of the Fokker-Planck-Kolmogorov equations have been found for two types of stochastic differential equations:

1. systems of linear equations
2. certain first order nonlinear equations.

The steady-state probability density can always be obtained for first order nonlinear systems, and has been found for a certain class of coupled nonlinear oscillator problems. Caughey and Atkinson (1968), obtained the transition probability density function for a class of piecewise linear systems excited by Gaussian white noise.

The exact steady-state probability density for first order nonlinear system excited by Gaussian white noise can readily be determined by direct integration. The Fokker-Planck equation for a stochastic differential equation of the type

$$dx = -f(x) dt + dw(t) \quad (1.17)$$

is given by

$$\frac{\partial q}{\partial t} = \frac{\partial}{\partial x} \left[f(x) q + D \frac{\partial q}{\partial x} \right] \quad (1.18)$$

where D is a positive constant. Direct integration of the above equation yields the steady-state probability distribution function $q_s(x)$ providing that it satisfies the condition $\frac{\partial q}{\partial t} = 0$

$$q_s(x) = C^{-1} \exp \left[- \int_0^x f(\xi) / D d\xi \right] \quad (1.19)$$

where C is the normalizing constant given by

$$C = \int_{-\infty}^{\infty} \exp \left[- \int_0^x f(\xi) / D d\xi \right] dx \quad (1.20)$$

Exact solutions of the steady state probability density function for nonlinear equations of second order excited by white noise have been found only for equations of the form

$$\ddot{x} + f(H) \dot{x} + g(x) = \dot{w}(t) \quad (1.21)$$

$$E [dw(t)^2] = 2Ddt \quad (1.22)$$

$$H = \frac{1}{2} \dot{x}^2 + \int_0^x g(\eta) d\eta \quad (1.23)$$

The associated Fokker-Planck equation is easily shown to be

$$\frac{\partial q}{\partial t} = - \dot{x} \frac{\partial q}{\partial x} + \frac{\partial}{\partial \dot{x}} [(g(x) + f(H) \dot{x}) q] + D \frac{\partial^2 q}{\partial \dot{x}^2} \quad (1.24)$$

and by direct integration, the steady-state probability density function is given by

$$q_s(x, \dot{x}) = \frac{\exp\left[-(1/D) \int_0^H f(\eta) d\eta\right]}{\int_{-\infty}^{\infty} \int_{-\infty}^{\infty} \exp\left[-(1/D) \int_0^H f(\eta) d\eta\right] dx d\dot{x}} \quad (1.25)$$

The same technique can be applied to the system of coupled nonlinear equations.

The main advantage of the Fokker-Planck equation approach over all of the other approaches considered here, including statistical linearization, is the exact solution it provides. However, this advantage must be balanced by the fact that such solutions have only been found for certain restricted classes of problems. Caughey showed that the stationary Fokker-planck equation can be solved and the first order probability density of the Markovian response process can be obtained provided:

1. The only energy dissipation in the system arises from damping forces that are proportional to the velocity.
2. The excitation is Gaussian white noise.
3. The correlation function matrix of the excitation is proportional to the damping matrix of the system.
4. The restoring force vector of the system is derivable from a potential.

The solution of the time-independent Fokker-Planck equation under these conditions represents a very significant accomplishment. However, it is a fact that most systems of practical interest do not satisfy the above mentioned conditions. Since, in general, it is not possible to obtain exact statistics for the response of nonlinear system excited by white noise, a number of techniques have been developed to treat a broader class of problems.

One of the approximate techniques based on the use of the Fokker-Planck equation known as the eigenfunction expansion was used by Wong (1964) and Payne (1967, 1968) for first order system, in which case the Sturm-Liouville theory applies. For many higher order systems the Fokker-Planck-Kolmogorov equations are of degenerate form. Atkin-

son(1970) has used eigenfunction expansion techniques for second order systems excited by white noise. Unfortunately, for many nonlinear systems of the second or higher order, the eigenvalue problem cannot be solved exactly. In some cases, perturbation techniques may be used to extend the class of systems which may be analyzed by this method. This requires that eigenvalues and eigenfunctions of an associated Fokker-Planck operator be known a priori, a situation which unfortunately occurs rather infrequently. The Rayleigh-Ritz method (Mikhlin, 1964) has been widely used to approximate the eigenvalues and eigenfunctions of the linear differential operators.

An approximate technique that has been used is the normal mode approach for stationary random response problems. This technique reduces a set of coupled nonlinear second order differential equations to a set of equations that include coupling only in the nonlinear terms, and is applicable for statistically uncorrelated excitations. The reduced equations may then be subjected to a number of approximate solution techniques such as the method of statistical linearization. In order to successfully apply this technique to a given multi-DOF dynamical system, the system must satisfy the following two conditions:

1. The linear system obtained by neglecting all system nonlinearities must possess normal modes.
2. The correlation function matrix of the excitation must be diagonalized by the same transformation that diagonalizes the linear mass, damping and stiffness matrices.

While the first condition may be acceptable in a number of situations, the second condition is quite restrictive. In particular, it precludes the application of the technique to all dynamical systems that are excited at only few points in space. However, such systems are of considerable interest physically and thus, the second restriction represents a rather severe limitation on the usefulness of the normal mode approach.

Another approximate method is the perturbation approach where the stochastically excited nonlinear system is treated in the same way as a deterministically excited system.

A power series expansion in terms of a small parameter which specifies the size of the non-linearity represents the solution for such systems. Substituting the assumed solution form into the original equations of motion and equating coefficient of like powers of the nonlinearity parameter then yields a set of linear differential equations for the terms in the solution expansion. A first order approximation is obtained by solving two linear systems. The first is the system which is obtained by setting all nonlinearities equal to zero, and the second is a system having an excitation which is a function of the solution of the first system. Practically speaking, it is almost impossible to extend this procedure beyond the first approximation except in very trivial cases since the probability density of the first order correction term is non-Gaussian.

In their analysis of nonlinear systems, Lyon (1960) and later Crandall (1963) applied the perturbation approach to a continuous nonlinear system. This proved useful in a variety of applications since the approach is not restricted to cases of uncorrelated excitation. The major source of difficulty however, arises in the solution of the equation for the first -order correction term. This is because generally, this equation has a non-Gaussian excitation. The complexity of this can be overwhelming even when a relatively simple multi-DOF system is considered. A scheme for reducing the computational difficulties was presented by Tung (1967). By using Foss's complex-mode approach to solve for the first-order correction term the computational difficulties were alleviated, but the overall complexity of the approach is still considerable

A third approximate technique is statistical linearization. This technique was developed independently by Booton(1954) and Caughey (1959). It is applicable to nonlinear stochastic differential equations. This approach overcomes many of the limitations encountered in the previous methods for studying the stationary random response of multi-DOF systems. It is based on the concept of replacing the nonlinear system by an equivalent linear system while minimizing the difference between the two systems. This concept has

been widely used in control theory and in the study of multi-DOF dynamical systems with stochastic excitation.

The accuracy of an approximate analysis based on statistical linearization is difficult to predict in general, but it is usually assumed that the approximate solution obtained is accurate to first order in the parameter specifying the size of the system nonlinearity. Wan and Yang (1972) showed that the accuracy of statistical linearization approach appear to be well within the limits of practical engineering usefulness. When studying a specific nonlinear system, the accuracy of statistical linearization should be assessed by comparing its results with results obtained by Monte Carlo simulation.

Applications to composites

Much of the recent work related to analysis of composites has been on the development of suitable finite elements for composite plates and shells. Studies considering static loading far outnumber those that consider dynamic loading. There have been only a few studies considering stochastic dynamic loading, and some of these are briefly discussed in this section, along with their limitations.

Witt and Sobczyk (1980) were the earliest researchers to study the random vibration of laminated plates. They used an analytical series formulation and modal analysis to study the stochastic bending response, but considered only linear behavior. Witt (1986) later extended the formulation to include transverse shear deformation in the plate.

Cederbaum, Elishakoff and Liberscu (1989) used an analytical formulation that included a first-order shear deformation theory together with modal analysis to study the linear random vibration of composite plates. Cederbaum (1990) later extended this to include viscoelastic material behavior.

Mei and Prasad (1989) appear to be the only researchers who have considered the non-linear random vibration of composite plates. They included transverse shear deformation, but considered non-linearity arising from large deformations and not from the consti-

tutive laws. They used an analytical formulation together with the method of equivalent linearization, and considered only a single modal response equation obtained through an approximate Galerkin approach.

There are several limitations in the works cited above:

1) None of the investigations include non-linear material behavior, which is quite important for filamentary composites.

2) They all use analytical formulations, rather than finite element based formulations, and therefore are readily applicable only for plates with simple geometries and boundary conditions (e.g., rectangular plates with simply supported or fixed boundaries).

3) They cannot be easily used in existing large-scale computer programs which are predominantly based on the finite element approach.

Harichandran and Hawaari (1992) performed nonlinear random vibration analysis of filamentary composites loaded in extension. They approximated the nonlinear shear stress-strain law in terms of a power series. The result of their work has shown that the non-linearity in the constitutive law results in significant increases in the shear strains, but does not significantly affect the normal strains.

2. Finite Element Formulation

2.1 General

The advent of computers has opened new horizons in the field of engineering design. In the realm of analysis for engineering design the finite element method has emerged as a powerful tool for modeling and analysis of solids and structures of complex geometries and variable material properties. Although the original applications of the finite element were in the area of stress analysis, its usage has spread to many other areas having similar mathematical bases such as heat transfer, fluid flow, electric and magnetic fields and several others. The finite element method is a numerical procedure which enables a problem with an infinite number of DOF to be converted to one with a finite number in order to simplify the solution technique.

The primary objective of the use of the finite element method in the analysis of structures is to calculate approximately the displacements, strains, stresses and other responses of the structure. The power of the method resides mainly in its versatility. The method can be applied to a variety of structures with arbitrary shape, loads, and support conditions. The finite element mesh can mix elements of different types and physical properties.

Today, the concept of finite elements is a very broad one. A most important formulation, which is widely used for the solution of practical problems, is the displacement-based finite element method. Due to its simplicity, generality and good numerical properties, this formulation has been used in major general-purpose analysis programs.

The basic process of the displacement based finite element method is that the complete structure is idealized as an assemblage of individual structural elements. The element stiffness matrices corresponding to the global degrees of freedom of the structural idealization are calculated and the total stiffness matrix is obtained by addition of element stiffness matrices. The solution of the equilibrium equations of the assemblage of elements yields the element displacements which are used to calculate the strains and stresses.

In two- and three-dimensional finite element analyses, we basically use the Ritz analysis technique with trial functions that approximate the actual displacements. The result is that the differential equations of equilibrium are not satisfied in general, but this error is reduced as the finite element idealization of the structure is refined.

2.2 Constitutive Equations

In the elementary theory of plates, certain assumptions are made regarding the stress distribution. Certain stresses are assumed to predominate, while others are neglected. In the theory of bending of beams and plates, the normal stress, σ_3 , which is perpendicular to the beam or plate midplane, is assumed to be negligible in comparison to the normal stresses, σ_1 or σ_2 . In other words, due to the geometry of the plate, the magnitudes that σ_3 can assume are several orders of magnitude less than the values of σ_1 and σ_2 which are induced by bending. Also, the assumption is made that any line perpendicular to the plate midplane before deformation remains perpendicular to the midplane after deformation, and it suffers neither extension nor contraction. As a result, the shear strains, γ_{13} and γ_{23} , and the normal strain, ϵ_3 , are zero. The shear stresses, τ_{13} and τ_{23} , are also neglected. These assumptions, which are made in the classical theory of plates, are termed Kirchhoff's hypothesis. For thin plates, the hypothesis results in the existence of a plane stress state. Thus one pertinent assumption in establishing the constitutive or stress-strain relationships for the laminae of a laminated composite is that the laminae, when in the composite, are in a plane stress state - which is not to say that the interlaminar shear stresses, τ_{13} and τ_{23} , will not be present between laminae once they are placed in the composite. However, these stresses may be neglected in establishing the laminae constitutive relations on which the laminae stress-strain relations will be formulated.

It is commonly known that most uni-directional filamentary composites display orthotropic characteristics, and behave essentially linearly when loaded parallel to or perpendicular to the fiber directions. However, when loaded in shear, they exhibit significantly

nonlinear behavior. Fig. 2.1 shows the global coordinate system x - y and material coordinate system 1-2 for a typical uni-directional composite element.

In view of the advantages and the disadvantages of the various nonlinear stress-strain models described in chapter 1, the model proposed by Hahn and Tsai seems to obtain an explicit relation for ϵ in terms of the loading and known material parameters including the nonlinear shear term. Hence, this model is adopted in this study.

Based on experimental results, Hahn (1973) proposed the following strain-stress (or inverse) law for plane stress problems:

$$\begin{Bmatrix} \epsilon_1 \\ \epsilon_2 \\ \gamma_{12} \end{Bmatrix} = \begin{bmatrix} S_{11} & S_{12} & 0 \\ S_{12} & S_{22} & 0 \\ 0 & 0 & S_{66} \end{bmatrix} \begin{Bmatrix} \sigma_1 \\ \sigma_2 \\ \tau_{12} \end{Bmatrix} + S_{66}^* \tau_{12}^2 \begin{Bmatrix} 0 \\ 0 \\ \tau_{12} \end{Bmatrix} \quad (2.1)$$

in which ϵ_1 and σ_1 are the normal strain and stress in the 1-direction (i.e., along the fiber direction), ϵ_2 and σ_2 are the normal strain and stress in the 2-direction, γ_{12} and τ_{12} are the engineering shear strain and shear stress corresponding to the material coordinates 1-2, and the square matrix on the right hand side is the linear compliance matrix $[S]$. The cubic

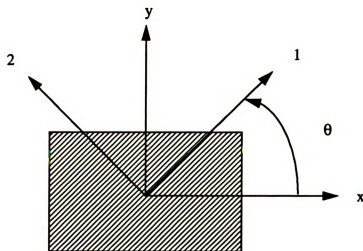


Figure 2.1 Coordinate systems

variation of γ_{12} as a function of τ_{12} in Eq. 2.1 describes the softening behavior of filamentary composites loaded in shear, and is sufficiently accurate. In finite element application, the stress-strain law is preferred. The inverse relation of the cubic shear strain-stress law may be written as $\tau_{12} = g(\gamma_{12})$, where $g(\gamma_{12})$ is the real solution for τ_{12} of the cubic

$$S_{66}^* \tau_{12}^3 + S_{66} \tau_{12} - \gamma_{12} = 0$$

letting $f(\gamma_{12}) = \frac{g(\gamma_{12})}{\gamma_{12}} - Q_{66}$, the stress-strain law may be written as

$$\begin{aligned} \begin{Bmatrix} \sigma_1 \\ \sigma_2 \\ \tau_{12} \end{Bmatrix} &= \begin{bmatrix} Q_{11} & Q_{12} & 0 \\ Q_{12} & Q_{22} & 0 \\ 0 & 0 & Q_{66} \end{bmatrix} \begin{Bmatrix} \epsilon_1 \\ \epsilon_2 \\ \gamma_{12} \end{Bmatrix} + f(\gamma_{12}) \begin{Bmatrix} 0 \\ 0 \\ \gamma_{12} \end{Bmatrix} \\ &= \begin{bmatrix} Q_{11} & Q_{12} & 0 \\ Q_{12} & Q_{22} & 0 \\ 0 & 0 & Q_{66} \end{bmatrix} \begin{Bmatrix} \epsilon_1 \\ \epsilon_2 \\ \gamma_{12} \end{Bmatrix} + f(\gamma_{12}) \begin{bmatrix} 0 & 0 & 0 \\ 0 & 0 & 0 \\ 0 & 0 & 1 \end{bmatrix} \begin{Bmatrix} \epsilon_1 \\ \epsilon_2 \\ \gamma_{12} \end{Bmatrix} \end{aligned} \quad (2.2)$$

or, more compactly as

$$\{\sigma'\} = [Q] \{\epsilon'\} + f(\gamma_{12}) [\text{diag}(0, 0, 1)] \{\epsilon'\} \quad (2.3)$$

in which $[Q] = [S]^{-1}$. In terms of elastic moduli and Poisson's ratios, the elements of $[S]$ and $[Q]$ are

$$S_{11} = 1/E_1, S_{22} = 1/E_2, S_{12} = -\nu_{12}/E_2 = -\nu_{21}/E_1, \text{ and } S_{66} = 1/G_{12}$$

$$Q_{11} = E_1/(1 - \nu_{12}\nu_{21}), Q_{22} = E_2/(1 - \nu_{12}\nu_{21})$$

$$Q_{12} = \nu_{12}E_1/(1 - \nu_{12}\nu_{21}) = \nu_{21}E_2/(1 - \nu_{12}\nu_{21})$$

For Eqs. 2.1 and 2.2 to be exact inverse relations, the function $f(\gamma_{12})$ is related to the solution of the cubic equation mentioned earlier, and contains terms involving fractional powers of γ_{12} . This poses computational difficulties in the method of equivalent lineariza-

tion used to perform the approximate random vibration analysis. In order to facilitate the analysis, it is assumed that the function $f(\gamma_{12})$ may be approximated by

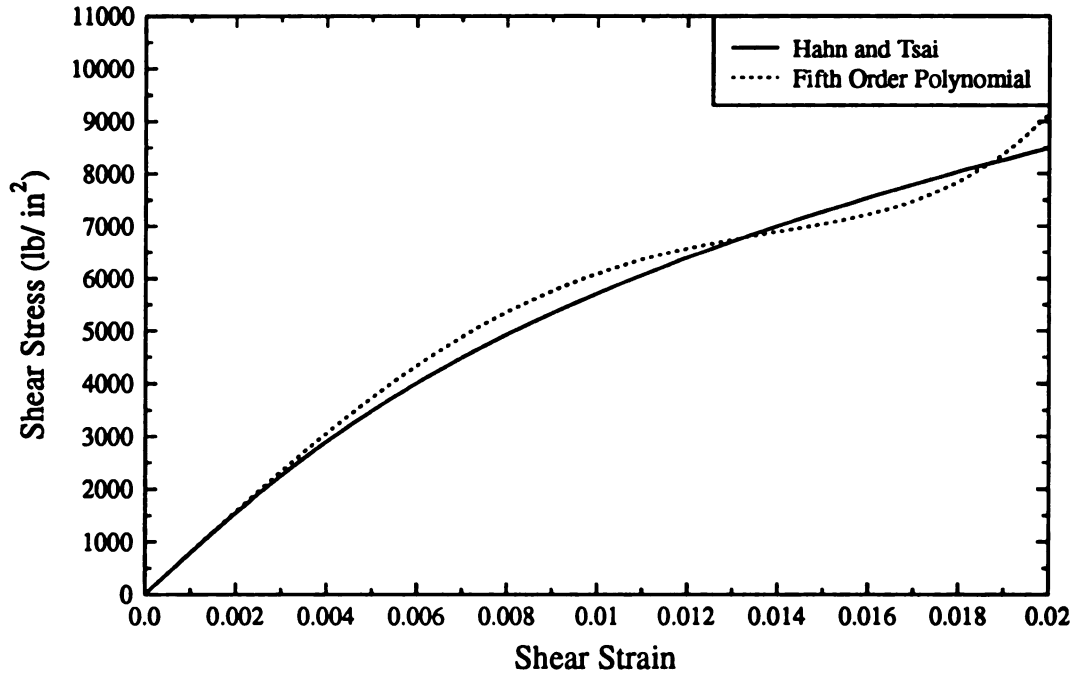


Figure 2.2 Fit of approximate stress-strain law for shear

$$f(\gamma_{12}) = a_1\gamma_{12}^2 + a_2\gamma_{12}^4 + \dots + a_n\gamma_{12}^{2n} = \sum_{i=1}^n a_i\gamma_{12}^{2i} \quad (2.4)$$

Note that the nonlinear term in eq. 2.2 is $f(\gamma_{12})\gamma_{12}$, which is therefore being approximated by an odd-powered series starting with the cubic term.

By suitable choice of the parameters a_i , the stress-strain law can be made to approximate the law in Eq. 2.1 for realistic values of γ_{12} . Fig. 2.2 shows the shear stress-strain law given by Eq. 2.1 for Boron/ Epoxy Narmco 5505, and the approximate curve using Eq. 2.2 and 2.4 with $n = 2$. The material properties used were: $S_{11} = 3.32 \times 10^{-8} \text{ in}^2 \text{ lb}^{-1}$, $S_{22} = 3.48 \times 10^{-7} \text{ in}^2 \text{ lb}^{-1}$, $S_{66} = 1.25 \times 10^{-6} \text{ in}^2 \text{ lb}^{-1}$, $S_{66}^* = 1.53 \times 10^{-14} \text{ in}^6 \text{ lb}^{-2}$

$a_1 = -2.259 \times 10^9$ lb/in², $a_2 = 3.505 \times 10^{12}$ lb/in². The fifth-order approximation is satisfactory for strains up to 0.02.

The stress-strain law in terms of the global coordinate system, x-y, may be written as

$$\{\sigma\} = [\bar{Q}] \{\varepsilon\} + f([T_3] \{\varepsilon\}) [T^*] \{\varepsilon\} \quad (2.5)$$

in which $\{\sigma\} = [\sigma_x \sigma_y \sigma_{xy}]^T$, $\{\varepsilon\} = [\varepsilon_x \varepsilon_y \gamma_{xy}]^T$, $[\bar{Q}] = [T]^{-1} [Q] [T]^{-T}$, and $[T]$ is the orthogonal rotational transformation matrix given by

$$[T] = \begin{bmatrix} \cos^2\theta & \sin^2\theta & 2\sin\theta\cos\theta \\ \sin^2\theta & \cos^2\theta & -2\sin\theta\cos\theta \\ -\sin\theta\cos\theta & \sin\theta\cos\theta & \cos^2\theta - \sin^2\theta \end{bmatrix} \quad (2.6)$$

$[T_3]$ is a row matrix consisting of the third row of $[T]^{-T}$, and $[T^*] = [T]^{-1} [\text{diag}(0, 0, 1)] [T]^{-T}$. Note that $f([T_3] \{\varepsilon\}) = f(\gamma_{12})$ in Eq. 2.5. since $Q_{16} = Q_{26} = 0$. A convenient form for the transformed lamina stiffnesses, \bar{Q} , has been given by Tsai and Pagano (1968):

$$\begin{aligned} \bar{Q}_{11} &= U_1 + U_2 \cos(2\theta) + U_3 \cos(4\theta) \\ \bar{Q}_{22} &= U_1 + U_2 \cos(2\theta) + U_3 \cos(4\theta) \\ \bar{Q}_{12} &= U_4 - U_3 \cos(4\theta) \\ \bar{Q}_{66} &= U_5 - U_3 \cos(4\theta) \\ \bar{Q}_{16} &= \frac{1}{2} U_2 \sin(2\theta) + U_3 \sin(4\theta) \\ \bar{Q}_{26} &= \frac{1}{2} U_2 \sin(2\theta) - U_3 \sin(4\theta) \end{aligned} \quad (2.7)$$

where

$$\begin{aligned}
U_1 &= \frac{1}{8} (3Q_{11} + 3Q_{22} + 2Q_{12} + 4Q_{66}) \\
U_2 &= \frac{1}{2} (Q_{11} - Q_{22}) \\
U_3 &= \frac{1}{8} (Q_{11} + Q_{22} - 2Q_{12} - 4Q_{66}) \\
U_4 &= \frac{1}{8} (Q_{11} + Q_{22} + 2Q_{12} - 4Q_{66}) \\
U_5 &= \frac{1}{8} (Q_{11} + Q_{22} - 2Q_{12} + 4Q_{66})
\end{aligned} \tag{2.8}$$

Note that only three of the invariants U_1 , U_4 and U_5 are independent. That is, these terms remain constant regardless of the angle θ . Thus, examining Eq. 2.8 reveals that each of the first four terms (independent terms) is composed of a constant term plus terms which change with the angle θ . Therefore, these are inherent lamina properties which are only dependent on the material being used and do not change with orientation of the lamina. This “invariant” concept is very useful in design with composite materials.

2.3 Finite Element Formulation using Classical Plate Theory

Numerical methods, such as the finite element method, are necessary in practical applications as they are able to model general geometries, boundary conditions, loading and materials. In this section, the derived expressions needed for the evaluation of the in-plane stiffness and mass matrices of the *isoparametric* four-node rectangular element shown in Fig. 2.3 , and the plate bending stiffness and mass matrices of the Melosh-Zienkiewicz-Cheung (*MZC*) nonconforming four- node rectangular element shown in Fig. 2.4.

2.3.1 In-plane formulation

Isoparametric finite elements are used for the in-plane extensional response. The element displacements are interpolated as

$$q_x = N_1 q_{x1} + N_2 q_{x2} + N_3 q_{x3} + N_4 q_{x4} \tag{2.9}$$

$$q_y = N_1 q_{y1} + N_2 q_{y2} + N_3 q_{y3} + N_4 q_{y4} \tag{2.10}$$

where q_x and q_y are the local element displacements at any point of the element, and q_{xi} and q_{yi} , ($i = 1, \dots, 4$), are the corresponding element displacement at the element nodes. The interpolation functions N'_i are defined in the natural coordinate system of the element, which has variables ξ and η that each vary from -1 to +1. The fundamental property of the interpolation function N'_i is that its value in the natural coordinates is unity at node i and is zero at all other nodes. Using these conditions the functions N'_i corresponding to a specific nodal point layout could be solved for in a systematic manner.

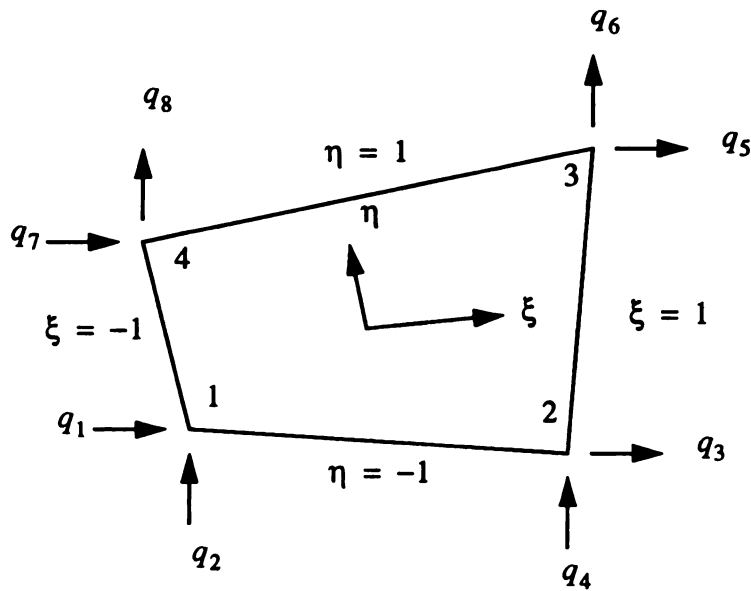


Figure 2.3 Nodal displacements for isoparametric plane stress element

As shown in Figure 2.3 the nodal displacements are:

$$\{q'_e\} = \{q_{xi}, q_{yi}\} \quad (i = 1, 2, 3, 4)$$

the in-plane displacements at the reference plane of a laminated composite plate can be expressed as

$$\begin{Bmatrix} q_x(\zeta, \eta) \\ q_y(\zeta, \eta) \end{Bmatrix} = \begin{bmatrix} N'_1 & 0 & N'_2 & 0 & N'_3 & 0 & N'_4 & 0 \\ 0 & N'_1 & 0 & N'_2 & 0 & N'_3 & 0 & N'_4 \end{bmatrix} \{q'_e\}$$

in which $\{q'_e\}$ is a vector of eight element nodal displacements, and N'_i are the interpolation functions:

$$N'_1(\xi, \eta) = \frac{1}{4}(1-\xi)(1-\eta) \quad (2.11)$$

$$N'_2(\xi, \eta) = \frac{1}{4}(1+\xi)(1-\eta) \quad (2.12)$$

$$N'_3(\xi, \eta) = \frac{1}{4}(1+\xi)(1+\eta) \quad (2.13)$$

$$N'_4(\xi, \eta) = \frac{1}{4}(1-\xi)(1+\eta) \quad (2.14)$$

The strain field within the element may be expressed as

$$\{\varepsilon\} = [B'] \{q'_e\} \quad (2.15)$$

where the strain-displacement matrix is given by

$$[B'] = \begin{bmatrix} \frac{\partial}{\partial x} & 0 \\ 0 & \frac{\partial}{\partial y} \\ \frac{\partial}{\partial y} & \frac{\partial}{\partial x} \end{bmatrix} [N'] = \begin{bmatrix} \frac{1}{a} \frac{\partial}{\partial \xi} & 0 \\ 0 & \frac{1}{b} \frac{\partial}{\partial \eta} \\ \frac{1}{b} \frac{\partial}{\partial \eta} & \frac{1}{a} \frac{\partial}{\partial \xi} \end{bmatrix} [N'] = \begin{bmatrix} N'_{i,x} & 0 \\ 0 & N'_{i,y} \\ N'_{i,y} & N'_{i,x} \end{bmatrix} \quad (2.16)$$

where $N'_{i,x}$ and $N'_{i,y}$ represent partial derivatives of N'_i with respect to x and y .

$$N'_{i,x} = \frac{\partial N'_i}{\partial x} = \frac{1}{a} N'_{i,\xi} \quad (i = 1, 2, 3, 4) \quad (2.17)$$

$$N'_{i,y} = \frac{\partial N'_i}{\partial y} = \frac{1}{b} N'_{i,\eta} \quad (i = 1, 2, 3, 4) \quad (2.18)$$

or more explicitly,

$$\begin{aligned} N_{1,x} &= -\frac{1}{4a}(1-\eta) & N_{1,y} &= -\frac{1}{4b}(1-\xi) \\ N_{2,x} &= \frac{1}{4a}(1-\eta) & N_{2,y} &= -\frac{1}{4b}(1+\xi) \\ N_{3,x} &= \frac{1}{4a}(1+\eta) & N_{3,y} &= \frac{1}{4b}(1+\xi) \\ N_{4,x} &= -\frac{1}{4a}(1+\eta) & N_{4,y} &= \frac{1}{4b}(1-\xi) \end{aligned}$$

2.3.2 Out-of-plane formulation

Consider the plate-bending element in Fig. 2.4. It was originally developed by Melosh, Zienkiewicz and Cheung (Melosh 1963, Zienkiewicz and Cheung 1964). As with other elements of this type, it has only one displacement in the z-direction.

This element is said to be nonconforming because it does not have normal-slope compatibility at the edges. There are some practical reasons for considering nonconforming plate-bending elements. General-purpose structural analysis programs usually permit six

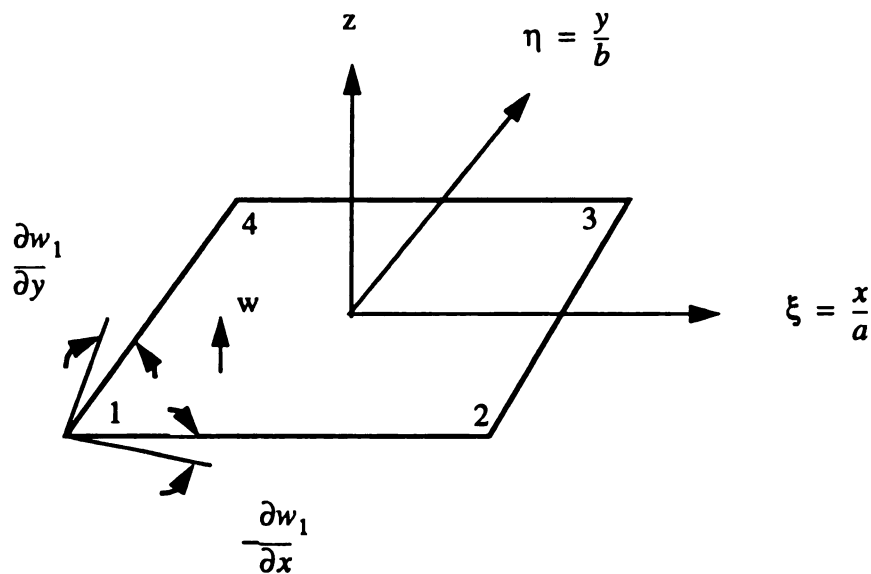


Figure 2.4 Nodal displacements for rectangular plate-bending element

nodal degrees of freedom, three displacements and three rotations. Compatible elements (C^1 elements) are capable of preserving interelement continuity of the field and its first derivatives at the nodes, but not interelement continuity of all second derivatives of the field. Such elements possess an additional nodal degree of freedom (i.e. $\frac{\partial^2 w}{\partial x \partial y}$) which does not fit well into a typical general-purpose program. On the other hand, several incompatible plate elements exist with only nodal displacements and rotations as degree of freedom. These elements fit well into general-purpose computer codes and permit the analysis of a variety of general structures. Such elements are particularly appealing because they can be used with plane stress elements to model plates and shells.

The displacement function chosen for this element is a complete cubic of ten terms plus two quadratic terms.

$$w = c_1 + c_2\xi + c_3\eta + c_4\xi^2 + c_5\xi\eta + c_6\eta^2 + c_7\xi^3 + c_8\xi^2\eta + c_9\xi\eta^2 + c_{10}\eta^3 + c_{11}\xi^3\eta + c_{12}\xi\eta^3 \quad (2.19)$$

Since the element does not preserve normal slope continuity between adjacent elements boundaries, it violates one of the conditions for convergence to the exact solution with a refined mesh. Convergence, however, has been proved by Walz, Fulton and Cyrus (1968), and numerical results obtained by Zeinkiewicz (1977) demonstrate the convergence rates and accuracy for both displacements and bending moments. It should be mentioned that rectangular elements are the most straight forward type of plate-bending elements. Triangular and quadrilateral elements are more versatile for general structural analysis. Zienkiewicz presents an excellent discussion of other plate-bending element formulations and types.

The displacement shape functions for the above element can be expressed as follows

$$N''_{ii} = \frac{1}{8} (1 + \xi_0) (1 + \eta_0) (2 + \xi_0 + \eta_0 - \xi^2 - \eta^2) \quad (2.20)$$

$$N''_{i2} = -\frac{1}{8}b\eta_i(1 + \xi_0)(1 - \eta_0)(1 + \eta_0)^2 \quad (2.21)$$

$$N''_{i3} = \frac{1}{8}a\xi_i(1 - \xi_0)(1 + \eta_0)(1 + \xi_0) \quad (2.22)$$

where $\xi_0 = \xi_i\xi$ and $\eta_0 = \eta_i\eta$ ($i = 1, 2, 3, 4$)

The curvatures at any point within the element are given by

$$\begin{Bmatrix} \kappa_x \\ \kappa_y \\ \kappa_{xy} \end{Bmatrix} = \nabla^2 [N''] \{q''_e\} = [B''] \{q''_e\} \quad (2.23)$$

where the generalized strain-displacement matrix $[B'']$ is

$$[B''_i] = \left\{ \frac{\partial^2}{\partial x^2} \quad \frac{\partial^2}{\partial y^2} \quad 2\frac{\partial^2}{\partial x\partial y} \right\} [N''_i] = \begin{bmatrix} N''_{i1,xx} & N''_{i2,xx} & N''_{i3,xx} \\ N''_{i1,yy} & N''_{i2,yy} & N''_{i3,yy} \\ 2N''_{i1,xy} & 2N''_{i2,xy} & 2N''_{i3,xy} \end{bmatrix} \quad (2.24)$$

The elements of $[B''_i]$ are:

$$N''_{i1,xx} = \frac{1}{4a^2}(1 + \eta_i\eta)(\xi^2 - 3\xi_i\xi - 1) \quad (2.25)$$

$$N''_{i2,xx} = 0 \quad (2.26)$$

$$N''_{i3,xx} = -\frac{1}{4a}\xi_i^3(1 + \eta_i\eta)(1 + 3\xi_i\xi) \quad (2.27)$$

$$N''_{i1,yy} = \frac{1}{4b^2}(1 + \xi_i\xi)(\eta_i^2 - 3\eta_i\eta - 1) \quad (2.28)$$

$$N''_{i2,yy} = -\frac{1}{8}\eta_i^2(1 + \xi_i\xi)(1 + \eta_i\eta)(1 - \eta_i^2\eta^2) \quad (2.29)$$

$$N''_{i3,yy} = 0 \quad (2.30)$$

$$2N''_{i1,xy} = \frac{1}{4ab}[\eta_i\xi_i(4 - 3\xi^2 - 3\eta^2) + 2\xi_i\eta_i(\xi_i\xi + \eta_i\eta) - 2(\xi\eta_i + \eta\xi_i)] \quad (2.31)$$

$$2N''_{i2,xy} = -\frac{1}{4a}\eta_i^2\xi_i(1+\eta_i\eta)(1-3\eta_i\eta) \quad (2.32)$$

$$2N''_{i3,xy} = \frac{1}{4b}\xi_i^2\eta_i(1+\xi_i\xi)(1-3\xi_i\xi) \quad (2.33)$$

The full out-of-plane strain-displacement matrix $[B'']$ can be written as

$$[B''] = \frac{1}{4a^2b^2} [[B''_1] [B''_2] [B''_3] [B''_4]]_{3 \times 12} \quad (2.34)$$

where

$$[B''_1] = \begin{bmatrix} 3\xi(1-\eta)b^2 & 0 & (1-3\xi)(1-\eta)ab^2 \\ 3\eta(1-\xi)a^2 & -(1-\xi)(1-3\eta)a^2b & 0 \\ (4-3\xi^2-3\eta^2)ab & -(1-\eta)(1+3\eta)ab^2 & -(1-\xi)(1+3\xi)a^2b \end{bmatrix}$$

$$[B''_2] = \begin{bmatrix} -3(1-\eta)\xi b^2 & 0 & -(1-\eta)(1+3\xi)ab^2 \\ 3\eta(1+\xi)a^2 & -(1+\xi)(1-3\eta)a^2b & 0 \\ -(4-3\xi^2-3\eta^2)ab & -(1-\eta)(1+3\eta)ab^2 & -(1+\xi)(1-3\xi)a^2b \end{bmatrix}$$

$$[B''_3] = \begin{bmatrix} -3\xi(1+\eta)b^2 & 0 & (1+\eta)(1+3\xi)ab^2 \\ -3\eta(1+\xi)a^2 & (1+\xi)(1+3\eta)a^2b & 0 \\ (4-3\xi^2-3\eta^2)ab & -(1+\eta)(1-3\eta)ab^2 & (1+\xi)(1-3\xi)a^2b \end{bmatrix}$$

$$[B''_4] = \begin{bmatrix} 3\xi(1+\eta)b^2 & 0 & (1+\eta)(1-3\xi)ab^2 \\ -3\eta(1-\xi)a^2 & (1-\xi)(1+3\eta)a^2b & 0 \\ -(4-3\xi^2-3\eta^2)ab & (1+\eta)(1-3\eta)ab^2 & (1-\xi)(1+3\xi)a^2b \end{bmatrix}$$

2.3.3 Formulation of the linear elemental stiffness matrix $[K_e]$

Composite laminates are constructed by bonding two or more laminae. Laminate deformations are assumed to be small with respect to the laminate thickness. Using the theory of thin laminates, strains are considered to vary linearly through the thickness and interlaminar deformations may be considered small at interior regions.

For combined in-plane and out-of-plane behavior, assuming plane section remain plane after bending, the strain at any point in the plate is

$$\{\varepsilon\} = \{\varepsilon^0\} + z\{\kappa\} = [[B'] + z[B'']] \{q_e\} = [B] \{q_e\} \quad (2.35)$$

The strain in material coordinates is

$$\{\varepsilon'\} = [T]^{-T}[B] \{q_e\} = [T]^{-T} [[B'] + z[B'']] \{q_e\} \quad (2.36)$$

The shear strain in material coordinates (i.e., the third element of $\{\varepsilon'\}$ is

$$\gamma'_{12} = [T_3] [B] \{q_e\} = [T_3] [[B'] + z[B'']] \{q_e\} \quad (2.37)$$

in which $[T_3]$ is the third row of $[T]^{-T}$

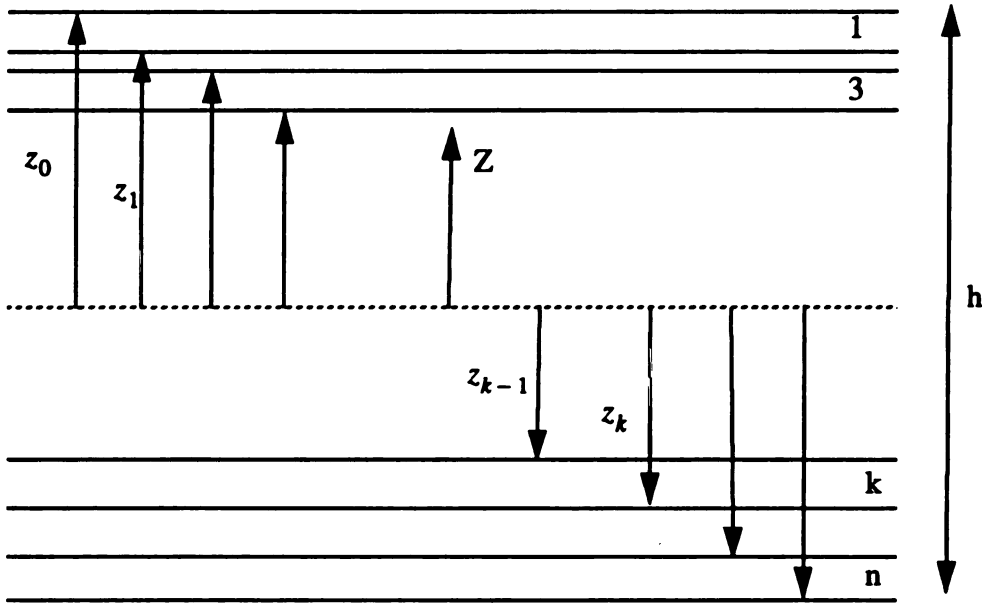


Figure 2.5 Layer nomenclature for laminate

As has been described previously, the plate element used in the formulation has 20 DOF: three displacements and two rotations at each of the four nodes..

The linear elemental stiffness matrix of a laminated plate with N laminae is

$$\begin{aligned}
[K_e] &= \int_V [B]^T [\bar{Q}] [B] dV \\
&= \sum_{k=1}^N \int_{-1}^1 \int_{-1}^1 \int_{z_{k-1}}^{z_k} [[B']^T + z[B'']^T] [\bar{Q}] [[B'] + z[B'']] dx dy dz \quad (2.38) \\
&= \sum_{k=1}^N \int_{-1}^1 \int_{-1}^1 \int_{z_{k-1}}^{z_k} [[B']^T + z[B'']^T] [\bar{Q}] [[B'] + z[B'']] |J| d\xi d\eta dz
\end{aligned}$$

where N is the number of laminae, z_k is the height from the reference plane to the bottom of the k th lamina (z_0 being the height to the top surface of the laminate as shown in figure 2.4), and $|J| = \frac{\partial}{\partial(\xi, \eta)}(x, y)$ is the determinant of the jacobian matrix for transformation from the x - y coordinate system to the ξ - η system. The integral with respect to z in Eq. 2.39 may be performed in closed-form, and the double integral with respect to ξ and η is normally computed by numerical Gauss integration. Expanding Eq. 2.38 the elemental stiffness matrix can be written as

$$[K_e] = \sum_{k=1}^N [[K'_e] + [K''_e] + [K'''_e] + [K''''_e]] \quad (2.39)$$

in which

$$[K'_e] = (z_k - z_{k-1}) \int_{-1}^1 \int_{-1}^1 [B']^T [\bar{Q}] [B'] |J| d\xi d\eta \quad (2.40)$$

$$[K''_e] = \frac{z_k^2 - z_{k-1}^2}{2} \int_{-1}^1 \int_{-1}^1 [B']^T [\bar{Q}] [B''] |J| d\xi d\eta \quad (2.41)$$

$$[K'''_e] = \frac{z_k^3 - z_{k-1}^3}{2} \int_{-1}^1 \int_{-1}^1 [B'']^T [\bar{Q}] [B'] |J| d\xi d\eta \quad (2.42)$$

$$[K''''_e] = \frac{z_k^3 - z_{k-1}^3}{3} \int_{-1}^1 \int_{-1}^1 [B'']^T [\bar{Q}] [B''] |J| d\xi d\eta \quad (2.43)$$

The Jacobian matrix $[J]$ is

$$[J] = \begin{bmatrix} \frac{\partial x}{\partial \xi} & \frac{\partial y}{\partial \xi} \\ \frac{\partial x}{\partial \eta} & \frac{\partial y}{\partial \eta} \end{bmatrix} = \begin{bmatrix} a & 0 \\ 0 & b \end{bmatrix} \quad (2.44)$$

2.3.4 Formulation of the elemental consistent mass matrix

The consistent mass matrix for the plate element is

$$\begin{aligned} [M_e] &= \int_V \rho N^T N dv \\ &= \sum_{k=1}^N \int_{00z_{k-1}}^{ab z_k} \int \int \rho [[N']^T + z[N'']^T] [[N'] + z[N'']] dx dy dz \\ &= \sum_{k=1}^N \int_{-1-1}^{1 1} \int_{-1-1}^{1 1} \int \rho [[N']^T + z[N'']^T] [[N'] + z[N'']] |J| d\xi d\eta dz \end{aligned} \quad (2.45)$$

Performing the integral with respect to z analytically, the elemental mass can be expressed as

$$[M_e] = \sum_{k=1}^N [[M'_e] + [M''_e] + [M'''_e] + [M''''_e]] \quad (2.46)$$

in which

$$[M'_e] = (z_k - z_{k-1}) \int_{-1-1}^{1 1} \int [N']^T [\bar{Q}] [N'] |J| d\xi d\eta \quad (2.47)$$

$$[M''_e] = \frac{z_k^2 - z_{k-1}^2}{2} \int_{-1-1}^{1 1} \int [N']^T [\bar{Q}] [N''] |J| d\xi d\eta \quad (2.48)$$

$$[M'''_e] = \frac{z_k^2 - z_{k-1}^2}{2} \int_{-1-1}^{1 1} \int [N'']^T [\bar{Q}] [N'] |J| d\xi d\eta \quad (2.49)$$

$$[M''''_e] = \frac{z_k^3 - z_{k-1}^3}{3} \int_{-1}^1 \int_{-1}^1 [N'']^T [\bar{Q}] [N''] |J| d\xi d\eta \quad (2.50)$$

2.3.5 Numerical Integration

In the integration of finite element matrices, a subroutine is called to evaluate the unknown function Φ given in Eq. 2.52 at given points, and these points may be anywhere on the element. A very important numerical integration procedure in which both the positions of the sampling points and the weights have been optimized is Gauss quadrature. Hence, for the two dimensional plate bending problem we have

$$\int_{-1}^1 \int_{-1}^1 \Phi(\xi, \eta) d\xi d\eta \approx \sum_{i,j} W_i W_j \Phi(\xi_i, \eta_j) \quad (2.51)$$

where W_i and W_j are the integration weights. The above mentioned scheme is directly applicable to the evaluation of matrices of rectangular elements in which all integration limits are -1 to +1.

The order of numerical integration to be used in the evaluation of stiffness and mass integrals depend on the degree of precision that the order of the numerical Gauss integration must satisfy. Since the shape functions have up to fifth order terms, we must satisfy the condition $2n - 1 \geq 5$. Therefore, the order of integration is taken to be $n = 3 \times 3$.

3. Equivalent Linearization

3.1 Introduction

Random vibration analysis of mechanical systems has become an important subject in recent years for various engineering applications. Forces due to earthquakes, turbulence in air or water, storm waves, and the forces experienced by a vehicle traversing rough terrain are examples where an understanding of random vibration theory is essential to the successful design of the structure. Composite materials used in high speed flight vehicles are usually exposed to fluctuating loads caused by the flow of turbulent air or rocket engines.

A common feature of such problems is that the excitation is often so complex that it can be described only statistically. In addition, most physical systems behave in a linear manner only for a limited range of the excitations, and since under random excitation larger responses can be expected, at least occasionally, it is often necessary to study nonlinear responses due to random excitations.

Exact solution of non-linear random vibration problems is possible only for simple systems. For realistic engineering problems an approximate method must be used.

One of the most widely used approximation techniques for nonlinear random vibration problems is equivalent linearization (or statistical linearization) in which the original nonlinear system is replaced by an effective linear system. This approach has proved quite useful for a broad range of engineering problems. Other methods such as Gaussian closure and energy balance are closely related and generally give similar response results as equivalent linearization while approaches such as the perturbation method may give somewhat different results.

The essence of the method of equivalent linearization is to replace a given non-linear system by a linear system in such a way that the difference between the two systems is min-

imized for all possible solutions of the associated linear system. The solution of the linear system is then taken as an approximate solution of the original nonlinear system. The minimization of the difference in the equations of motion with respect to the linear system parameters does not necessarily guarantee that a minimization of the difference in the corresponding solutions will be achieved. It has been shown that the method of equivalent linearization gives good results even for strong nonlinearities.

3.2 Formulation

Consider the response to external load of a nonlinear multi-DOF vibratory system: Generally, The dynamic equations of motion of a composite plate discretized into finite elements may be written as

$$[M] \{\ddot{q}\} + [C] \{\dot{q}\} + [K] \{q\} + \phi(q, \dot{q}, \ddot{q}) = \{Q(t)\} \quad (3.1)$$

in which $[M]$ is the consistent or lumped mass matrix obtained by assembling the element mass matrices, $[C]$ is the damping matrix (usually specified indirectly through modal damping ratios), $[K]$ is the linear stiffness matrix obtained by assembling the linear element stiffness matrices, $\{\phi\}$ is a vector of nonlinear terms obtained by assembling the element load vectors $\{\phi_e\}$, $\{q\}$, $\{\dot{q}\}$, and $\{\ddot{q}\}$ are the displacement, velocity and acceleration vectors and $\{Q(t)\}$ is an excitation vector. It is assumed in this study that $\{Q(t)\}$ is a zero mean Gaussian vector random process.

In the case when $\phi(q, \dot{q}, \ddot{q})$ is non-zero and nonlinear, attention is directed toward techniques of approximate analysis. Equivalent linearization offers a systematic and readily automated method for generating an approximate solution of Eq. 3.1.

In the process of obtaining an approximate solution of Eq. 3.1, let us consider an auxiliary (equivalent) system which is described by a linear differential equation of the form

$$([M] + [M_e]) \{\ddot{q}\} + ([C] + [C_e]) \{\dot{q}\} + ([K] + [K_e]) \{q\} = \{Q(t)\} \quad (3.2)$$

where $[M_e]$, $[C_e]$, and $[K_e]$ are deterministic mass, damping and stiffness matrices.

The difference $\{\delta\}$ between Eq. 3.1 and 3.2 may be written as (Spanos, 1976; Spanos and Iwan, 1978)

$$\begin{aligned}\{\delta\} &= M\ddot{q} + C\dot{q} + Kq + \phi - (M + M_e)\ddot{q} + -(C + C_e)\dot{q} - (K + K_e)q \\ &= \phi(q, \dot{q}, \ddot{q}) - M_e\ddot{q} - C_e\dot{q} - K_eq\end{aligned}\quad (3.3)$$

In order to determine the matrices $[M_e]$, $[C_e]$ and $[K_e]$ of the equivalent linear system it is necessary to establish a criterion for the minimization of $\{\delta\}$, based on a suitable norm of this vector. Here the Euclidean norm defined as

$$\|\{\delta\}\|_2^2 = \{\delta\}^T \{\delta\} \quad (3.4)$$

will be used as a measure of $\{\delta\}$.

The minimization of δ is performed according to the criterion

$$E[\{\delta\}^T \{\delta\}] = E\{\delta_1^2 + \delta_2^2 + \dots + \delta_n^2\} = \text{minimum} \quad (3.5)$$

where $\delta_1, \delta_2, \dots, \delta_n$ are the elements of δ .

Using the linearity of the expectation operator $E[\]$, Eq 3.5 can be written as

$$\sum_{i=1}^n D_i^2 = \text{minimum} \quad (3.6)$$

where $i = 1, 2, 3, \dots, n$ and D_i is defined by

$$D_i^2 = E\{\delta_i^2\} = E\left[\left[\phi_i - \sum_{j=1}^n (m_{ij}^e \ddot{q}_j + c_{ij}^e \dot{q}_j + k_{ij}^e q_j)\right]^2\right] \quad (3.7)$$

Minimization is with respect to the class of functions of t which are solutions of Eq. 3.2.

The necessary conditions for Eq. 3.7 to be true are

$$\frac{\partial}{\partial m_{ij}^e} E[\{\delta\}^T \{\delta\}] = \frac{\partial}{\partial m_{ij}^e} (D_i^2) = 0 \quad (3.8)$$

$$\frac{\partial}{\partial c_{ij}^e} E[\{\delta\}^T \{\delta\}] = \frac{\partial}{\partial c_{ij}^e} (D_i^2) = 0 \quad (3.9)$$

$$\frac{\partial}{\partial k_{ij}^e} E[\{\delta\}^T \{\delta\}] = \frac{\partial}{\partial k_{ij}^e} (D_i^2) = 0 \quad (3.10)$$

where m_{ij}^e , c_{ij}^e and k_{ij}^e are the (i, j) elements of the matrices $[M_e]$, $[C_e]$ and $[K_e]$, respectively.

The expansion of Eqs. 3.8, 3.9 and 3.10 gives the following

$$E\{\phi_i \hat{q}\} = E\{\hat{q} \hat{q}^T\} \begin{bmatrix} [K_i^*]^T \\ [C_i^*]^T \\ [M_i^*]^T \end{bmatrix} \quad (3.11)$$

where $[M_i^*]$, $[C_i^*]$ and $[K_i^*]$ are the i th rows of the matrices M_e , C_e and K_e , respectively, and

$$\{\hat{q}\} = [q, \dot{q}, \ddot{q}]^T \quad (3.12)$$

So far the method of statistical linearization has been presented irrespective of the particular probability density which is used in computing the expectations appearing in Eq. 3. 11. The formulation is facilitated by assuming that the excitation of the original nonlinear system is Gaussian. Therefore, the response of the equivalent linear system to this excitation is also Gaussian. Utilizing Kazakov's formula (1965) for Gaussian random vectors:

$$E\{f(\eta) \eta\} = E\{\eta \eta^T\} E\{\nabla f(\eta)\} \quad (3.13)$$

we obtain

$$E[\phi_i\{\hat{q}\}] = E[\{\hat{q}\}\{\hat{q}\}^T] E \left\{ \begin{array}{c} \frac{\partial \phi_i}{\partial \{q\}} \\ \frac{\partial \phi_i}{\partial \{\dot{q}\}} \\ \frac{\partial \phi_i}{\partial \{\ddot{q}\}} \end{array} \right\} \quad (3.14)$$

Comparison of Eqs. 3.11 and 3.14 shows that the elements of the matrices $[M^*]$, $[C^*]$ and $[K^*]$ are given by the simple expressions

$$m^*_{ij} = E \left\{ \frac{\partial \phi_i}{\partial \{\ddot{q}_j\}} \right\} \quad (3.15)$$

$$c^*_{ij} = E \left\{ \frac{\partial \phi_i}{\partial \{\dot{q}_j\}} \right\} \quad (3.16)$$

$$k^*_{ij} = E \left\{ \frac{\partial \phi_i}{\partial \{q_j\}} \right\} \quad (3.17)$$

These results are due to Kazakov (1965). They were first used for stationary nonlinear random vibration analysis by Atalik and Utku (1976). Subsequently, Spanos (1978, 1980) pointed out that they are also applicable for non-stationary problems.

For the laminated composite plate, the nonlinear force vector is only a function of the generalized displacement coordinate q . Thus the nonlinearity will affect only the stiffness matrix and consequently, $[C^*] = [M^*] = [0]$.

3.3 Derivation of the Nonlinear Elemental Stiffness Matrices

Consider virtual displacements $\{\delta q_e\}$. The elemental virtual work done is

$$\delta W = \{\delta q_e\}^T \{R_e\}$$

where $\{R_e\}$ are the nodal loads on the element. The internal virtual work is

$$\delta U = \int_V \{\delta \epsilon\}^T \{\sigma\} dV$$

setting $\delta W = \delta U$ and using the strain displacement relations

$$\{\delta \epsilon\}^T = \{\delta q_e\}^T [B]^T$$

and the constitutive law in Eq.2.5 yields

$$\begin{aligned} \{\delta q_e\}^T \{R_e\} &= \int_V \{\delta q_e\}^T [B]^T \{ [\bar{Q}] \{\epsilon\} + f(\gamma_{12}) [T^*] \{\epsilon\} \} dV \\ &= \{\delta q_e\}^T \left[\int_V [B]^T [\bar{Q}] \{\epsilon\} dV + \int_V [B]^T f(\gamma_{12}) [T^*] \{\epsilon\} dV \right] \end{aligned} \quad (3.18)$$

since Eq. 3.18 must hold for any arbitrary virtual displacements $\{\delta q_e\}^T$, the following equation must hold:

$$\begin{aligned} \{R_e\} &= \left[\int_V [B]^T \{ [\bar{Q}] [B] dV \right] \{q_e\} + \int_V [B]^T f(\gamma_{12}) [T^*] [B] \{q_e\} dV \\ &= [K_e] \{q_e\} + \{\phi_e\} \end{aligned} \quad (3.19)$$

where $[K_e]$ is the elemental stiffness matrix given in Eq. 2.39 and

$$\begin{aligned} \{\phi_e\} &= \int_V [B]^T f(\gamma_{12}) [T^*] [B] \{q_e\} dV \\ &= \sum_{k=100z_{k-1}}^N \iiint f(\gamma_{12}) [B]^T [T^*] [B] \{q_e\} dx dy dz \end{aligned} \quad (3.20)$$

is the elemental vector of nonlinear terms.

For the functional form of $f(\gamma_{12})$ given by

$$f(\gamma_{12}) = \sum_{i=1}^n a_i \gamma_{12}^{2i} \quad (3.21)$$

the nonlinear vector in the above equation may be written as

$$\{\phi_e\} = \sum_{i=1}^n \{\phi_{e,i}\} \quad (3.22)$$

in which

$$[\phi_e] = \sum_{k=1}^N \sum_{i=1}^n a_i \int_{i00z_{k-1}}^{ab z_k} \gamma_{12}^{2i} [B]^T [T^*] [B] \{q_e\} dx dy dz \quad (3.23)$$

Since the nonlinear vector ϕ is a function of the displacement vector $\{q\}$ only, the nonlinearity will affect only the stiffness matrix. Hence, $c^* = m^* = 0$. The resulting equivalent stiffness matrix can be written as

$$[K^*_e] = E \left[\frac{\partial}{\partial \{q_e\}} \{\phi_e\} \right] = \sum_{k=1}^N \sum_{i=1}^n a_i \int_{-1-1z_{k-1}}^{1 1 z_k} [B]^T [T^*] [B] [A] |J| d\xi d\eta dz \quad (3.24)$$

and requires the evaluation of

$$[A] = E \left[\frac{\partial}{\partial \{q_e\}} \gamma_{12}^{2i} \{q_e\} \right] \quad (3.25)$$

The partial derivative is

$$\frac{\partial}{\partial \{q_e\}} \gamma_{12}^{2i} \{q_e\} = \gamma_{12}^{2i} [I] + 2i \{q_e\} \gamma_{12}^{2i-1} \frac{\partial \gamma_{12}}{\partial \{q_e\}} \quad (3.26)$$

and since $\gamma_{12} = [T_3] [B] \{q_e\}$, Eq. 3.25 becomes

$$[A] = E \{ ([T_3] [B] \{q_e\})^{2i} [I] + 2i \{q_e\} ([T_3] [B] \{q_e\})^{2i-1} [T_3] [B] \} \quad (3.27)$$

Consider the first term of the above equation

$$\begin{aligned} E ([T_3] [B] \{u_e\})^{2i} &= ([T_3] [[B'] + z[B'']] \{q_e\})^{2i} \\ &= ([T_3] [[B'] \{q_e\} + z[T_3] [B'']] \{q_e\})^{2i} \end{aligned} \quad (3.28)$$

Using the Binomial expansion

$$(a + bz)^{2i} = \sum_{l=0}^{2i} \binom{2i}{l} a^{2i-l} b^l z^l \quad (3.29)$$

Eq. 3.28 may be expanded as

$$\begin{aligned} E([T_3] [B] \{q_e\})^{2i} &= \sum_{l=0}^{2i} \binom{2i}{l} ([T_3] [B'] \{q_e\})^{2i-l} ([T_3] [B''] \{q_e\})^l z^l \\ &= \sum_{l=0}^{2i} E \left[\binom{2i}{l} \left(\sum_{j'=1}^3 \sum_{k'=1}^{20} T_{3j'} B'_{j'k'} q_{e,k'} \right)^{2i-l} \right. \\ &\quad \left. \times \left(\sum_{j''=1}^3 \sum_{k''=1}^{20} T_{3j''} B''_{j''k''} q_{e,k''} \right)^l \right] \end{aligned} \quad (3.30)$$

or in condensed form

$$E([T_3] [B] \{q_e\})^{2i} = \sum_{l=0}^{2i} \alpha_l z^l \quad (3.31)$$

where α_l is given by

$$\begin{aligned} \alpha_l &= \sum_{j_1=1}^3 \sum_{k_1=1}^{20} \sum_{j_2=1}^3 \sum_{k_2=1}^{20} \dots \sum_{j_{2i}=1}^3 \sum_{k_{2i}=1}^{20} E[q_{e,k_1} q_{e,k_2} q_{e,k_3} \dots q_{e,k_{2i}}] \\ &\quad \times \binom{2i}{l} \left(\prod_{m=1}^{2i} T_{3j_m} \right) \left(\prod_{m=1}^{2i-l} B'_{j_m k_m} \right) \left(\prod_{m=2i-l+1}^{2i} B''_{j_m k} \right) \end{aligned} \quad (3.32)$$

For the case where $i=2$, which corresponds to a fifth order approximation to $f(\gamma_{12})$, the expanded form of Eq. 3.31 is

$$\begin{aligned}
\sum_{l=0}^{2i} \alpha_l z^l &= \sum_{j_1=1}^3 \sum_{k_1=1}^{20} \sum_{j_2=1}^3 \sum_{k_2=1}^{20} \sum_{j_3=1}^3 \sum_{k_3=1}^{20} \sum_{j_4=1}^3 \sum_{k_4=1}^{20} T_{3j_1} B'_{j_1 k_1} T_{3j_2} B'_{j_2 k_2} T_{3j_3} B'_{j_3 k_3} T_{3j_4} B'_{j_4 k_4} \\
&\quad \times E[q_{e,k_1} q_{e,k_2} q_{e,k_3} q_{e,k_4}] \\
&+ 4z \sum_{j_1=1}^3 \sum_{k_1=1}^{20} \sum_{j_2=1}^3 \sum_{k_2=1}^{20} \sum_{j_3=1}^3 \sum_{k_3=1}^{20} \sum_{j_4=1}^3 \sum_{k_4=1}^{20} T_{3j_1} B'_{j_1 k_1} T_{3j_2} B'_{j_2 k_2} T_{3j_3} B'_{j_3 k_3} T_{3j_4} B''_{j_4 k_4} \\
&\quad \times E[q_{e,k_1} q_{e,k_2} q_{e,k_3} q_{e,k_4}] \\
&+ 6z^2 \sum_{j_1=1}^3 \sum_{k_1=1}^{20} \sum_{j_2=1}^3 \sum_{k_2=1}^{20} \sum_{j_3=1}^3 \sum_{k_3=1}^{20} \sum_{j_4=1}^3 \sum_{k_4=1}^{20} T_{3j_1} B'_{j_1 k_1} T_{3j_2} B'_{j_2 k_2} T_{3j_3} B''_{j_3 k_3} T_{3j_4} B''_{j_4 k_4} \\
&\quad \times E[q_{e,k_1} q_{e,k_2} q_{e,k_3} q_{e,k_4}] \\
&+ 4z^3 \sum_{j_1=1}^3 \sum_{k_1=1}^{20} \sum_{j_2=1}^3 \sum_{k_2=1}^{20} \sum_{j_3=1}^3 \sum_{k_3=1}^{20} \sum_{j_4=1}^3 \sum_{k_4=1}^{20} T_{3j_1} B'_{j_1 k_1} T_{3j_2} B''_{j_2 k_2} T_{3j_3} B''_{j_3 k_3} T_{3j_4} B''_{j_4 k_4} \\
&\quad \times E[q_{e,k_1} q_{e,k_2} q_{e,k_3} q_{e,k_4}] \\
&+ z^4 \sum_{j_1=1}^3 \sum_{k_1=1}^{20} \sum_{j_2=1}^3 \sum_{k_2=1}^{20} \sum_{j_3=1}^3 \sum_{k_3=1}^{20} \sum_{j_4=1}^3 \sum_{k_4=1}^{20} T_{3j_1} B''_{j_1 k_1} T_{3j_2} B''_{j_2 k_2} T_{3j_3} B''_{j_3 k_3} T_{3j_4} B''_{j_4 k_4} \\
&\quad \times E[q_{e,k_1} q_{e,k_2} q_{e,k_3} q_{e,k_4}] \tag{3.33}
\end{aligned}$$

Now consider the second term in Eq. 3.25 which can be expressed as follows:

$$\begin{aligned}
&E[\{q_e\} ([T_3] [B]) \{q_e\}]^{2i-1} [T_3] [B] \\
&= E\{q_e\} \sum_{l=0}^{2i-1} \binom{2i-1}{l} ([T_3] [B'] \{q_e\})^{2i-1-l} ([T_3] [B''] \{q_e\})^l \\
&\quad \times [T_3] [[B'] z^l + [B''] z^{l+1}] \tag{3.34} \\
&= \sum_{l=0}^{2i-1} \{\beta_l\} [[B'] z^l + [B''] z^{l+1}]
\end{aligned}$$

where $\{\beta_l\}$ is given by

$$\{\beta_l\} = E\left(\{q_e\} \sum_{l=0}^{2i-1} \binom{2i-1}{l} ([T_3] [B'] \{q_e\})^{2i-1-l} ([T_3] [B''] \{q_e\})^l\right) \quad (3.35)$$

The p^{th} element of $\{\beta_l\}$ is

$$\begin{aligned} \beta_{l,p} = & \sum_{j_1=1}^3 \sum_{k_1=1}^{20} \sum_{j_2=1}^3 \sum_{k_2=1}^{20} \dots \sum_{j_{2i-1}=1}^3 \sum_{k_{2i-1}=1}^{20} E[q_{e,k_1} q_{e,k_2} q_{e,k_3} \dots q_{e,k_{2i-1}}] \\ & \times \binom{2i-1}{l} \left(\prod_{m=1}^{2i-1} T_{3j_m} \right) \left(\prod_{m=1}^{2i-1-l} B'_{j_m k_m} \right) \left(\prod_{m=2i-l}^{2i-1} B''_{j_m k} \right) \end{aligned} \quad (3.36)$$

where $\binom{2i}{l}$ indicates the binomial coefficient. The expectations in Eqs. 3.32 and 3.36 represent $2i$ th-order moments of the zero-mean Gaussian vector $\{q_e\}$. The higher-order even moments may be expressed in terms of the covariances as follows:

$$E[q_{e,k_1} q_{e,k_2} \dots q_{e,k_{2i}}] = \sum E[q_{e,k_1} q_{e,k_2}] E[q_{e,k_3} q_{e,k_4}] \dots E[q_{e,k_{2i-1}} q_{e,2i}] \quad (3.37)$$

in which the summation is taken over all possible ways of dividing the $2i$ variables into i combinations of pairs [the number of terms in the summation is $1.3.5\dots(2i-3)(2i-1)$].

The effort required to compute the α_l and $\beta_{l,p}$ coefficient by Eqs. 3.31 and 3.34 is substantial. However, a special algorithm described in chapter 4 that carefully takes into account the symmetries involved in the summations has been developed, and the computational effort has been reduced by a factor of more than 20.

Finally the equivalent stiffness matrix can be written as

$$[K^*]_e = \sum_{k=1}^N \sum_{i=1}^n a_i \int_{i-1}^1 \int_{1-z_{k-1}}^1 \int_{z_k} [B]^T [T^*] [B] [A] |J| d\xi d\eta dz \quad (3.38)$$

where $[A]$ is given by

$$[A] = \sum_{l=0}^{2i} \alpha_l z^l [I] + 2i \sum_{l=0}^{2i-1} \{\beta_l\} [T_3] [[B'] z^l + [B''] z^{l+1}] \quad (3.39)$$

Expanding $[B]^T [T^*] [B]$, $[K^*]$ can be split into

$$[K^*_e] = [K^{*'}_e] + [K^{''*}_e] + [K^{''''*}_e] \quad (3.40)$$

where

$$[K^{*'}_e] = \sum_{k=1}^N \sum_{i=1}^n a_i \int_{-1}^1 \int_{-1}^1 [B']^T [T^*] [B'] [A_1] |J| d\xi d\eta \quad (3.41)$$

$$[K^{''*}_e] = \sum_{k=1}^N \sum_{i=1}^n a_i \int_{-1}^1 \int_{-1}^1 [[B']^T [T^*] [B''] + [B'']^T [T^*] [B']] [A_2] |J| d\xi d\eta \quad (3.42)$$

$$[K^{''''*}_e] = \sum_{k=1}^N \sum_{i=1}^n a_i \int_{-1}^1 \int_{-1}^1 [B'']^T [T^*] [B''] [A_3] |J| d\xi d\eta \quad (3.43)$$

and $[A_1]$, $[A_2]$, and $[A_3]$ are

$$\begin{aligned} [A_1] &= \int_{z_{k-1}}^{z_k} [A] dz \\ &= \sum_{l=0}^{2i} \alpha_l \left(\frac{z_k^{l+1} - z_{k-1}^{l+1}}{l+1} \right) [I] \\ &\quad + 2i \sum_{l=0}^{2i-1} \{\beta_l\} [T_3] \left[[B'] \left(\frac{z_k^{l+1} - z_{k-1}^{l+1}}{l+1} \right) + [B''] \left(\frac{z_k^{l+2} - z_{k-1}^{l+2}}{l+2} \right) \right] \end{aligned} \quad (3.44)$$

$$\begin{aligned}
[A_2] &= \int_{z_{k-1}}^{z_k} z [A] dz \\
&= \sum_{l=0}^{2i} \alpha_l \left(\frac{z_k^{l+2} - z_{k-1}^{l+2}}{l+2} \right) [I]
\end{aligned} \tag{3.45}$$

$$+ 2i \sum_{l=0}^{2i-1} \{\beta_l\} [T_3] \left[[B'] \left(\frac{z_k^{l+2} - z_{k-1}^{l+2}}{l+2} \right) + [B''] \left(\frac{z_k^{l+3} - z_{k-1}^{l+3}}{l+3} \right) \right]$$

(3.46)

$$\begin{aligned}
[A_3] &= \int_{z_{k-1}}^{z_k} z^2 [A] dz \\
&= \sum_{l=0}^{2i} \alpha_l \left(\frac{z_k^{l+3} - z_{k-1}^{l+3}}{l+3} \right) [I]
\end{aligned} \tag{3.47}$$

$$+ 2i \sum_{l=0}^{2i-1} \{\beta_l\} [T_3] \left[[B'] \left(\frac{z_k^{l+3} - z_{k-1}^{l+3}}{l+3} \right) + [B''] \left(\frac{z_k^{l+4} - z_{k-1}^{l+4}}{l+4} \right) \right]$$

The general expression for $[A_q]$, $q = 1, 2, 3$ can be written concisely as

$$\begin{aligned}
[A_q] &= \int_{z_{k-1}}^{z_k} z^{q-1} [A] dz \\
&= \sum_{l=0}^{2i} \alpha_l \left(\frac{z_k^{l+q} - z_{k-1}^{l+q}}{l+q} \right) [I] \\
&\quad + 2i \sum_{l=0}^{2i-1} \{\beta_l\} [T_3] \left[[B'] \left(\frac{z_k^{l+q} - z_{k-1}^{l+q}}{l+q} \right) + [B''] \left(\frac{z_k^{l+q+1} - z_{k-1}^{l+q+1}}{l+q+1} \right) \right]
\end{aligned} \tag{3.48}$$

3.4 Random Vibration Analysis

Since computation of $[K_e^*]$ requires the mean and covariance of the displacement responses to be known, an iterative approach must be used, in which each iteration consists of a linear random vibration analysis. Linear random vibration analysis is well-known and is only summarized here. Time-domain or frequency-domain techniques can be used for the analysis, and the main steps using a frequency domain approach are as follows:

1. Using the stiffness matrix $[K_e] + [K_e^*]$ (with $[K_e^*] = [0]$ in the first iteration) and mass matrix $[M]$, determine the frequencies, ω_j , and mode shapes, $\{\psi_j\}$, for a chosen number of modes (say n modes).
2. Perform a linear random vibration analysis to determine the covariance matrix of the nodal displacements $\{u\}$. The rs th element of the covariance matrix is given by

$$E[q_r q_s] = \sum_{j=1}^n \sum_{k=1}^n \frac{\psi_{rj} \psi_{sk}}{M_j M_k} \sum_{l=1}^n \sum_{m=1}^n \psi_{lj} \psi_{mk} \int_{-\infty}^{\infty} H_j(-\omega) H_k(\omega) S_{lm}(\omega) d\omega \tag{3.49}$$

in which ψ_{rj} are elements of the mode shape matrix, $M_j = \{\psi_j\}^T [M] \{\psi_j\}$ is the j th modal mass, $H_j(\omega) = (\omega_j^2 - \omega + 2i\omega_j\omega)^{-1}$ is the j th modal frequency re-

sponse function, and $S_{lm}(\omega)$ is the cross spectral density function for the excitations P_l and P_m . Note that for synchronous loading only the auto spectra are non-zero, and the double summation over l and m may be reduced to a single summation. For certain classes of excitation spectra, closed form solutions can be used to rapidly compute the integrals in Eq. 3.49 (Harichandran 1992), while for more general cases numerical integration must be implemented.

3. Compute the equivalent element stiffness matrices $[K^*_e]$ from Eq. 3.40 through 3.47, and assemble the global equivalent stiffness matrix $[K^*]$.

The three steps outlined above are repeated until convergence is reached in the covariances of the nodal displacements. One method of checking for convergence is by using the nodal displacement variances, and the m th iteration is assumed to have converged if

$$\frac{\sqrt{\sum_i (\sigma_{q_r, m} - \sigma_{q_r, m-1})^2}}{\sqrt{\sum_i \sigma_{q_r, m}^2}} < \epsilon \quad (3.50)$$

in which $\sigma_{q_i} = \sqrt{E[q_i q_i]}$.

The covariances of the strains within an element may be computed by replacing ψ_{rj} and ψ_{sk} in Eq. 3.49 with strains corresponding to modes j and k in the final iteration. The covariances of the stresses may be computed from the covariances of the strains and the nonlinear constitutive equations.

3.5 Computation of Strains and Stresses

The multidirectional composite laminate consists of laminae of various fiber orientations. In this form the stiffness of each lamina may differ significantly from adjacent laminae. Since the strain components in thin laminates vary linearly through the laminate thickness, discontinuities in the in-plane stress components will occur at laminae interfaces.

1
2
3

in

T

fe

Th

and

Hence, it is imperative that the detailed state of stresses be established for each lamina. In this study strain and stress components are computed within each lamina using the techniques outlined below.

In global coordinates, the strain at any point (x,y,z) in the element is computed as follows

$$\{\varepsilon\} = [[B'] + z[B'']] \{q_e\} \quad (3.51)$$

The covariance matrix of the strains in global coordinates is given by

$$[\Sigma_\varepsilon] = [\{\varepsilon\} \{\varepsilon\}^T] = [[B'] + z[B'']] [\Sigma_{q_e}] [[B'] + z[B'']]^T \quad (3.52)$$

in which $[\Sigma_{q_e}]$ is the covariance matrix of the nodal displacements.

In local coordinates, the strain can be expressed as

$$\{\varepsilon'\} = [T]^{-T} \{\varepsilon\} = [T]^{-T} [[B'] + z[B'']] \{q_e\} \quad (3.53)$$

The covariance matrix of the strains in local coordinates is computed through

$$[\Sigma_{\varepsilon'}] = [T]^{-T} [[B'] + z[B'']] [\Sigma_{q_e}] [[B'] + z[B'']]^T [T]^{-1} \quad (3.54)$$

For stresses, it is easier to compute the stresses in local coordinate first and then transfer to global coordinates. In local coordinates the stresses at any point (x,y,z) are given by

$$\{\sigma'\} = [Q] \{\varepsilon'\} + f(\gamma_{12}) \begin{bmatrix} 0 & 0 & 0 \\ 0 & 0 & 0 \\ 0 & 0 & 1 \end{bmatrix} \{\varepsilon'\} \quad (3.55)$$

The normal stresses in local coordinates are

$$\begin{Bmatrix} \sigma'_{11} \\ \sigma'_{22} \end{Bmatrix} = \begin{bmatrix} Q_{11} & Q_{12} \\ Q_{21} & Q_{22} \end{bmatrix} \begin{Bmatrix} \varepsilon'_{11} \\ \varepsilon'_{22} \end{Bmatrix} \quad (3.56)$$

and the shear stress is



$$\tau'_{12} = Q_{66}\gamma_{12} + f(\gamma_{12})\gamma_{12} = Q_{66}\gamma_{12} + \sum_i a_i \gamma_{12}^{2i+1} \quad (3.57)$$

From Eq. 3.54 the covariance matrix of the normal stresses is

$$[\Sigma_{\sigma'_N}] = \begin{bmatrix} Q_{11} & Q_{12} \\ Q_{21} & Q_{22} \end{bmatrix} [\Sigma_{\epsilon'_N}] \begin{bmatrix} Q_{11} & Q_{12} \\ Q_{21} & Q_{22} \end{bmatrix}^T = [Q_N] [\Sigma_{\epsilon'_N}] [Q_N]^T \quad (3.58)$$

From Eq. 3.55 the covariance matrix of the shear stress can be expressed as follows

$$E[\tau'^2_{12}] = E[Q_{66}^2 \gamma_{12}^2] + 2Q_{66} \sum_i a_i E[\gamma_{12}^{2i+2}] + \sum_i a_i \sum_j a_j E[\gamma_{12}^{2i+2j+2}] \quad (3.59)$$

Since γ_{12} is a gaussian random variable, $E[\gamma_{12}^{2k}]$ can be expanded as follows

$$E[\gamma_{12}^{2k}] = 1 \times 2 \times \dots \times (2k-1) \times (\sigma_{\gamma_{12}}^2)^k \quad (3.60)$$

in which, $\sigma_{\gamma_{12}}^2 = E[\gamma_{12}^2]$. Note that $\sigma_{\gamma_{12}}^2$ was obtained in the computation of the strain in the local coordinates using Eq. 3.52.

In global coordinate the stresses can be computed easily through

$$[\Sigma_{\sigma}] = [T]^{-1} \begin{bmatrix} [\Sigma_{\sigma'}] & 0 \\ 0 & E[\tau'^2_{12}] \end{bmatrix} [T]^{-T} \quad (3.61)$$

in which $[\Sigma_{\sigma'}]$ is the covariance matrix of the stresses in local coordinates, computed by using Eqs.3.58 and 3.59.

3.6 Laminate Strength Analysis

From a design point of view, it is important to be able to predict failure due to excessive strains or stresses. The maximum strain criterion is one of the failure criterion used in the analysis of unidirectional fiber composites. In this criterion the orthotropic lamina is characterized by six ultimate strain allowables.

If any one of the ultimate strains is exceeded in any lamina, it is deemed to have failed. Ultimate strains in material coordinates for Narmco 5505 (the material used in the numerical examples presented in Chapter 5) at room temperature are

$$\varepsilon_1^+ = 0.0040 \qquad \varepsilon_2^+ = 0.0027 \qquad \gamma_{12}^+ = 0.011$$

$$\varepsilon_1^- = 0.0065 \qquad \varepsilon_2^- = 0.0038 \qquad \gamma_{12}^- = 0.011$$

As each ply fails, the laminate stiffness is recalculated to reflect the deletion of the failed lamina. The lamina failure strains can be used to predict of the laminate ultimate strength.

Alternatively, failure in composite laminates have also been expressed in terms of stresses. The most common ones are the Tsai-Hill and Tsai-Wu criteria (Jones 1975).

4. Optimizing Computational Effort

4.1 Introduction

Finite element programs can be computation-intensive. For example, even small problems of size n may require a computation time in the order of $O(n^4)$. In nonlinear problems the computation time becomes worse because convergence iteration is required. The nonlinear random vibration analysis outlined in the previous chapter is extremely computation-intensive and unless the computational effort is alleviated, the user will be restricted to analyze only small problems. In order to investigate a reasonably large problem, there is an urgent need to drastically reduce the required number of computations and consequently minimize execution time.

In this chapter a novel optimization technique is developed to make use of the symmetry inherent in the mathematical expressions. The improved performance of this technique is presented later in this chapter and is compared to the straight forward FORTRAN implementation. A number of simple techniques is also used to reduce the computation time for the types of formulas that involve operations on multiple matrices.

4.2 FORTRAN Implementation

This section provides a general description of the FORTRAN code developed for this problem.

The program is logically divided into a number of different modules. Each module corresponds to a separate logical computation unit as defined in the general *flow-chart* of Fig. (4.1). This logical separation was adopted in order to simplify the implementation and greatly enhance the readability of the code. The modular design should also greatly facilitate future modifications and extensions to the existing code. This is true even if major changes and additions are required. The corresponding modifications may be added between the units of Fig.4.1 or within each unit without affecting other units.

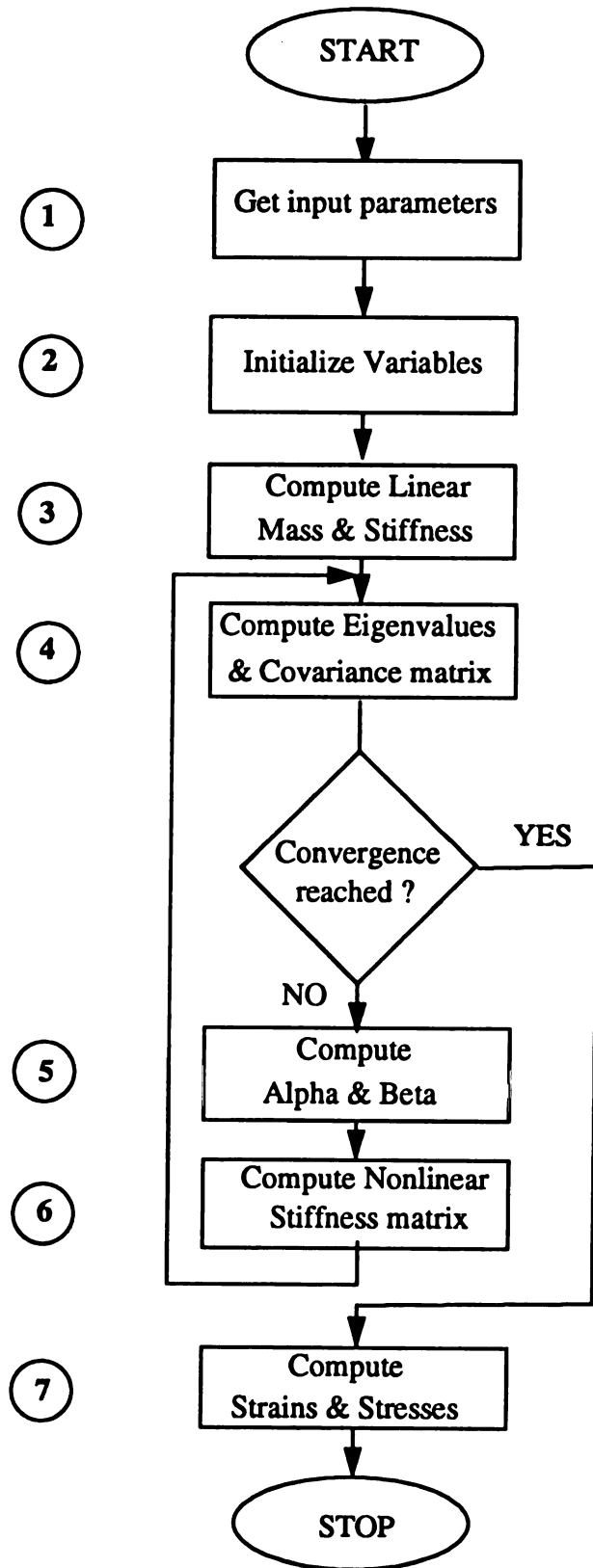


Figure 4.1 General flow-chart for Plate.f program

Figure 4.1 shows the general *flow-chart* for the main program. Each step in the flow-chart is described in detail below:

1. The user is prompted to input a number of parameters that completely control the size, variation and behavior of the problem. The implementation is quite automated and allows for a large variety of problem sizes, loading conditions, support conditions, number of laminae, and different thicknesses and fiber orientation angles for each lamina.
2. All static variables are initialized, and the topography of the plate based on the input parameters is generated. Elements are generated along a rectangular grid. The values of Z_k and Z_{k-1} based on the number of laminae are also computed. These values represent the distances from the mid-plane to the top and bottom of each lamina L_i . The signs for Z_k and Z_{k-1} are determined according to the position of lamina L_i with respect to the mid-plane (i.e. if L_i is below the mid-plane, Z_k and Z_{k-1} will both be negative). Finally, B' and B'' are computed according to the formulation previously introduced in chapter 2. These computations are done for each Gauss point within an element.
3. The elemental stiffness and mass matrices are computed using 3×3 Gauss quadrature. These matrices are then assembled using the topography matrix computed in step 1. The global structural mass and stiffness matrices are then obtained by eliminating the restrained DOF specified by the user.
4. The eigenvalues are computed using the structural mass and stiffness matrices determined in step 3 for the first iteration or in step 6 for subsequent iterations. In the first iteration, only the linear mass and stiffness matrices are used. In subsequent iterations, the stiffness matrix includes both linear and nonlinear terms. The eigenvalues are then sorted and the corresponding eigenvectors are computed. The DOF chosen by the user are loaded with excitations having the user specified spectral densities $S(\omega)$. Finally, the structural covariance matrix is computed using Eq.

- 3.49 and convergence based on Eq. 3.50 is checked using a tolerance of 0.001. Covariance matrices corresponding to elemental DOF are extracted from the structural covariance matrix as needed.
5. The coefficient α and β , as introduced in Eqs. 3.32 and 3.35, are computed. These intensive computations are performed for each element and at each Gauss point, and is the most time-consuming part of the whole program. It is here, that two major optimization techniques that drastically reduce the number of computations are introduced. These techniques are described in details in the following sections. The individual values of the α and β coefficients for any given pair of indices $\langle i, j \rangle$ may be computed independently and this will facilitate the parallelization of this step as discussed in chapter 6.
 6. Using the values of α and β , the elemental nonlinear stiffness matrix for each lamina is computed. These matrices are assembled and the restrained DOFs are eliminated to obtain the final nonlinear stiffness matrix for the whole laminate. The nonlinear stiffness matrix is then added to the linear one to obtain the total stiffness matrix.
 7. Steps 4 through 6 are repeated until convergence is obtained.
 8. After convergence, the final covariance matrix is used to obtain the covariances of the local and global strains and stresses. These values are computed at the center of the element chosen by the user for each lamina.

4.3 Optimization Techniques

The time needed to evaluate any given formula is directly proportional to the number of arithmetic operations performed by the corresponding code. When computing the nonlinear stiffness matrix by statistical linearization, the execution time was found to be large especially for computing the α and β coefficients. The actual time to execute a given instruction that involves arithmetic operations also depends on the precision of the variables

involved (i.e., the multiplication of double precision numbers requires about twice the amount of time needed for the multiplication of single precision numbers). Hence, minimizing the number of arithmetic operations performed by the program can greatly reduce the total computation time. Since code normally represents the direct implementation of a given problem, any technique to optimize such code will have to preserve the integrity of the implementation. Thus, optimization has to be done at the semantic level. For example, a computation that involves the multiplication of a number of variables may be totally skipped if at least one of these variables has a value of zero. Checking for zero values within a matrix V is only justified if it is known a priori that V is mostly sparse. The rest of this section describes in details a number of techniques developed and implemented to minimize the required number of instructions and thus optimize the execution time. Also, a detailed comparison between the non-optimized and the optimized versions of the code is presented.

4.3.1 Optimizing α and β

The computation of Eqs. 3.31 requires the evaluation of five sub-equations of the following type

$$\alpha = \sum_{j_1=1}^3 \sum_{k_1=1}^{20} \sum_{j_2=1}^3 \sum_{k_2=1}^{20} \sum_{j_3=1}^3 \sum_{k_3=1}^{20} \sum_{j_4=1}^3 \sum_{k_4=1}^{20} F \quad (4.1)$$

where F is

$$F = T_{3j_1} B'_{j_1 k_1} T_{3j_2} B'_{j_2 k_2} T_{3j_3} B'_{j_3 k_3} T_{3j_4} B'_{j_4 k_4} E[q_{e, k_1} q_{e, k_2} q_{e, k_3} q_{e, k_4}] \quad (4.2)$$

A direct implementation of Eq. 4.1 is shown in Fig 4.2, where each Do-loop represents the corresponding summation in the equation. Based on this implementation the expression F has to be evaluated approximately N times, where $N \equiv 13 \times 10^6$. The time required to execute the code in Fig. 4.2 is approximately $T_{\alpha} = N \times C(F)$, where $C(F)$ represents the computation time required to multiply the twelve double precision variables

```

DO J1 = 1, 3, 1
  DO K1 = 1, 20, 1
    DO J2 = 1, 3, 1
      DO K2 = 1, 20, 1
        DO J3 = 1, 3, 1
          DO K3 = 1, 20, 1
            DO J4 = 1, 3, 1
              DO K4 = 1, 20, 1
                tttcov = cove(ielem,k1,k2)*cove(ielem,k3,k4)+
                  +cove(ielem,k1,k3)*cove(ielem,k2,k4)+
                  +cove(ielem,k1,k4)*cove(ielem,k2,k3)

alpha2(ic,ielem,1) = alpha2(ic,ielem,1) +
                  +tt3(J1)*tbn2(J1,k1)*tt3(j2)*
                  + tbn2(J2,K2)*tt3(J3)*tbn2(j3,k3)*
                  + tt3(j4)*tbn2(j4,k4)*ttcov
          :::
        :::
      :::
    :::
  :::

```

Figure 4.2 Direct implementation of α

in Eq. 4.2. Let t_{dp} represents the time required to multiply two double precision numbers. The amount of time, T_{α_i} becomes $T_{\alpha_i} = 12 \times N \times t_{dp}$ which is approximately $1.56 \times 10^7 t_{dp}$. Hence the total amount of time required to compute Eq. 3.31 may be expressed as

$$T_{\alpha} = \sum_{i=1}^5 T_{\alpha_i} \quad (4.3)$$

Since the computation time, T_{α_i} for each of the sub-equation α_i is approximately the same, $T_{\alpha} \cong 5 \times T_{\alpha_i}$, for all i . According to the formulation of the nonlinear stiffness matrix $[K^*]$, α must be evaluated at each Gauss point, for each element and in each lamina. Hence, the overall time spent by the program in evaluating α may be approximated by

$$T = n \times m_x \times m_y \times G^2 \times T_{\alpha} \quad (4.4)$$

where n = the number of laminae in the problem, $m_x \times m_y$ = total number of elements, and G = order of the Gauss integration used.

To appreciate the magnitude of computing T , assume $n = 5$ laminae, $m_x = 20$, $m_y = 20$ and $G = 3$. The total time T then becomes $T = 1.4 \times 10^{13} t_{dp}$.

The computational optimizations for the α and β coefficients involve the combination of three types of techniques:

1. The reverse Pascal triangle indexing scheme to optimize Eq. 4.2
2. Elimination of zero-valued computations in the evaluation of F in Eq. 4.2
3. Unrolling of compound *DO-loops* in Eq. 4.1

These techniques are discussed in details in the next subsections, and then the computational time for the optimized and non-optimized computations of the expression T are compared.

4.3.2 Covariance optimization

The computation of Eq. 4.2 involves the evaluation of

$$\begin{aligned}
 E[q_{k_1}q_{k_2}q_{k_3}q_{k_4}] &= E[q_{k_1}q_{k_2}] \times E[q_{k_3}q_{k_4}] \\
 &+ E[q_{k_1}q_{k_3}] \times E[q_{k_2}q_{k_4}] \\
 &+ E[q_{k_1}q_{k_4}] \times E[q_{k_2}q_{k_3}]
 \end{aligned} \tag{4.5}$$

Note that Eq. 4.5 requires three multiplications and two additions of double precision variables, and will be executed N (13 million) times in evaluating Eq. 4.1. Reducing these number of computations will have a significant effect on the overall computation.

Given that the covariance matrix is symmetric, $E[q_{k_1}q_{k_2}] = E[q_{k_2}q_{k_1}]$ for any k_1 and k_2 and thus, rearranging the indices $k_1k_2k_3k_4$ in any order in Eq. 4.5 will produce the same numerical result. Hence, Eq. 4.5 need to be actually evaluated for only one of these arrangements. All other arrangements may substitute this computed value provided an efficient indexing scheme can be devised.

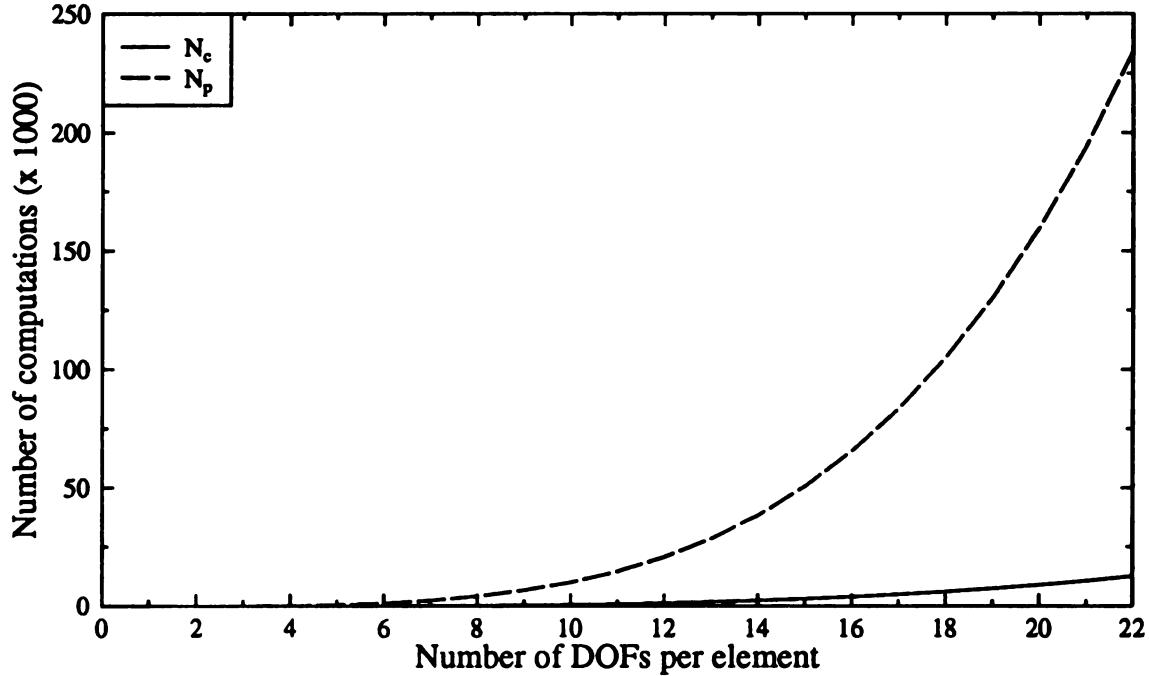


Figure 4.3 Number of Permutations (N_p) vs. Combinations (N_c).

The execution of Eq. 4.1 produces all possible permutations $N_p = 20^4$ of k_1, k_2, k_3 and k_4 . This requires the evaluation of Eq. 4.5 for all these permutations. Given an efficient indexing scheme, this number of permutations actually reduces to the number of all possible combinations with repetition (i.e., including combinations such as (1 1 2 3), (3 2 1 3), etc...). The number of these combinations N_c may be expressed as

$$N_c = \binom{n+r-1}{r} = \frac{(n+r-1)!}{r!(n-1)!} \quad (4.6)$$

where n and r represent the total number of *DOF* per element and the number of *DO-loops* in Eq. 4.1 respectively. For our problem $n = 20$ and $r = 4$. A comparison between the relative magnitudes of Eq. 4.6 and the number of permutation is shown in Fig. 4.3. The figure outlines the major saving in terms of computational time when n increases. Note that for $n = 20$, the indexing scheme reduces the overall execution time by approximately a factor of 20.

4.3.3 The indexing scheme

In evaluating Eq. 4.1, all possible permutations $(k_1k_2k_3k_4)$ will be generated by the four k -DO-loops. The previous discussion showed that for any given set of indices, we need only compute the value of one of all such permutations. This computed value may be saved by the program in a one-dimensional array (*offset* (N_c)) to be used as a special access structure. Later, any of the remaining permutations may access this stored value by means of an indexing scheme. This approach is known as dynamic programming. A necessary condition in dynamic programming is that the cost of the indexing scheme should be less than the cost of performing the actual evaluation. Next, we present an efficient indexing scheme, show its correctness and that it greatly outperforms the straightforward implementation.

To illustrate how the scheme works, we provide the following example: Let $n = 4$ and $r = 4$. Fig. 4.4 lists all possible combinations of $(k_1k_2k_3k_4)$. Note that these combinations will be produced in ascending order of indices due to cascading of the *DO-loops* as shown below:

```
DO K1 = 1, 20, 1
  DO k2 = k1, 20, 1
    DO k3 = k2, 20, 1
      DO k4 = k3, 20, 1
        :::
      END DO
    END DO
  END DO
END DO
```

The indexing problem may be outlined as follows: Given any permutation of indices $P = (k_1k_2k_3k_4)$, the problem is to locate the corresponding combination of indices, C , for which the value of F has already been computed and stored in *offset* N_c .

Since the combinations are produced in ascending order of indices, the combination C is the permutation that has the indices k_i sorted in ascending order.

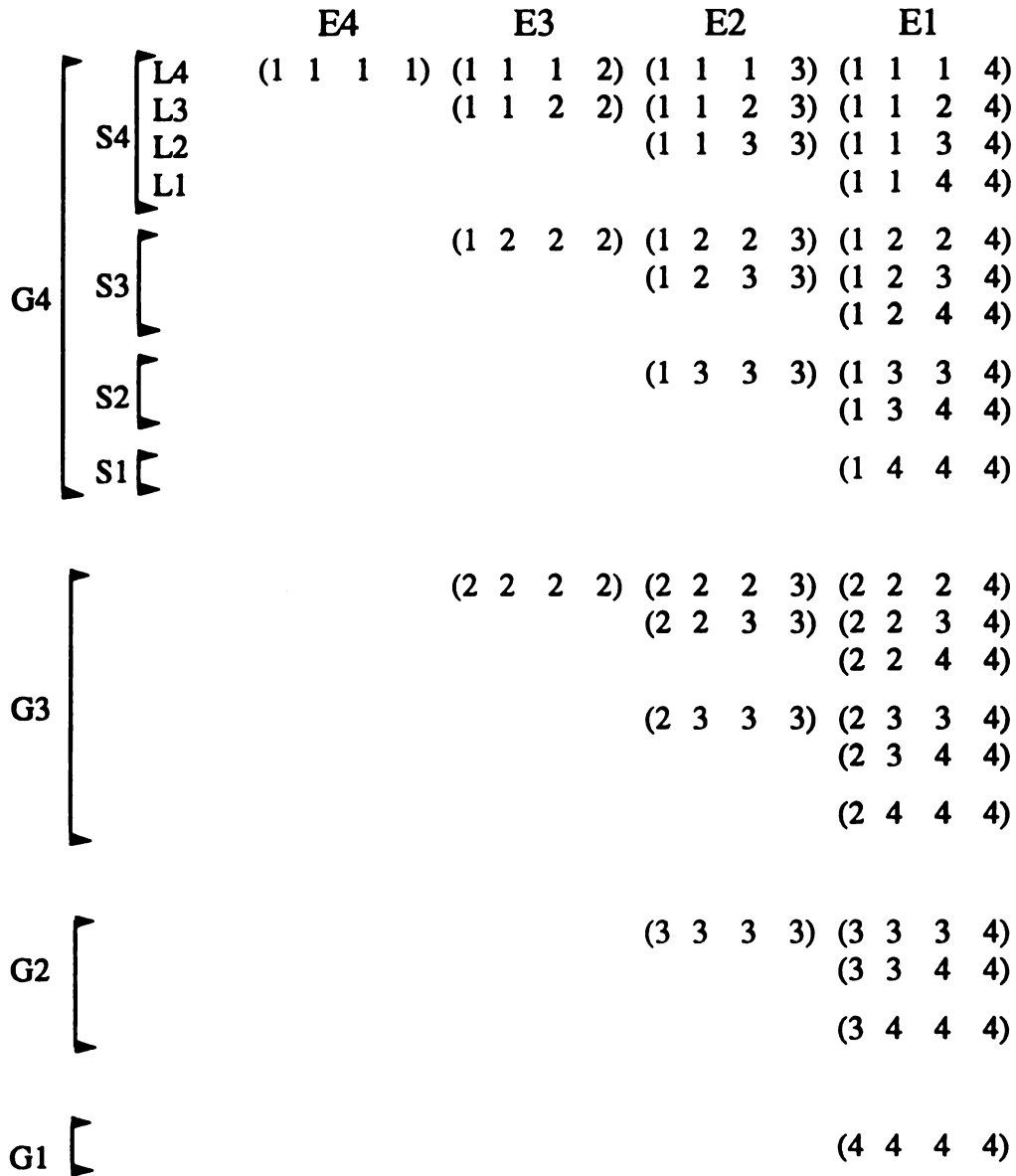


Figure 4.4 Derivation of reverse Pascal triangle

In order to locate combination C corresponding to P , the correct index of C in the array (*offset*) has to be computed. To illustrate the indexing scheme, termed reversed Pascal triangle (RPT), let $n = 4$ and $r = 4$. Fig. 4.4 displays all the combinations produced by the four k -DO-loops in the code segment presented earlier. Note that in Fig. 4.4, the combinations can be divided into four groups (g_1, g_2, g_3, g_4) where each group has the same number in the first column. Within each group, the combinations may be split again into subgroups (s_1, s_2, s_3, s_4) based on the number in the second column. The division based on the third column is shown as a separate lines (l_1, l_2, l_3, l_4) within a subgroup and that based on the 4th column corresponds to entries (e_1, e_2, e_3, e_4) within each line.

In the following, we determine the number of combinations in each line, subgroup and group. We note that l_1 will always have one combination since it corresponds to the last combination starting at 4. l_2 corresponds to starting with 3, and thus has two entries (3 and 4). Similarly, l_3 starts with 2 and has 3 entries (2, 3 and 4) and l_4 has 4 entries.

Subgroup s_1 has only one line, l_1 , since it corresponds to starting with 4. s_2 has l_1 and l_2 resulting in 3 ($l_1 + l_2 = 1 + 2$) entries. s_3 has 6 ($l_1 + l_2 + l_3 = 1 + 2 + 3$) and s_4 has 10 entries ($l_1 + l_2 + l_3 + l_4 = 1 + 2 + 3 + 4$). The same trend holds for the groups and thus $g_1 = 1 (s_1)$, $g_2 = 5 (s_1 + s_2)$, etc..... To reach a given group g_i ($i = 1, 2, 3, 4$), we have to skip groups g_1, g_2, \dots, g_{i-1} . Thus, we have to skip $e_g = \sum_{j=1}^{i-1} g_j$ entries. Similarly, a subgroup s_i may be reached by skipping $e_s = \sum_{j=1}^{i-1} s_j$ entries within the given group. The number of entries in each category, as computed above, is represented in Table 4.7. This is done to motivate the use of the reverse Pascal triangle (RPT).

Note that the entries in this table correspond to those of the Pascal triangle. This observation generalizes the indexing scheme since Table 4.7 can now be generated for any combination of n and r .

TABLE 4.1 Number of terms in each group

<i>l</i>	1	2	3	4
<i>l</i>	1	2	3	4
<i>s</i>	1	3	6	10
<i>g</i>	1	4	10	20

Next, an example is presented to verify and show how the indexing scheme helps locate the correct combination C to any given permutation P .

Example: Let $P = (3\ 2\ 2\ 3)$, then by sorting the entries of P in ascending order we obtain the combination $C = (2\ 2\ 3\ 3)$. The pre-computed value of the combination C in the *offset* array is stored at location

$$N_c - \text{RPT}(1,2) - \text{RPT}(2,2) - \text{RPT}(3,3) - \text{RPT}(4,3)$$

$$= N_c - \sum_{j=1}^4 \text{RPT}(j, C(j)) = N_c - \sum_{j=1}^r \binom{n+r-C(j)-j}{r-j+1} = 35 - 5 - 4 - 1 - 1 = 24$$

Note that the column (second) indices in the RPT array are the element of C .

The following code segment illustrates how *offset* is computed

```

OFFSET = NC
DO J = 1, r
  OFFSET = OFFSET - RPT (J, C(J))
END DO

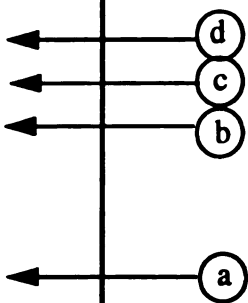
```

Thus, $\text{value}(P) = \text{offset}(24)$. This is graphically illustrated in Fig. 4.5 for the same example.

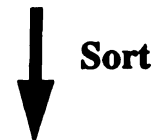
The corresponding RPT table is extracted from the Pascal triangle in Fig. 4.6. A table that represents the RPT indexing structure for the specific problem size treated in this work is also presented in Fig. 4.10 at the end of the chapter, where $n = 20$ *DOF* and $r = 4$ *DO-loops*.

Note that the ij th element in the table of Fig. 4.6 or in Fig. 4.7 is given by $\binom{n+r-i-j}{r-j+1}$, where $n = 4$ and $r = 4$ for the former, and $n = 20$ and $r = 4$ for the later, and with $\binom{l}{m}$ defined as being zero when $l < m$.

offset	Combinations
1	1, 1, 1, 1
2	1, 1, 1, 2
3	1, 1, 1, 3
4	1, 1, 1, 4
5	1, 1, 2, 2
6	1, 1, 2, 3
7	1, 1, 2, 4
8	1, 1, 3, 3
9	1, 1, 3, 4
10	1, 1, 4, 4
11	1, 2, 2, 2
12	1, 2, 2, 3
13	1, 2, 2, 4
14	1, 2, 3, 3
15	1, 2, 3, 4
16	1, 2, 4, 4
17	1, 3, 3, 3
18	1, 3, 3, 4
19	1, 3, 4, 4
20	1, 4, 4, 4
21	2, 2, 2, 2
22	2, 2, 2, 3
23	2, 2, 2, 4
24	2, 2, 3, 3
25	2, 2, 3, 4
26	2, 2, 4, 4
27	2, 3, 3, 3
28	2, 3, 3, 4
29	2, 3, 4, 4
30	2, 4, 4, 4
31	3, 3, 3, 3
32	3, 3, 3, 4
33	3, 3, 4, 4
34	3, 4, 4, 4
35	4, 4, 4, 4



$P = (3, 2, 2, 3)$



$C = (2, 2, 3, 3)$

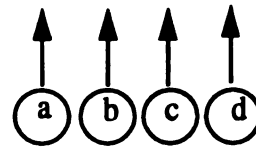


Figure 4.5 Combinations for which F is computed

i \ j	1	2	3	4
1	15	5	1	0
2	10	4	1	0
3	6	3	1	0
4	3	2	1	0

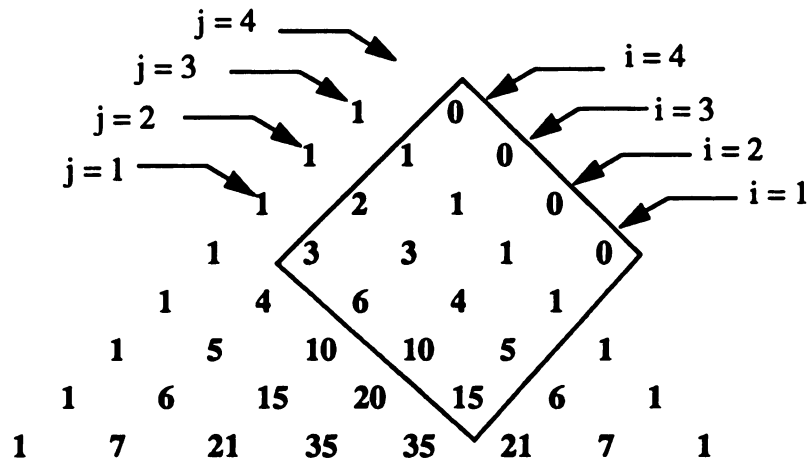


Figure 4.6 Pascal triangle and RPT table

4.3.4 Elimination of zero-valued computations

In the previous section, an indexing scheme to help minimize the number of computations involved in evaluating Eq. 4.5 was generalized. While the scheme was shown to be effective and efficient in reducing the computation time of $E[q_k, q_{k_2}, q_k, q_{k_4}]$, evaluating F in Eq. 4.1 still requires eight double precision multiplications and has to be executed $N \approx 13 \times 10^6$ times. Reducing this total number of evaluations should also improve the computation time of Eq. 4.1. Next, a technique that aims to reduce N by eliminating all

$i \backslash j$	1	2	3	4	5	6	7	8	9	10	11	12	13	14	15	16	17	18	19	20
1	7315	5985	4845	3876	3060	2380	1820	1365	1001	715	495	330	210	126	70	35	15	5	1	0
2	1330	1140	969	816	680	560	455	364	286	220	165	120	84	56	35	20	10	4	1	0
3	190	171	153	136	120	105	91	78	66	55	45	36	28	21	15	10	6	3	1	0
4	19	18	17	16	15	14	13	12	11	10	9	8	7	6	5	4	3	2	1	0

Figure 4.7 RPT offset array needed for indexing

computations of F that involve a zero-valued variable is introduced, a code segment for the computation of α is presented in Fig. 4.8 to illustrate the technique.

```

DO J1 = 1, 3, 1
  DO K1 = 1, 20, 1
    if (abs(tbn2(J1,K1)) .gt. MinTol) then
      L1 = (K1-1) * 8000
      DO J2 = 1, 3, 1
        ts1 = TT3(J1) * TT3(J2)
        DO K2 = 1, 20, 1
          if (abs(tbn2(J2,K2)) .gt. MinTol) then
            L2 = (K2-1) * 400
            bs1 = tbn2(J1,K1) * tbn2(J2,K2)
            DO J3 = 1, 3, 1
              DO K3 = 1, 20, 1
                if (abs(tbn2(J3,K3)) .gt. MinTol) then
                  L3 = (K3-1) * 20
                  bs2 = bs1 * tbn2(J3,K3)
                  DO J4 = 1, 3, 1
                    ts3 = ts2 * TT3(J4)
                    DO K4 = 1, 20, 1
                      if (abs(b1(J4,K4)) .gt. MinTol) then
                        XpVal = ev(ielem,iOffst(K4 + L3 + L2 + L1))
                        if (abs(XpVal) .gt. 0.d-12) then
                          alpha1(ic) = alpha1(ic)+ts3*XpVal*bs2*b1(J4,K4)
                        end if
                      end if
                    end if
                  end if
                end if
              end if
            end if
          end if
        end if
      end if
    end if
  end if
end if

```

:::

Figure 4.8 Segment of code for computing α .

Given that some of matrices involved in the computation of F are sparse (have a large number of zero-valued entries), the evaluation of Eq. 4.1 may be optimized as follows:

Within the scope of any DO-loop, for index k_i , check the entry of sparse matrix M corresponding to (j_i, k_i) . If $M(j_i, k_i) \leq MinTol$ then, the value of F will be approximately zero in all succeeding DO-loop computations, and hence the subsequent loops may be skipped.

4.3.5 Unrolling of DO-loops

One of the well known techniques in optimizing FORTRAN programs is the unrolling of DO-loops. Unrolling means to move, completely or partially, the independent portion of the computations outside the affected DO-loops. These computations may involve actual numerical values, defined constants (π , e , etc.), simple variables or even matrices. The main criteria necessary to move a computation outside of a given DO-loop is that the variables in the computation are required to be independent of the given DO-loop's index. Unrolling a computation with m arithmetic operations outside a DO-loop with n -iterations will save approximately $m \times (n - 1)$ operations.

In this program implementation, the unrolling technique was extensively utilized to optimize cascaded DO-loops and further enhance the performance of the program. To illustrate the benefits of this technique, the computation of the displacement covariance matrix is shown in the code segment in Fig. 4.8

```
do I1=1,60,1
  do J1=1,60,1
    cov(I1,J1) = 0.d0
    do I2=1,60,1
      do J2=1,60,1
        ztmp = 0.d0
        do I3=1,ndof,1
          do J3=1,ndof,1
            ztmp = ztmp + g(I3,I2) * g(J3,J2)
          end do
        end do
      end do
    cov(I1,J1)=cov(I1,J1)+ztmp*z(I1,I2)*z(J1,J2)*dint(I2,J2)
    end do
  end do
end do
```

Figure 4.9 Code segment illustrating unrolling of Do-loops

In the code of Fig. 4.8, the sub-computation

$$C = Z(i_1, i_2) \times Z(j_1, j_2) \times dint(i_2, j_2)$$

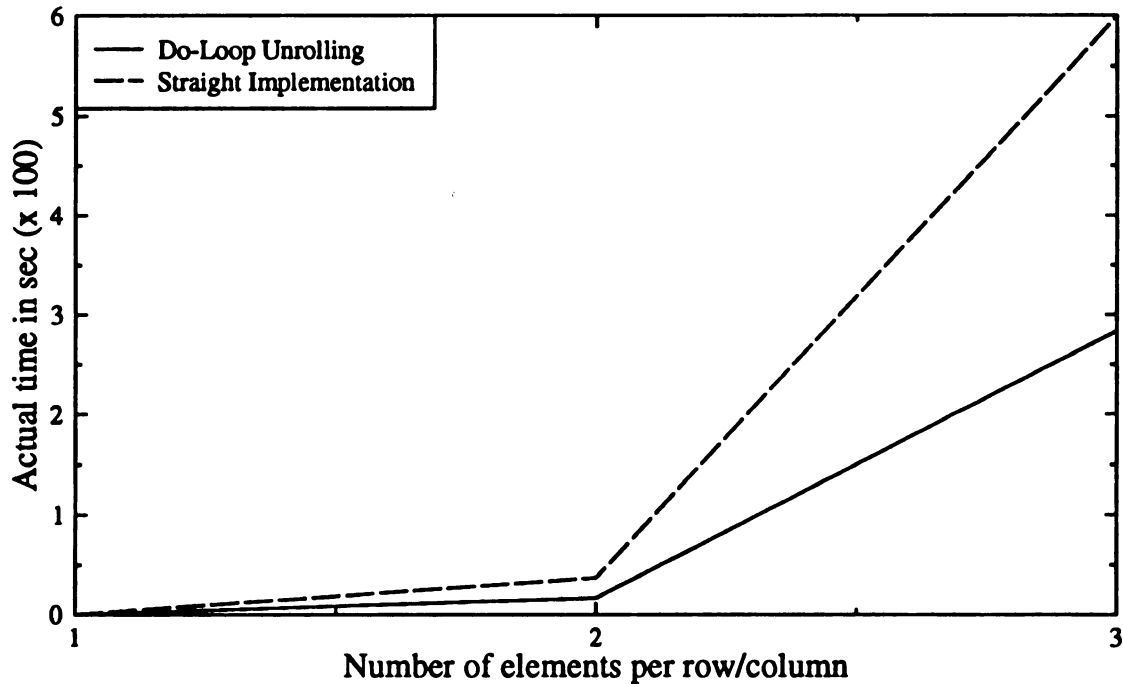


Figure 4.10 Do-Loop Unrolling vs. Straight Implementation.

is totally independent of the DO-loops corresponding to i_3 and j_3 . Thus, C may be moved outside these *DO-loops* resulting in the saving of $OPS(C) \times (ndof^2 - 1)$, where $OPS(C)$ is the number of arithmetic operations in the computation. When all the DO-loops for the above implementation are considered, the total number of operations saved by this simple technique is approximately $OPS(C) \times (ndof^2 - 1) \times 60^4$. The actual timing for the above illustration was measured on a Sun SPARC ELC workstation and is shown in Fig. 4.9 where it is compared to the straight forward implementation for different DO-loop dimensions. The computation time was measured using the UNIX *time* command.

Because of its wide applicability, this technique was used throughout the program. The interested reader is encouraged to go through the program listing to realize the importance of this technique in reducing the overall execution time of the program.

Table 4.8 presents a final comparison between a straight-forward implementation and the optimized version of the program. Four separate runs were made with the same loading

conditions and geometry while varying the number of layers. Note that the total time for each run is directly dependent on the number of iterations required for convergence and hence, in the above table, the time for 5 laminae (4 iterations) is less than the time for 4 laminae (5 iterations). The fourth column of the table, i.e. the ratio of non-optimized to optimized time, suggests an average ratio of 40. For this specific example (with 4 laminae), the optimized version takes only around two hours, while the straight implementation takes

TABLE 4.2 Comparison of total times.

Stacking Sequence	Optimized (sec)	Non-optimized (sec)	Non-Opt/Opt
[30/-30]	4100.6	150871	36.8
[30/0/-30]	3734.4	170136.5	45.5
[30/30/-30/-30]	6968.4	299230.3	43.0
[30/30/0/-30/-30]	5558.2	280187.6	50.4

roughly 3.5 days. All times in the table were measured on Sun SPARC 10 workstations.

5. Numerical Results

5.1 General

In this chapter a number of numerical examples of in-plane and out-of-plane responses of laminated cantilever plates are presented. Various types of loading, fiber orientations and stacking sequences are considered, and displacement, strain and stress responses are computed. In addition, the twisting effect due to shear coupling in unsymmetrical laminated composites is discussed. The basic units of length and force are taken to be inches and pounds.

5.2 In-Plane Loading

5.2.1 Extensional loading

To study the effect of material nonlinearity on the response of a composite laminated plate loaded in extension, a cantilevered plate made of Boron/Epoxy Narmco 5505 was considered. The plate was modeled with nine finite elements and excited by the boundary loads shown in Fig. 5.1, 5.5 and 5.9, with P being a zero-mean white noise excitation. A white noise has a spectral density function (SDF) that is constant at all frequencies. i.e.,

$$S(\omega) = S_0, \quad -\infty < \omega < \infty$$

While the r.m.s. of the load, which is the square root of the area under the SDF, is undefined for white noise, the response can be evaluated in closed-form. The intensity of the load is therefore characterized by the level of the SDF, S_0 . Note that since the r.m.s. load has units of lb, S_0 has units of $\text{lb}^2 \text{ sec}$.

The level of the excitation spectrum, S_0 , was increased from 1000 to 12000 $\text{lb}^2 \text{ sec}$ and the displacement, strain and stress responses computed. The fifth order approximation shown in Fig. 2.2 was used for the nonlinear shear stress-strain relation. Three cases of extensional loading are investigated and the results are discussed below.

Case I: A single-ply plate with fiber orientation α . Two values of α , 30° and 60° were used for comparison purposes.

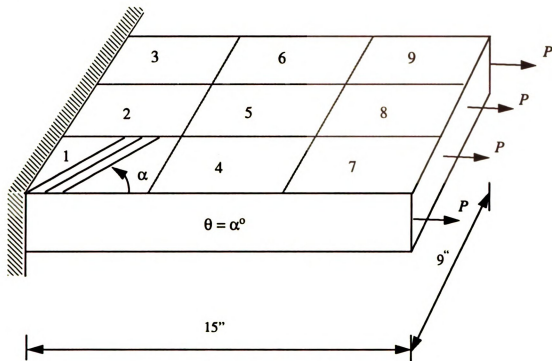


Figure 5.1 One-ply plate loaded in tension

Table 5.1 shows the first five undamped natural frequencies of the plate from the first and last iteration of the analysis, for the excitation level $S_0 = 12000 \text{ lb}^2 \text{ sec}$. The values from the first iteration correspond to the case where nonlinearity is neglected, while the values from the last iteration show the effect of nonlinearity. The natural frequencies show relatively small decreases ranging from 2 to 4%.

Table 5.2 shows the number of iterations required for convergence of the root mean square (r.m.s.) nodal displacements according to the criterion in Eq. 3.50, with a tolerance $\epsilon = 0.001$. The number of iterations increases with excitation load level, but shows a slight oscillations for S_0 between 7000 and 9000 $\text{lb}^2 \text{ sec}$. This is probably due to the slight oscillation in the approximate fifth-order shear stress-strain law in Fig. 2.2.

TABLE 5.1 First five natural frequencies from linear (first iteration) and nonlinear (last iteration) analysis for load level $S_0 = 12000 \text{ lb}^2 \text{ sec}$

Mode	[30°]		[60°]	
	First Iteration	Last Iteration	First Iteration	Last Iteration
1	25.5	24.6	15.8	15.3
2	52.8	49.7	47.6	46.6
3	96.7	95.0	74.5	70.2
4	139.4	134.0	95.2	93.2
5	170.5	163.2	101.5	96.7

TABLE 5.2 Number of iterations required for convergence

Load level, S_0 ($\text{lb}^2 \text{ s}$)	No. of Iterations	
	[30°]	[60°]
1000	3	3
2000	4	4
3000	4	4
4000	4	5
5000	5	5
6000	5	6
7000	5	6
8000	6	7
9000	6	7
10000	6	6
11000	6	6
12000	6	6

Fig. 5.2 shows the variation of the absolute r.m.s. shear strain in material coordinates at the center of element 2 of the plate with the excitation level. For $S_0 = 12000 \text{ lb}^2 \text{ sec}$, the r.m.s. shear strain is about 0.0055 for the [60°] and 0.0045 for [30°]. The peak shear strains

be expected to be in excess of three times the r.m.s. strain (i.e. in excess of 0.016 for $[60^\circ]$ and 0.0135 for $[30^\circ]$).

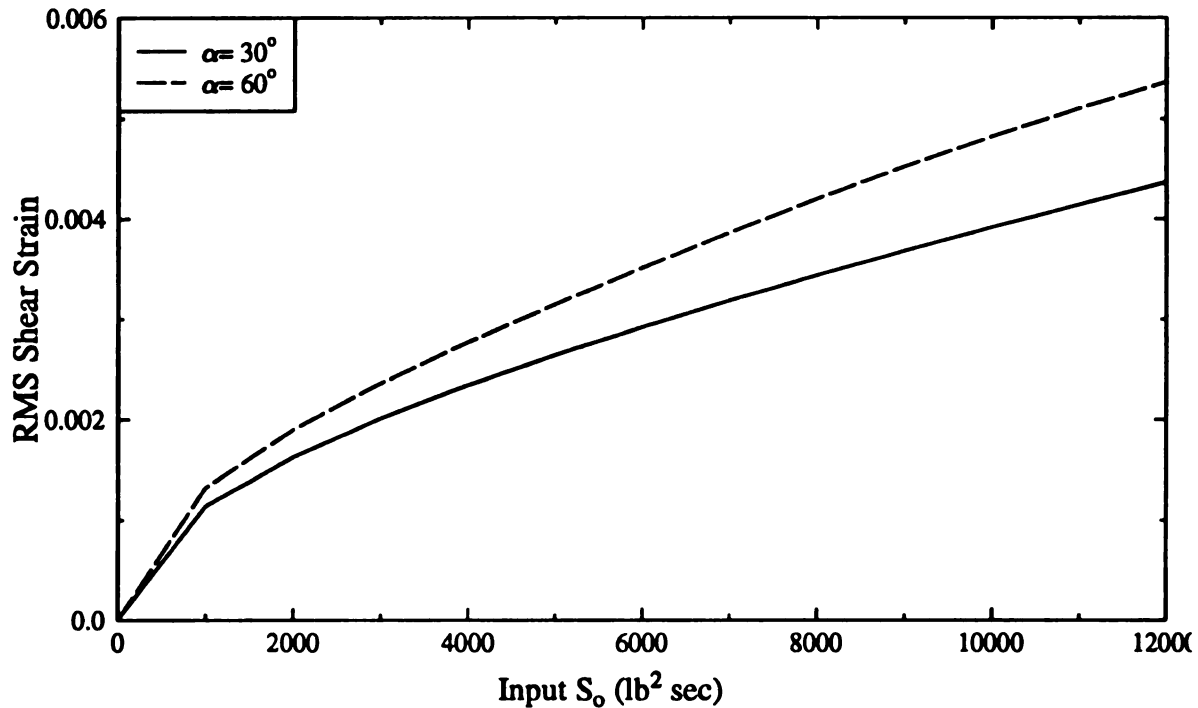


Figure 5.2 Variation of absolute r.m.s. shear strain at the center of element 2 with excitation load level

The variation of the normalized r.m.s. x -displacement of the front right corner node with excitation spectrum level, S_0 , is shown in Fig. 5.3. The displacement is normalized by dividing by the linear response (for which $[K^*] = [0]$). The figure illustrates that the proportional increase in the displacement due to non-linearity steadily increases with the excitation level.

The variation of the normalized r.m.s. strains and stresses (in the material directions) at the center of element 2 with the excitation level are shown in Fig. 5.4 and 5.5. Again, the normalizations have been performed by dividing by the corresponding linear responses. The non-linearity in the constitutive law results in significant increases in the shear strains and stresses, but does not significantly affect the normal strains.

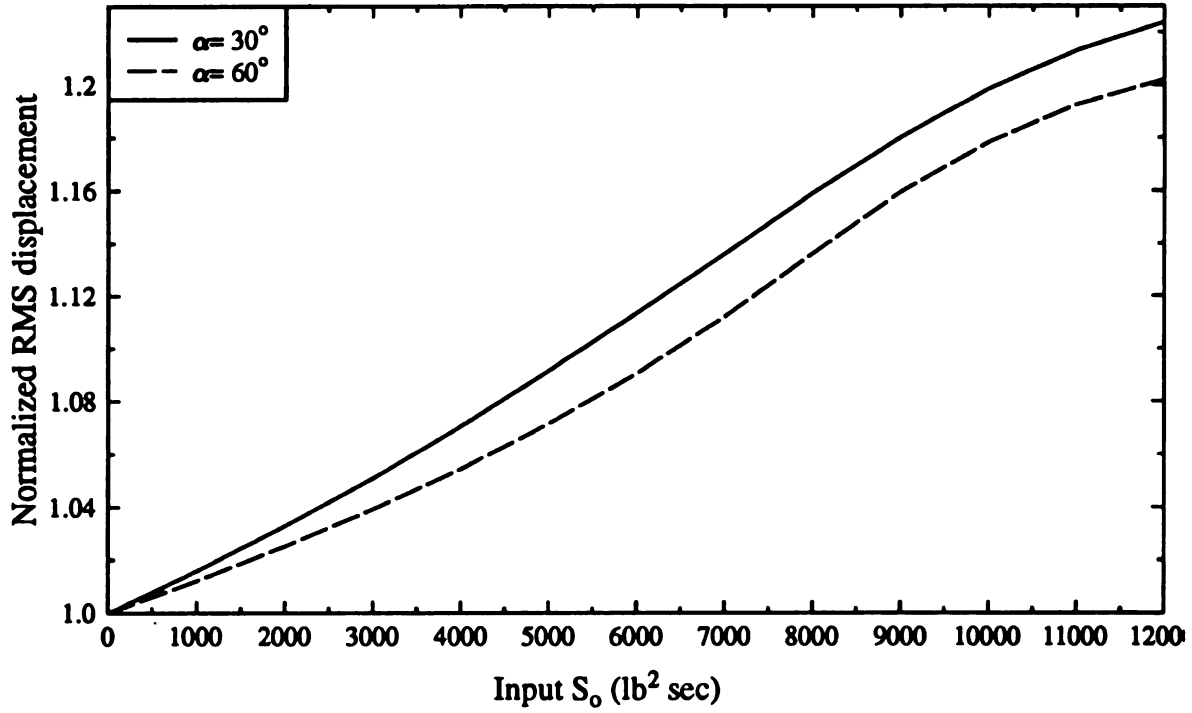


Figure 5.3 Variation of normalized r.m.s. displacement at free corner nodes with excitation load

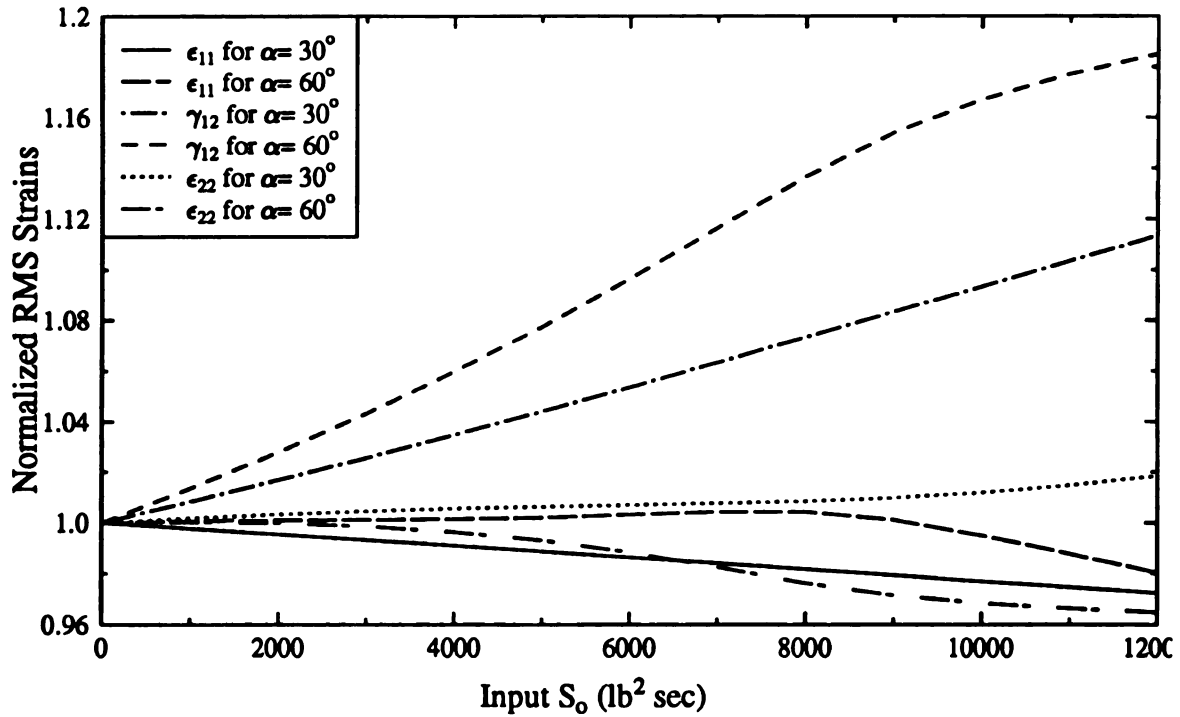


Figure 5.4 Variation of normalized r.m.s. strains at the center of element 2 with excitation load level

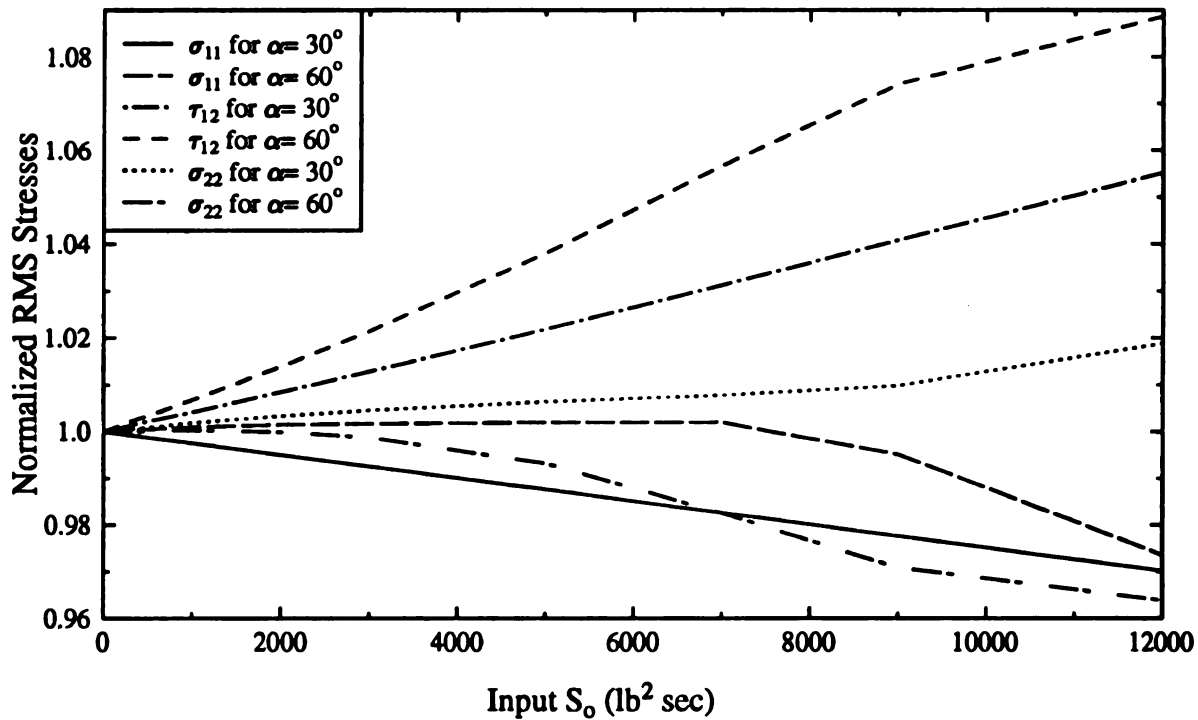


Figure 5.5 Variation of normalized r.m.s. stresses at the center of element 2 with excitation load level

Case II: Two-ply laminated plate with fiber orientation α and $-\alpha$ in the top and bottom layers, respectively, as shown in Figure 5.6. The total thickness of the plate is identical to case I.

Table 5.3 shows the first five undamped natural frequencies of the laminated plate shown in Fig. 5.5. Due to the nonlinearity effect, the natural frequencies show decreases ranging from 1 to 4%.

Table 5.4 shows that the number of iterations required for convergence increases with the excitation load level since the nonlinearity becomes more pronounced at higher loads. For any applied load level, the number of iterations required for convergence for the $[30^\circ/-30^\circ]$ laminate is less than that for the $[60^\circ/-60^\circ]$ laminate. This indicates that the nonlinearity has a more pronounced effect for the $[60^\circ/-60^\circ]$ laminate.

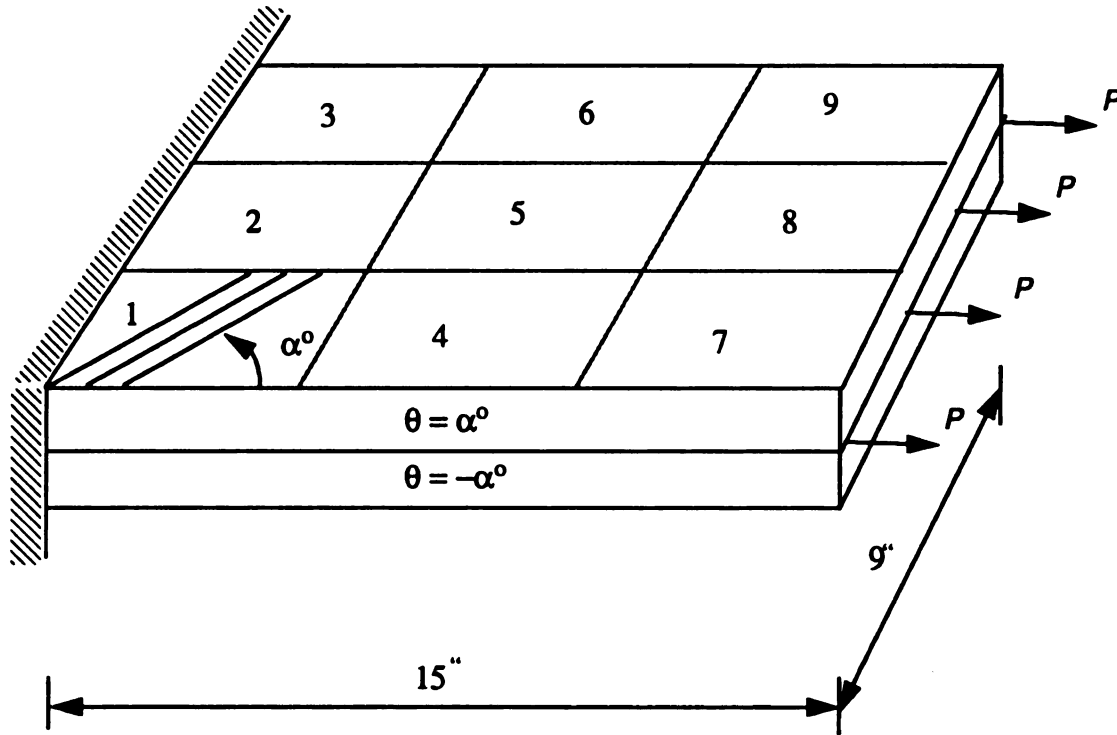


Figure 5.6 Two-ply laminated plate loaded in tension

The absolute shear strain in the material coordinates at the center of element 2 is shown in Fig. 5.7 and clearly the response is nonlinear. For any given excitation level the shear strain for the $[60^\circ/-60^\circ]$ laminate exceeds that for the $[30^\circ/-30^\circ]$ laminate.

The normalized r.m.s. x-displacement of the front corner node is shown in Fig. 5.8. The figure illustrates the effect of nonlinearity which is significant for the $[60^\circ/-60^\circ]$ laminate and negligible for the $[30^\circ/-30^\circ]$ laminate.

TABLE 5.3 First five natural frequencies from linear (first iteration) and nonlinear (last iteration) analysis for load level $S_0 = 12000 \text{ lb}^2 \cdot \text{sec}$

Mode	$[30^\circ/-30^\circ]$		$[60^\circ/-60^\circ]$	
	First Iteration	Last Iteration	First Iteration	Last Iteration
1	24.1 HZ	23.8 HZ	15.6 HZ	15.2 HZ
2	74.5	73.9	46.4	45.4
3	92.2	91.4	86.7	84.9
4	152.5	150.3	95.0	92.3
5	215.8	213.4	103.7	100.0

TABLE 5.4 Number of iterations required for convergence

Load level, S_0 (lb^2s)	No. of iterations	
	[30°/-30°]	[60°/-60°]
1000	3	3
2000	3	4
3000	3	4
4000	3	4
5000	3	4
6000	4	4
7000	4	5
8000	4	5
9000	4	5
10000	4	5
11000	4	5
12000	4	5

The variation of the normalized r.m.s. shear and normal strains and stresses in material directions at the center of element 2 with the excitation level are shown in Fig. 5.9 and 5.10. The nonlinearity in the constitutive law results in significant increases in the normal and shear strains and normal stresses for the [60°/-60°] laminate.

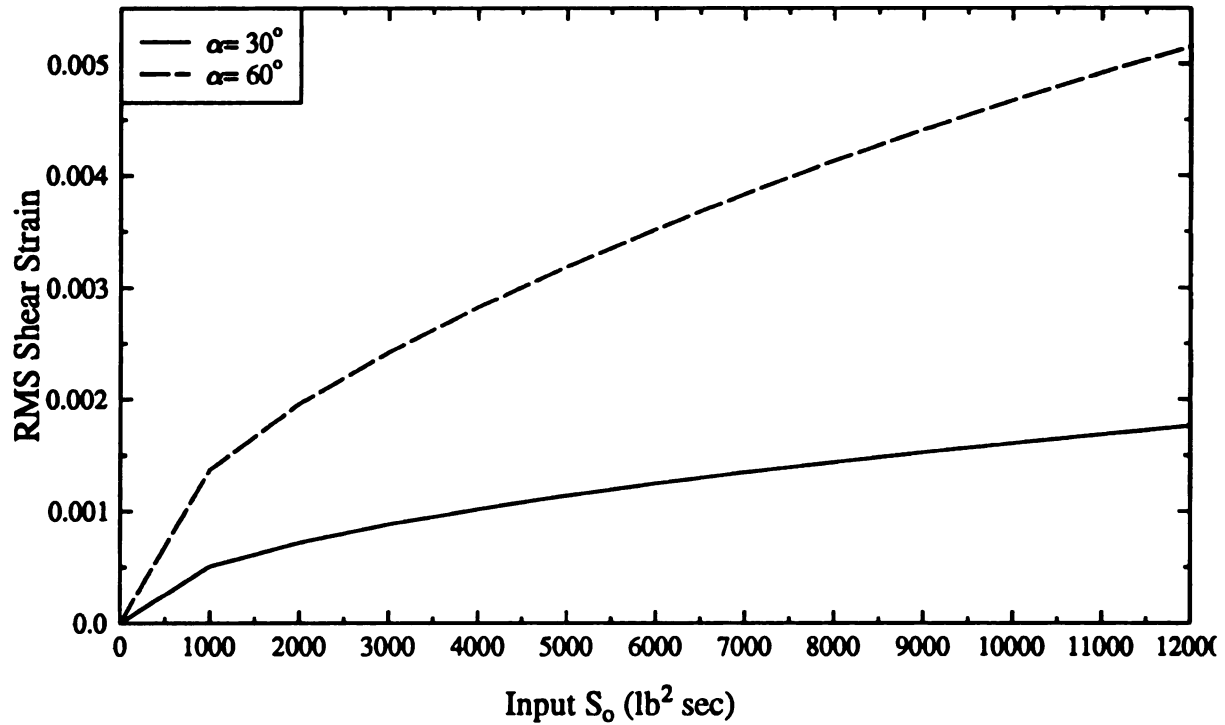


Figure 5.7 Variation of absolute r.m.s. shear strain at the center of element 2 with excitation load level

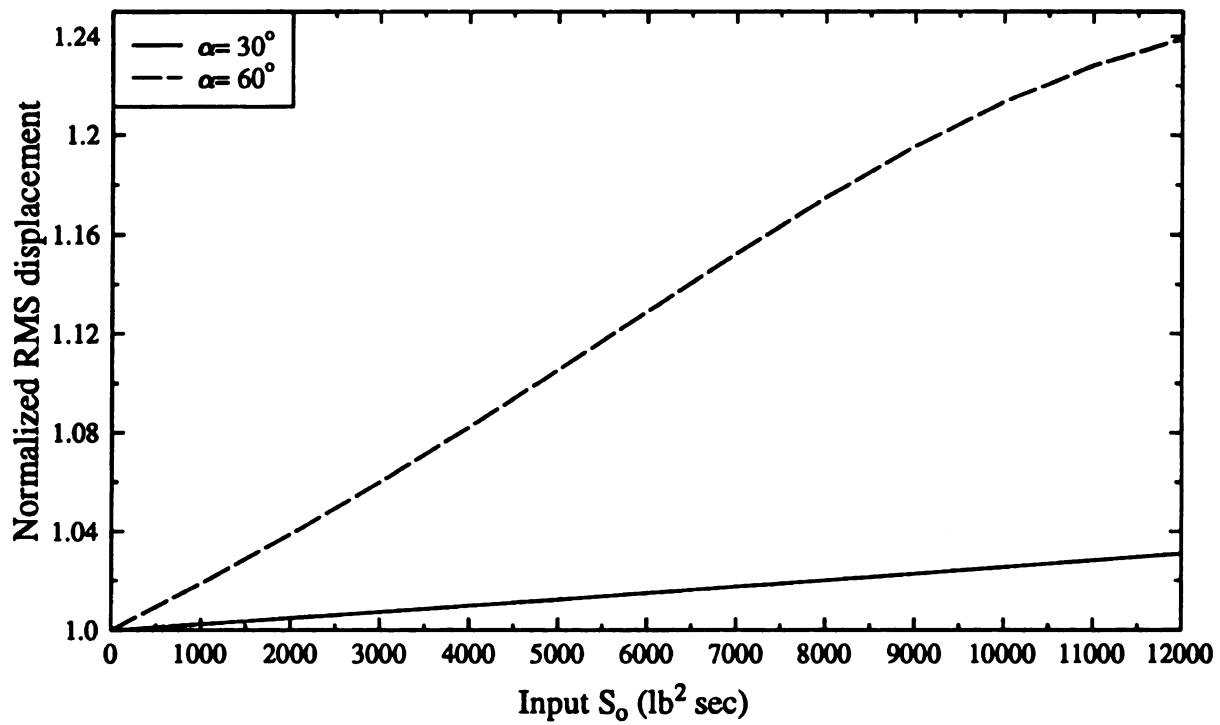


Figure 5.8 Variation of normalized r.m.s. displacement at free corner nodes with excitation load level

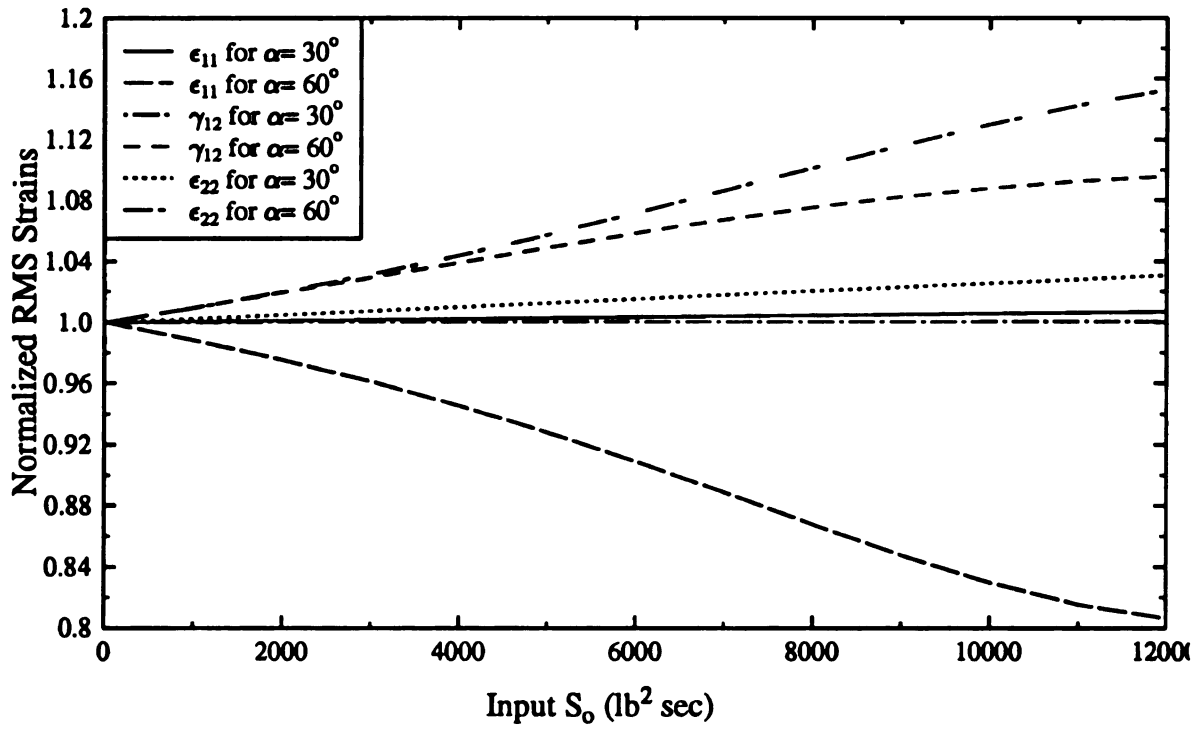


Figure 5.9 Variation of normalized r.m.s. strains at the center of element 2 with excitation load level

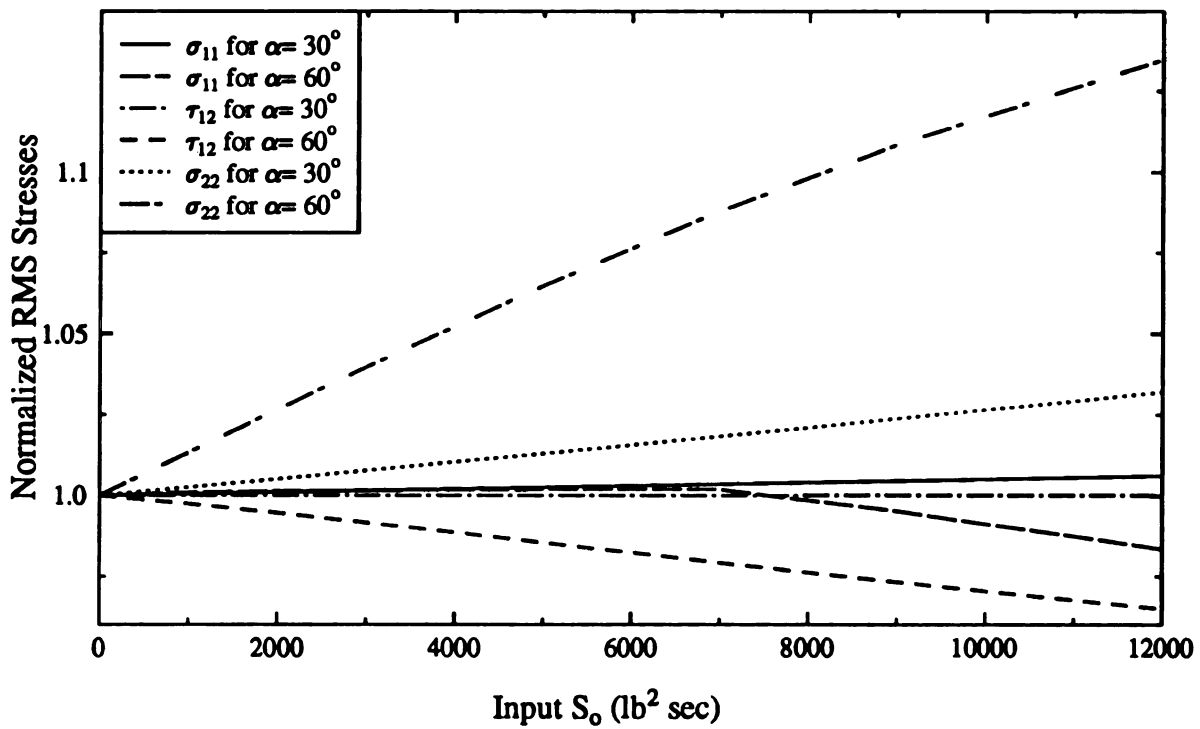


Figure 5.10 Variation of normalized r.m.s. stresses at the center of element 2 with excitation load level

Case III: Three-ply laminated plate with fiber orientation of α , 0 and $-\alpha$ in the top, middle and bottom layers, respectively, as shown in Fig.5.11. The total thickness of the plate is the same as in cases I and II.

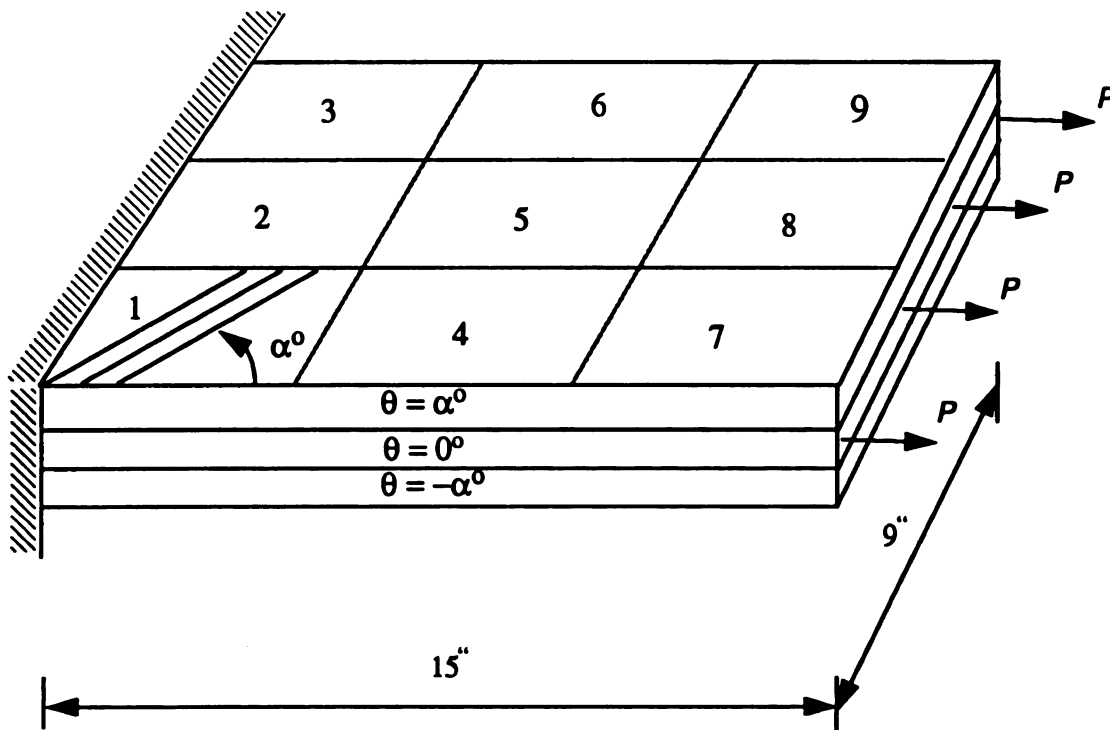


Figure 5.11 Three-ply laminated plate loaded in tension

Table 5.5 shows that the values of the first five natural frequencies from the nonlinear analysis (last iteration) are very close to those from the linear analysis (first iteration). This indicates that the nonlinearity has very little effect on the three-ply $[30^\circ/0^\circ/-30^\circ]$ and $[60^\circ/0^\circ/-60^\circ]$ laminates.

The number of iterations required for convergence as shown in Table 5.6 seems to be invariant with the increasing load level. This confirms that the nonlinearity of the constitutive law has a negligible effect on the three-ply laminated plate shown in Fig.5.9.

The variation of the absolute r.m.s. shear strain in the material coordinates at the center of element 2 with excitation load level is significantly less than for the two cases dis-

cussed previously. Fig. 5.12 and 5.13 show that the nonlinearity has negligible on the normalized r.m.s. shear & normal strains and stresses

TABLE 5.5 First five natural frequencies from linear (first iteration) and nonlinear (last iteration) analysis for load level $S_0 = 12000 \text{ lb}^2 \text{ sec}$.

Mode	[30°/0°/-30°]		[60°/0°/-60°]	
	First Iteration	Last Iteration	First Iteration	Last Iteration
1	23.2 HZ	23.4 HZ	17.9 HZ	17.9 HZ
2	81.4	81.6	65.2	65.1
3	101.5	101.6	80.7	80.4
4	146.9	147.8	110.0	109.6
5	260.6	261.3	215.3	215.3

TABLE 5.6 Number of iterations required for convergence

Load level, S_0 ($\text{lb}^2 \text{ s}$)	No. of iterations	
	[30°/0°/-30°]	[60°/0°/-60°]
1000	3	3
2000	3	3
3000	3	3
4000	3	3
5000	3	3
6000	3	3
7000	3	3
8000	3	3
9000	3	3
10000	3	3
11000	3	4
12000	3	4

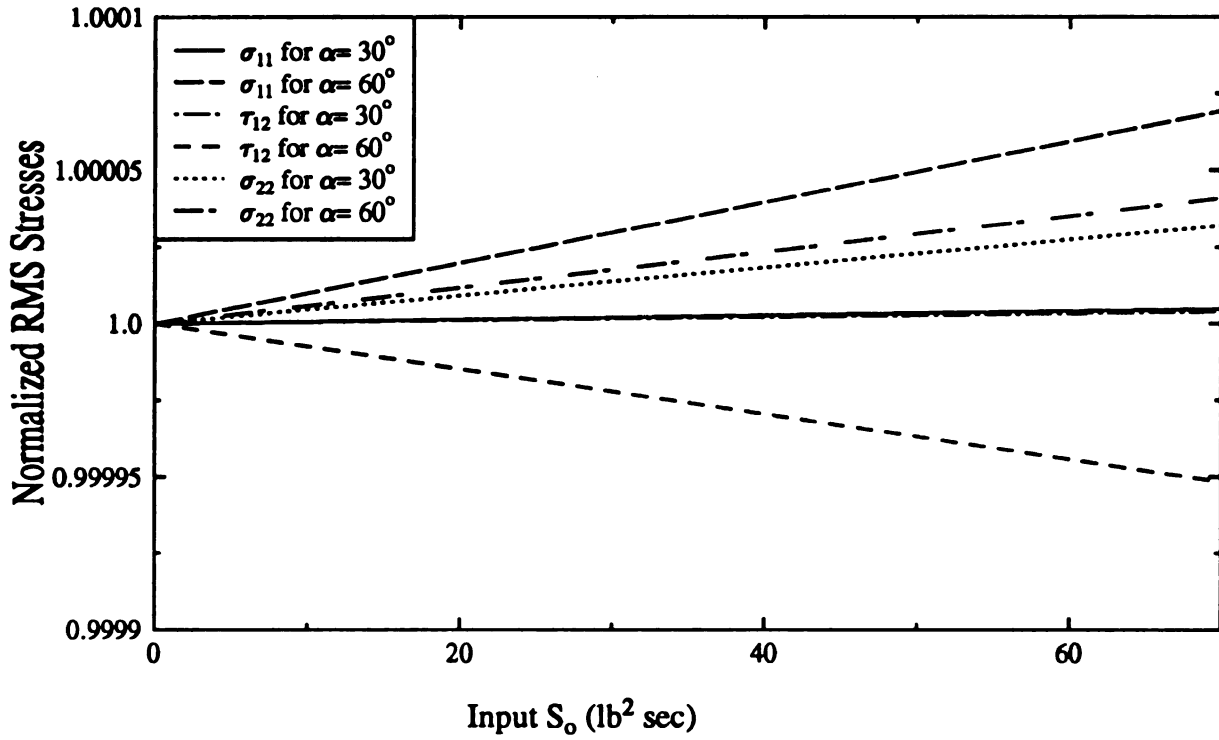


Figure 5.12 Variation of normalized r.m.s. stresses at the center of element 2 with excitation load level

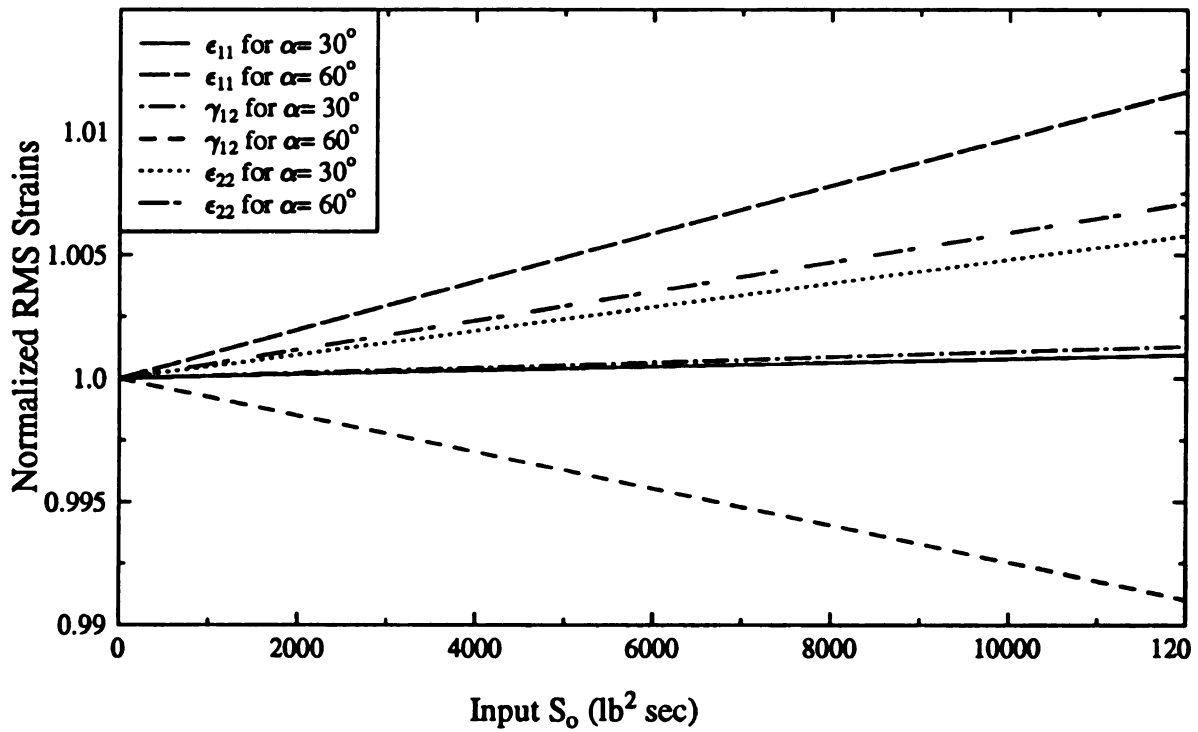


Figure 5.13 Variation of normalized r.m.s. strains at the center of element 2 with excitation load level

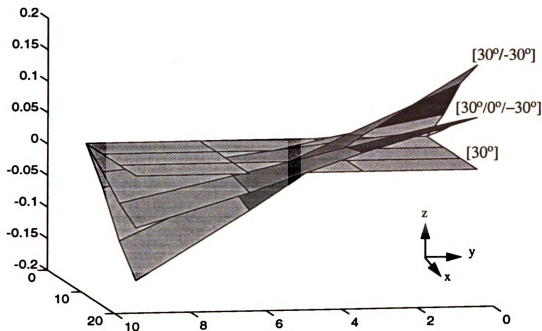


Figure 5.14 Twisting due to extensional loading for $[30^\circ]$, $[30^\circ/0^\circ/-30^\circ]$ and $[30^\circ/-30^\circ]$ at $S_0 = 8000$

The reason for the behavior exhibited by the three-ply plate is the presence of the middle layer with a fiber angle of 0° . Due to its fiber orientation, this layer is stiffer than the others, carries a larger share of the load, and since it responds essentially linearly to extensional load the overall response is approximately linear.

Fig. 5.14 shows the twisting effect which exists in unsymmetrical laminates. This important phenomena is due to the induced out-of-plane displacements by the extensional load. As expected the coupling between the in-plane loading and out-of-plane displacement is observed for cases I and II. Also, the figure indicates that less twisting is induced in the three-ply plate than in the two-ply plate.

5.2.2 Shear loading

The same cantilever plate used in the in-plane extensional loading with the same material properties and the same geometry is considered again, but now the loads are applied along the in-plane DOF in the y-direction. The white noise excitation spectrum level, S_0 , was increased from 1000 to 4000 lb² sec.

Case I: One-ply plate with fiber orientation α . Two values of α , 30° and 60° were used. Figure 5.15 shows the plate and the loaded DOF.

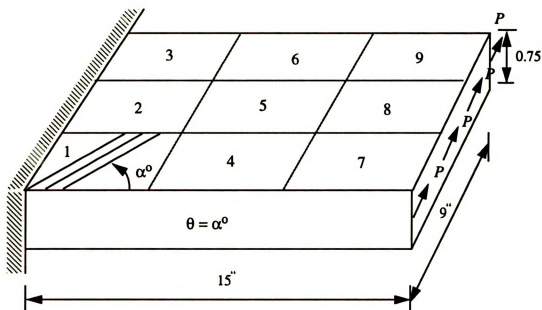


Figure 5.15 One-ply plate loaded in shear

Table 5.7 shows the effect of nonlinearity on the first five values of the natural frequencies from linear and nonlinear analysis for excitation level $S_0 = 4000$ lb² sec. Due to the effect of the nonlinearity, the values of the natural frequencies dropped by approximately 3 percent for both [30°] and [60°] one-ply plates.

The number of iterations required for convergence, listed in Table 5.8 increases with excitation load level since the nonlinearity becomes more dominant for higher loads. Table 5.8 also shows that a very large number of iterations are required at $S_0 > 5000$ lb² sec. This

is because for very high load levels, the shear response exceeds the range for which the approximate fifth-order shear stress-strain law is applicable.

TABLE 5.7 First five natural frequencies from linear (first iteration) and nonlinear (last iteration) analysis for load level $S_0 = 4000 \text{ lb}^2 \text{ sec}$.

Mode	[30°]		[60°]	
	First Iteration	Last Iteration	First Iteration	Last Iteration
1	25.5 HZ	24.7 HZ	15.7 HZ	15.5 HZ
2	52.8	50.6	47.6	46.7
3	96.7	95.5	74.5	72.0
4	139.4	133.2	95.2	94.0
5	170.5	166.1	101.5	98.5

TABLE 5.8 Number of iterations required for convergence

Load level, S_0 ($\text{lb}^2 \text{ s}$)	No. of Iterations	
	[30°]	[60°]
1000	4	4
2000	5	4
3000	5	4
4000	5	4
5000	8	4
6000	12	4
7000	21	5

The variation of the absolute shear strain in the material coordinates at the center of element 2 with excitation load level is shown in Fig. 5.16. The responses for the [30°] ply exhibits more nonlinearity than that of the [60°] ply. For $S_0 = 4000 \text{ lb}^2 \text{ sec}$, the r.m.s. shear strain is about 0.0062 for the [30°] ply. The peak shear strain would be expected to be in excess of three times the r.m.s. strain, which places it near the upper limit for which the fifth-order shear stress-strain law of Fig. 2.2 is applicable. For shear strains exceeding 0.02, the fifth-order law increases very rapidly, resulting in poor convergence.

The variation of the normalized r.m.s. y-displacement of the corner nodes with the excitation spectrum level S_0 is shown in Fig. 5.17. The figure illustrates that the proportional increase in the displacement due to the nonlinearity increases with the excitation level. The apparent increase in stiffness of the $[30^\circ/-30^\circ]$ laminate as S_0 exceeds $4000 \text{ lb}^2 \text{ sec}$ is again due to the fact that the approximate fifth-order stress-strain law breaks down for the high loads.

Figs. 5.18 and 5.19 show the normalized r.m.s normal and shear strains and stresses in material coordinates at the center of element 2 with the excitation level. The nonlinearity in the constitutive law has a significant effect on the shear strain for the $[30^\circ]$ ply (about 13%), but it shows negligible effect for the $[60^\circ]$ ply (less than 2%). Nonlinearity has a negligible effect on all stresses.

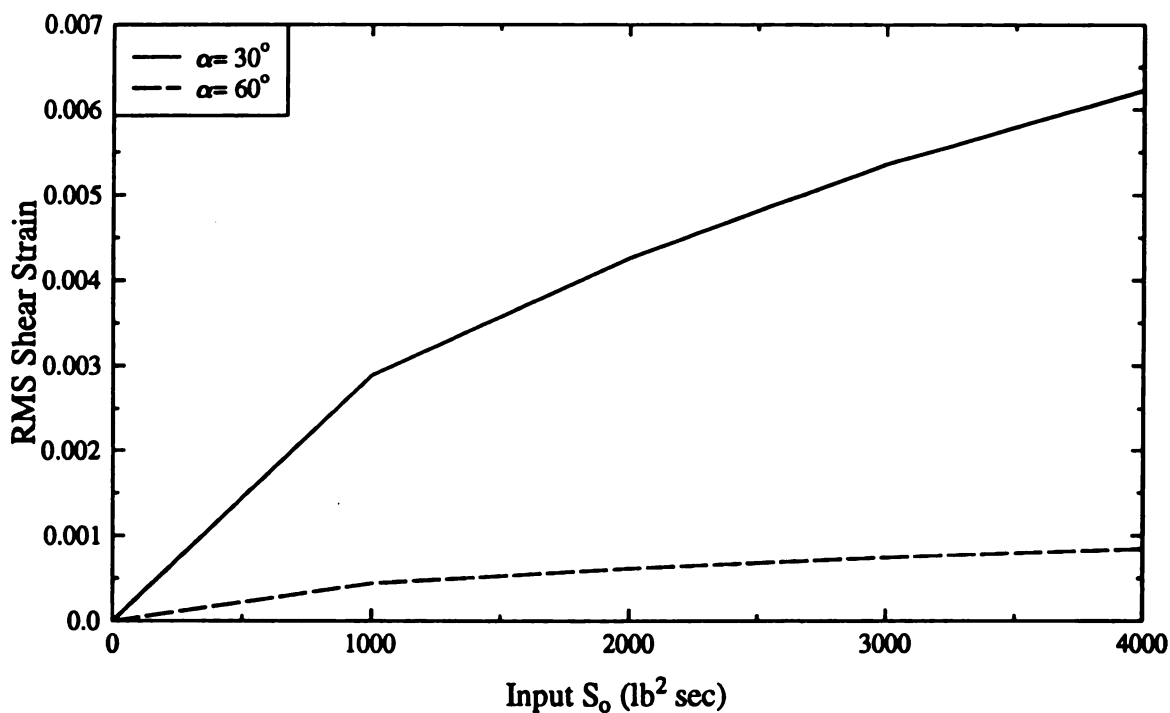


Figure 5.16 Variation of absolute r.m.s shear strain at the center of element 2 with excitation load level

Normalized RMS displacement

F

1

Normalized RMS Strains

0

Fig

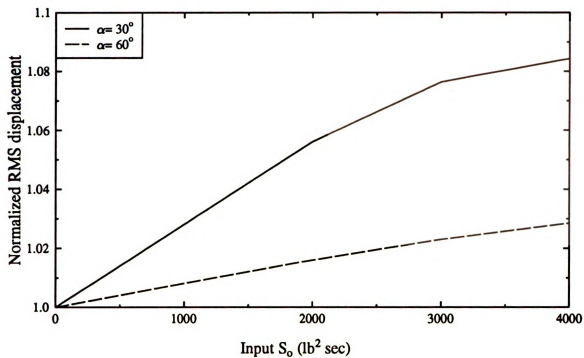


Figure 5.17 Variation of normalized r.m.s. displacement at free corner nodes with excitation level

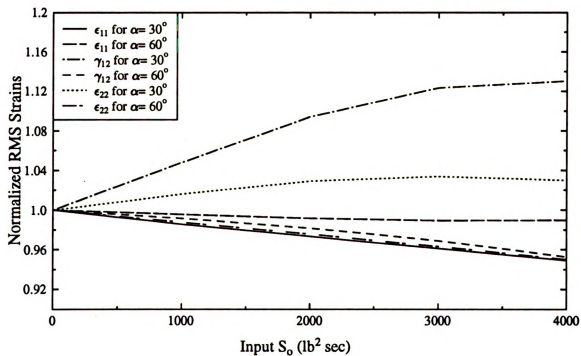


Figure 5.18 Variation of normalized r.m.s. strains at the center of element 2 with excitation load level

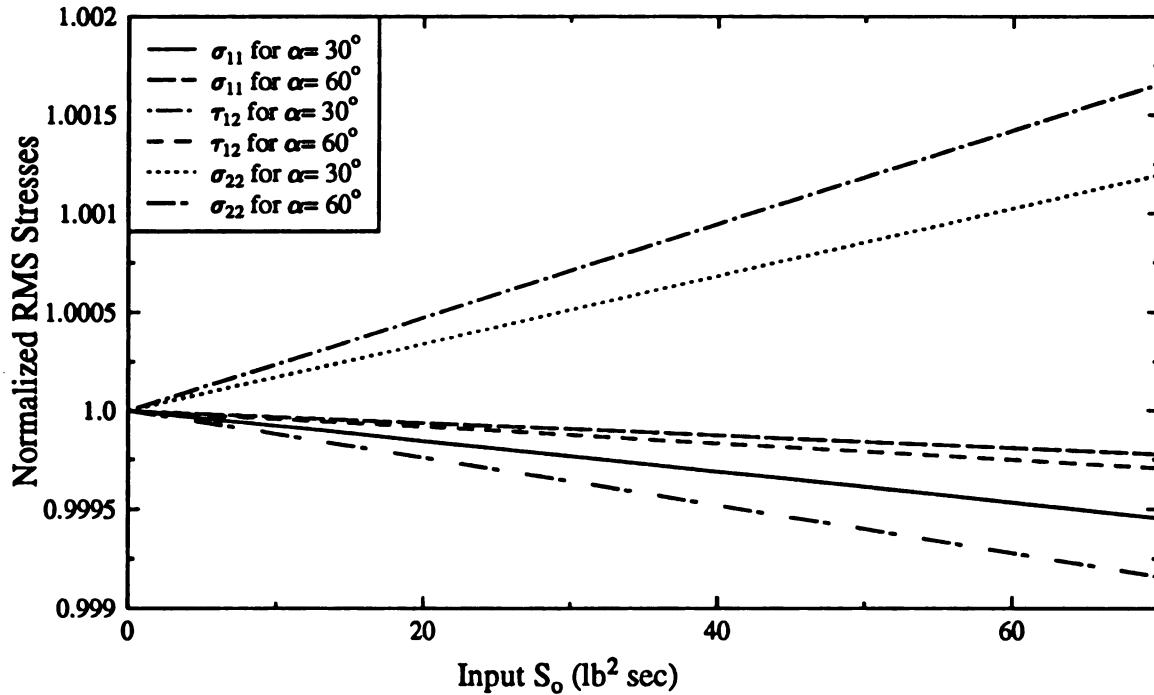


Figure 5.19 Variation of normalized r.m.s. stresses at the center of element 2 with excitation load level

Case II: Three-ply laminated plate with fiber orientation of α , 0 and $-\alpha$ in top, middle and bottom layers, respectively, as shown in Fig. 5.17. The total plate thickness is the same as in Case I. The level of excitation was increased from 5000 to 30000 lb² sec.

Table 5.9 shows the first five undamped natural frequencies from the linear and non-linear analysis (first and last iteration) of the three-ply laminated plate for the load spectrum level $S_o=30000$ lb² sec. Due to the softening effect of the shear nonlinearity, the natural frequencies show about 3 to 7% decreases. The laminate with the $[30^\circ/0^\circ/-30^\circ]$ arrangement is stiffer than the $[60^\circ/0^\circ/-60^\circ]$ laminate, as indicated by the higher natural frequencies.

Table 5.10 shows the number of iterations required for convergence of the r.m.s. nodal displacement. For the $[30^\circ/0^\circ/-30^\circ]$ laminate the number of iterations remain constant with the excitation load level, but the number of iterations increases with the excitation spectrum level for the $[60^\circ/0^\circ/-60^\circ]$ laminate. A large number of iterations are required for the $[60^\circ/0^\circ/$

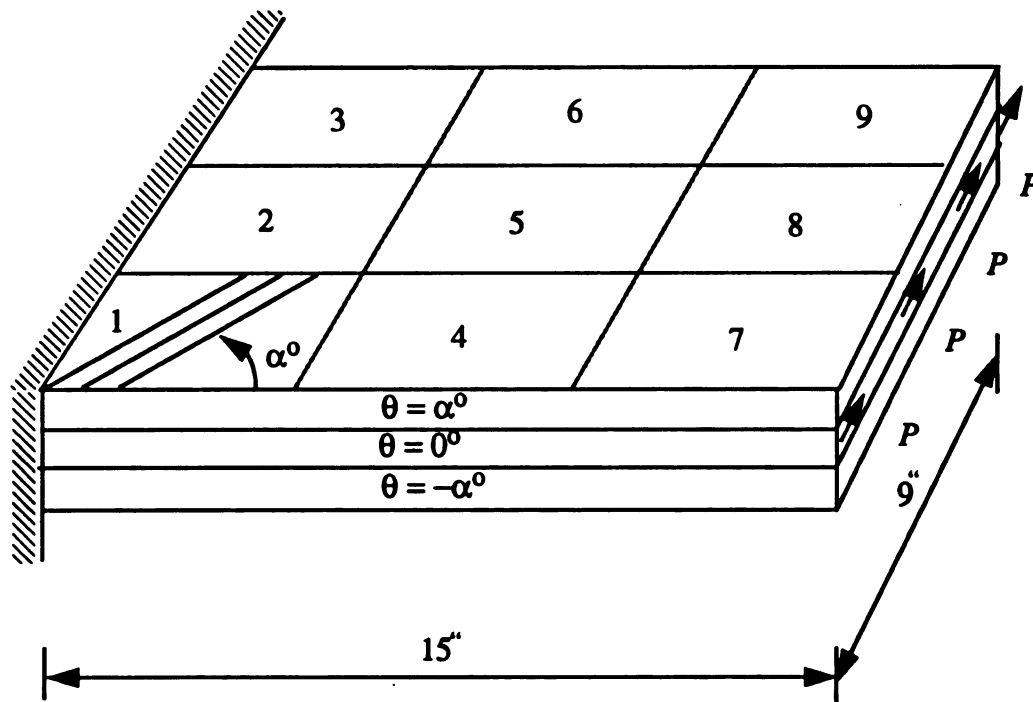


Figure 5.20 Tree-ply laminated plate loaded in shear

-60°] laminate at $S_0=25,000 \text{ lb}^2 \text{ sec}$. This indicates that the fifth order shear stress-strain law is not applicable for the $[60^\circ/0^\circ/-60^\circ]$ laminate at any load level about and beyond $25000 \text{ lb}^2 \text{ sec}$.

TABLE 5.9 First five natural frequencies from linear (first iteration) and nonlinear (last iteration) analysis for load level $S_0 = 30000 \text{ lb}^2 \text{ sec}$

Mode	$[30^\circ/0^\circ/-30^\circ]$		$[60^\circ/0^\circ/-60^\circ]$	
	First Iteration	Last Iteration	First Iteration	Last Iteration
1	23.4 HZ	21.8 HZ	18.0 HZ	17.7 HZ
2	81.6	79.7	65.3	64.0
3	101.6	100.4	80.7	78.1
4	147.9	137.7	110.0	106.6
5	261.3	253.6	215.3	213.3

TABLE 5.10 Number of iterations required for convergence

Load level, S_0 (lb^2s)	No. of iterations	
	[30°/0°/-30°]	[60°/0°/-60°]
5000	4	5
10000	5	6
15000	5	6
20000	5	6
25000	5	9
30000	5	14

Fig. 5.21 shows the variation of the absolute r.m.s. shear strain in material coordinates at the center of element 2 with excitation load level. The responses are clearly nonlinear. The effect of nonlinearity is comparable for both the [30°/0°/-30°] and [60°/0°/-60°] laminates.

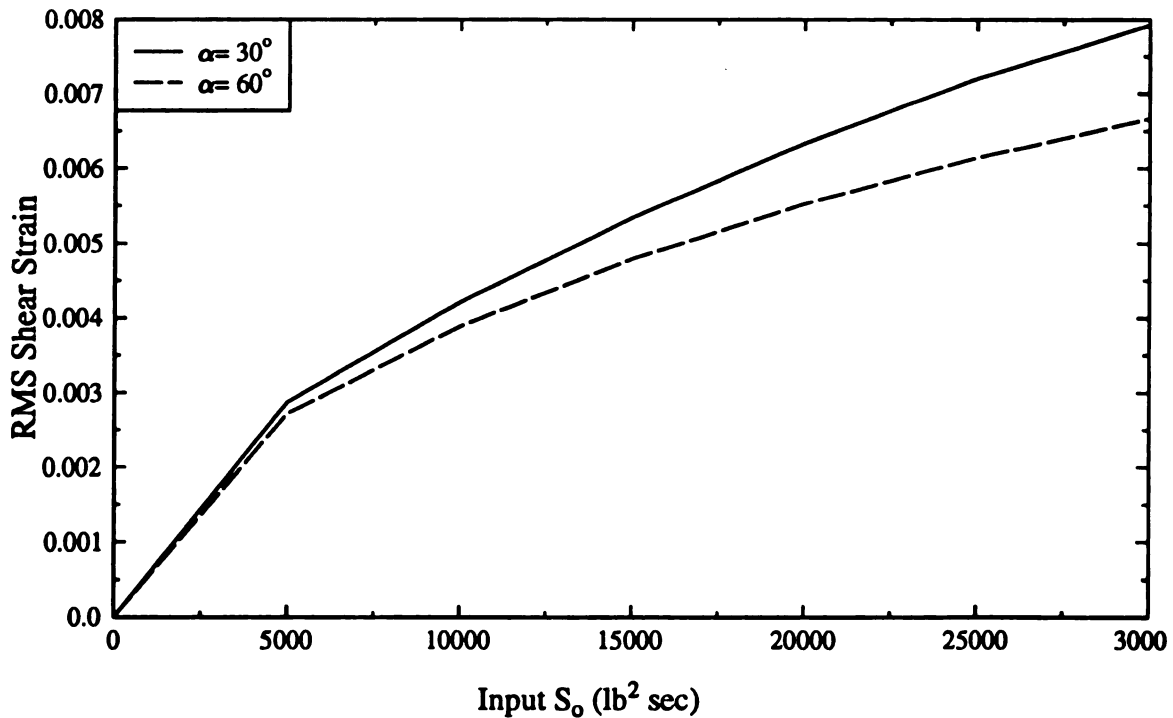


Figure 5.21 Variation of absolute r.m.s. shear strain at the center of element 2 with excitation load level

tati

the

tici

the

the

ati

rec

no

Normalized RMS displacement

The variation of the normalized r.m.s. y-displacement due to nonlinearity with excitation level, S_o , is shown in Fig. 5.22. There is a steady increase in the displacement with the excitation spectrum level due to the effect of nonlinearity. The fifth order approximation is not applicable for the $[60^\circ/0^\circ/-60^\circ]$ laminate at load levels above $20000 \text{ lb}^2 \text{ sec}$.

Fig 5.23 shows that the nonlinearity in the constitutive law has a significant effect on the shear strain of the $[30^\circ/0^\circ/-30^\circ]$ laminate and a negligible effect on the shear strain of the $[60^\circ/0^\circ/-60^\circ]$ laminate. The normalized normal strain in material direction 1 (ϵ_{11}) is relatively insensitive to nonlinear effects, whereas the normalized normal strain in material direction 2 (ϵ_{22}) shows a significant increase for both angles. Fig. 5.24 shows that nonlinearity is again negligible for all stresses.

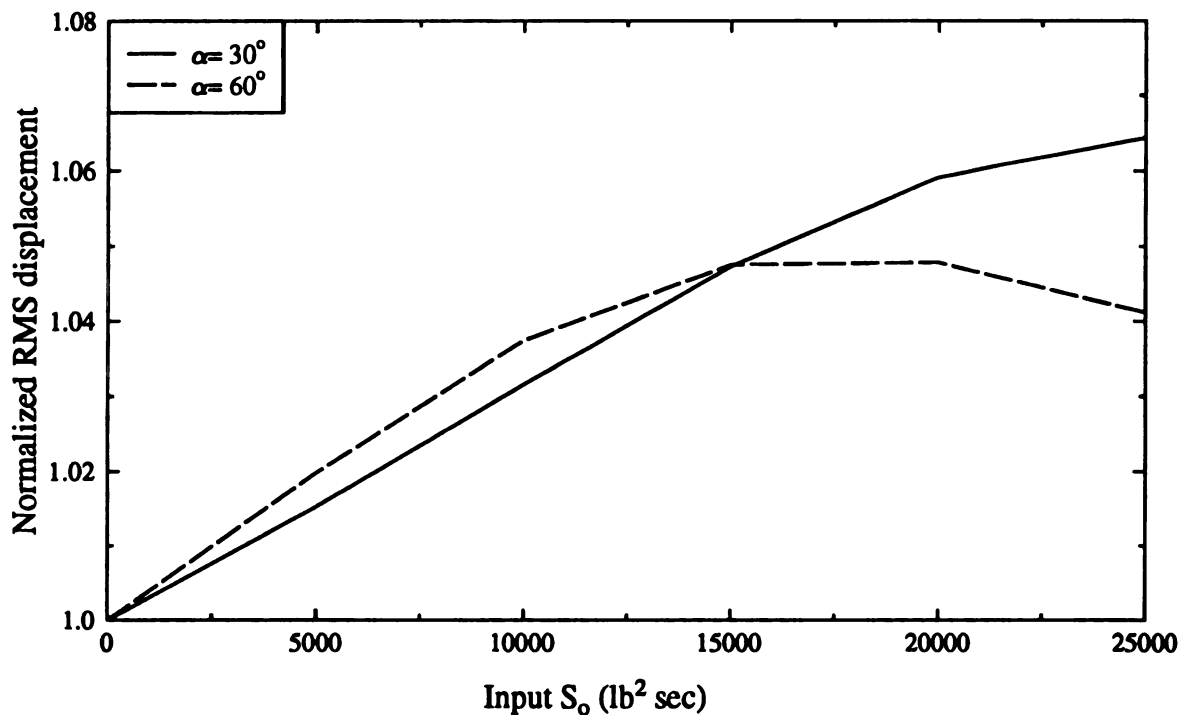


Figure 5.22 Variation of normalized r.m.s. displacement at free corner nodes with excitation load level

1.0
1.1
1.2
1.3
1.4
1.5
1.6
1.7
1.8
1.9
2.0
Normalized RMS Strains

Fig

1.0
1.1
1.2
1.3
1.4
1.5
1.6
1.7
1.8
1.9
2.0
Normalized RMS Stresses

Fig

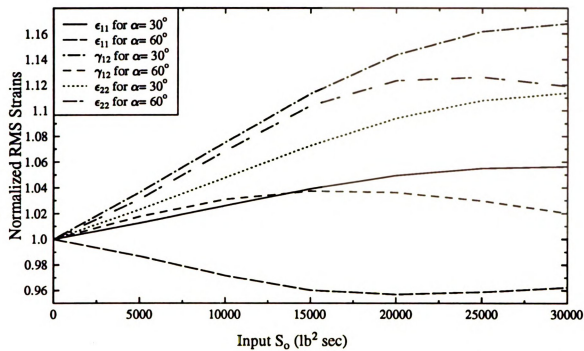


Figure 5.23 Variation of normalized r.m.s. strains at the center of element 2 with excitation load level

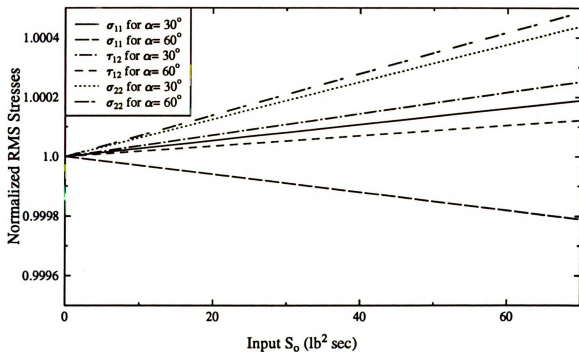


Figure 5.24 Variation of normalized r.m.s. stresses at the center of element 2 with excitation load level

5.3 Out

The
the same
z-directi
Ca
used. Fi

and no
ply ha
stiffer
neglig
al dis
load

5.3 Out-Of-Plane Loading

The same cantilever plate used in the in-plane extensional loading is considered with the same material properties and the same geometry, but now the out-of-plane DOF in the z-direction are loaded. The level of excitation was increased from 5 to 80 lb² sec.

Case I: One-ply plate with fiber orientation α . Two values of α , 30° and 60° were used. Figure 5.25 shows the plate and the loaded DOF.

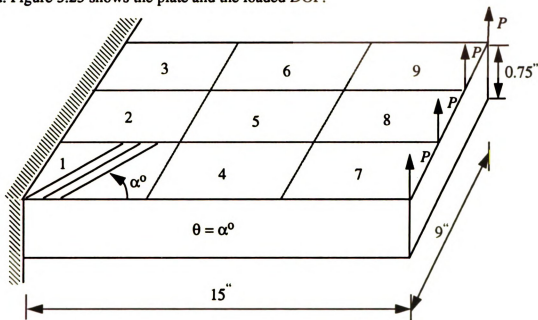


Figure 5.25 One-ply plate with fiber orientation α .

Table 5.11 shows the first five undamped natural frequencies of the plate from linear and nonlinear analysis for the excitations level corresponding to $S_0 = 80$ lb² sec. The [30°] ply has higher natural frequencies than the [60°] ply which indicates that the former ply is stiffer. Due to the softening effect of the shear nonlinearity, the natural frequencies show negligible decrease for the [60°] ply, and a slight decrease for the [30°] ply.

Table 5.12 shows the number of iterations required for convergence of the r.m.s. nodal displacements. The number of iterations remains approximately constant for the range of loads and comparable for [30°] and [60°]

TAE
here

of e

give

lam

the e

for t

mal

citati

resu

TABLE 5.11 First five natural frequencies from linear (first iteration) and nonlinear (last iteration) analysis for load level $S_0 = 80 \text{ lb}^2 \text{ sec}$

Mode	[30°]		[60°]	
	First Iteration	Last Iteration	First Iteration	Last Iteration
1	25.5	24.6	15.7	15.4
2	52.8	51.3	47.6	47.1
3	96.7	95.5	74.5	71.7
4	139.4	135.8	95.2	93.7
5	170.5	166.6	101.5	99.3

TABLE 5.12 Number of iterations required for convergence

Load level, S_0 ($\text{lb}^2 \text{ s}$)	No. of iterations	
	[30°]	[60°]
5	3	3
10	3	3
20	4	4
40	4	4
60	4	4
80	4	4

The variation of the absolute r.m.s. shear strains in material coordinates at the center of element 2 are shown in Fig. 5.26. The responses are clearly nonlinear. Note that for any given excitation level, the shear strain for the [30°] laminate is less than that for the [60°] laminate. The variation of the normalized r.m.s. z-displacement of the corner nodes with the excitation spectrum level, S_0 , is shown in Fig. 5.27. The nonlinearity is less pronounced for the fiber orientation of [30°] than for [60°]. The variation of the normalized r.m.s. normal and shear strains and stresses in material directions at the center of element 2 with excitation level are shown in Figs. 5.28 and 5.29. The nonlinearity in the constitutive law results in a slight increase of most strains and stresses.

0.012

0.01

0.005

0.00

0.00

0.00

0

Figure

1.

Normalized RMS displacement

1

1

1

F

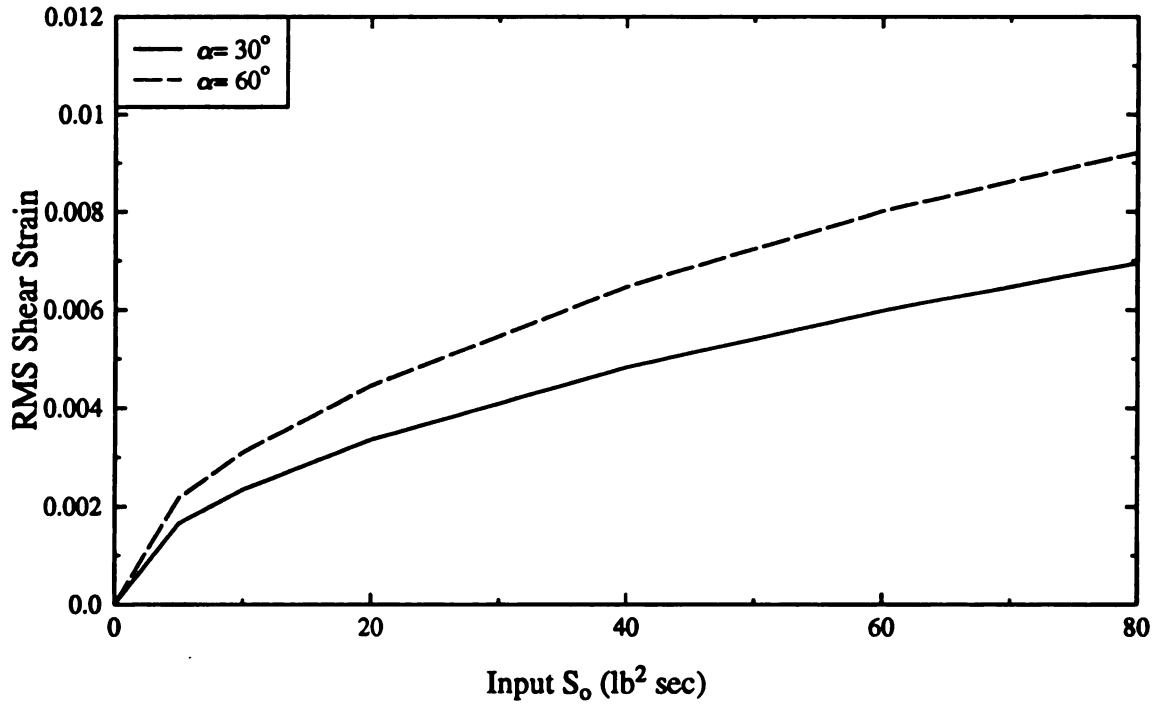


Figure 5.26 Variation of absolute r.m.s. shear strain at the center of element 2 with excitation load level

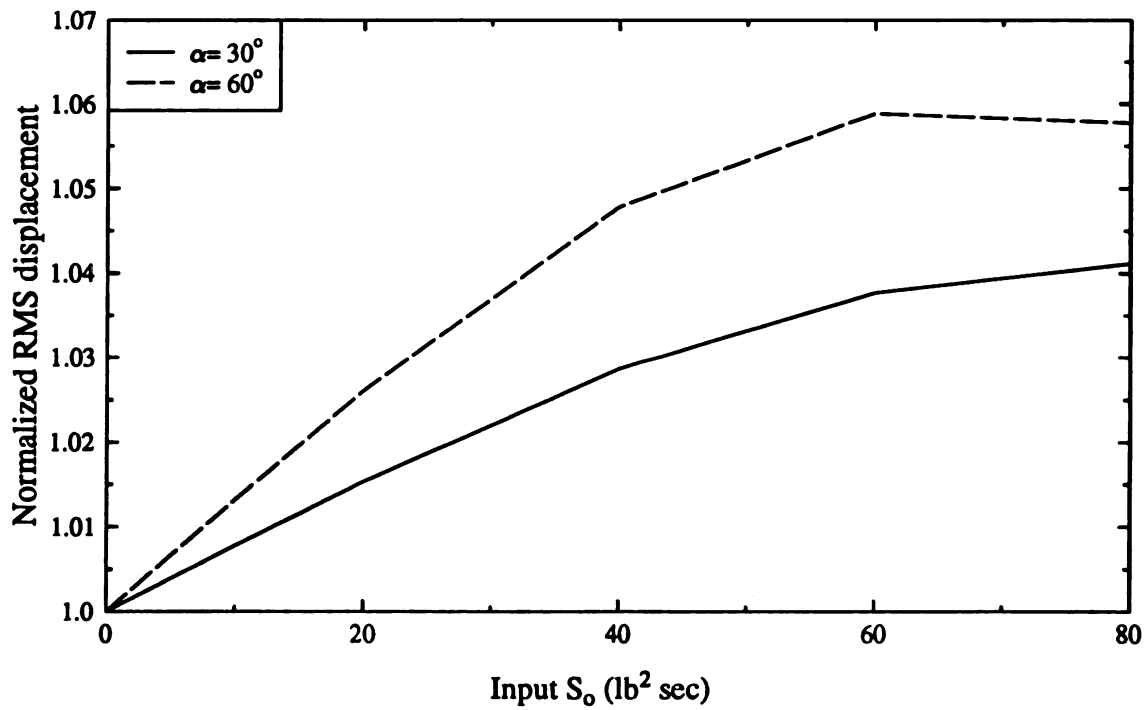


Figure 5.27 Variation of normalized r.m.s. displacement at free corner node with excitation load level

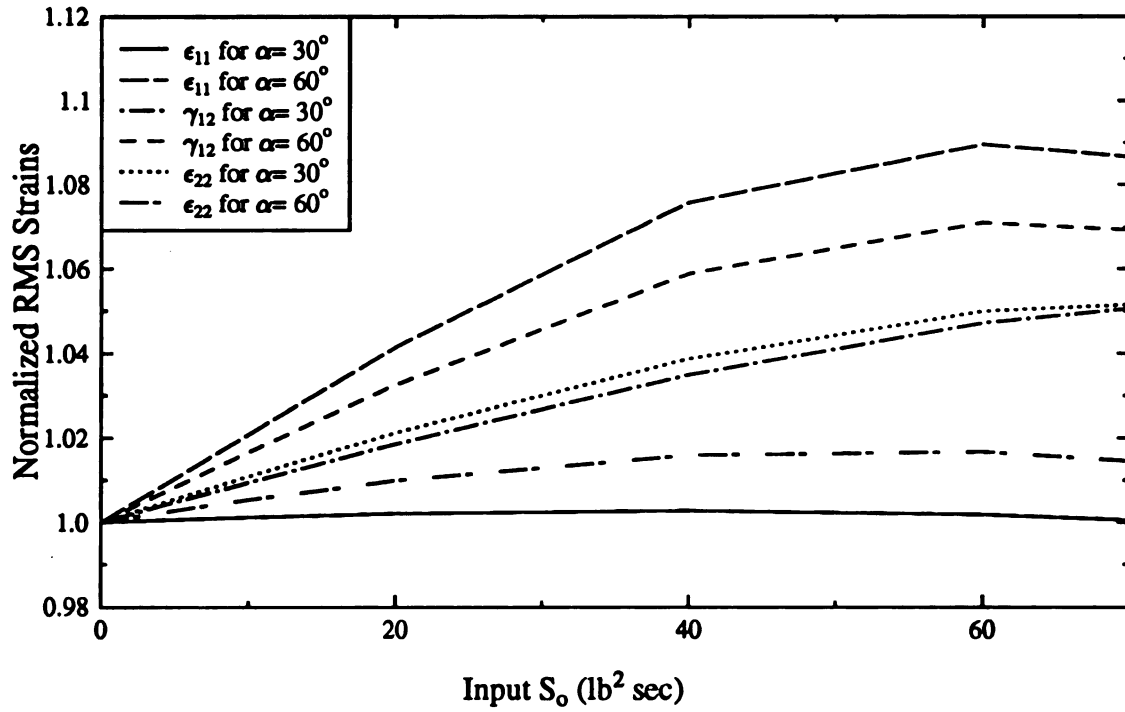


Figure 5.28 Variation of normalized r.m.s. strains at the center of element 2 with excitation load level

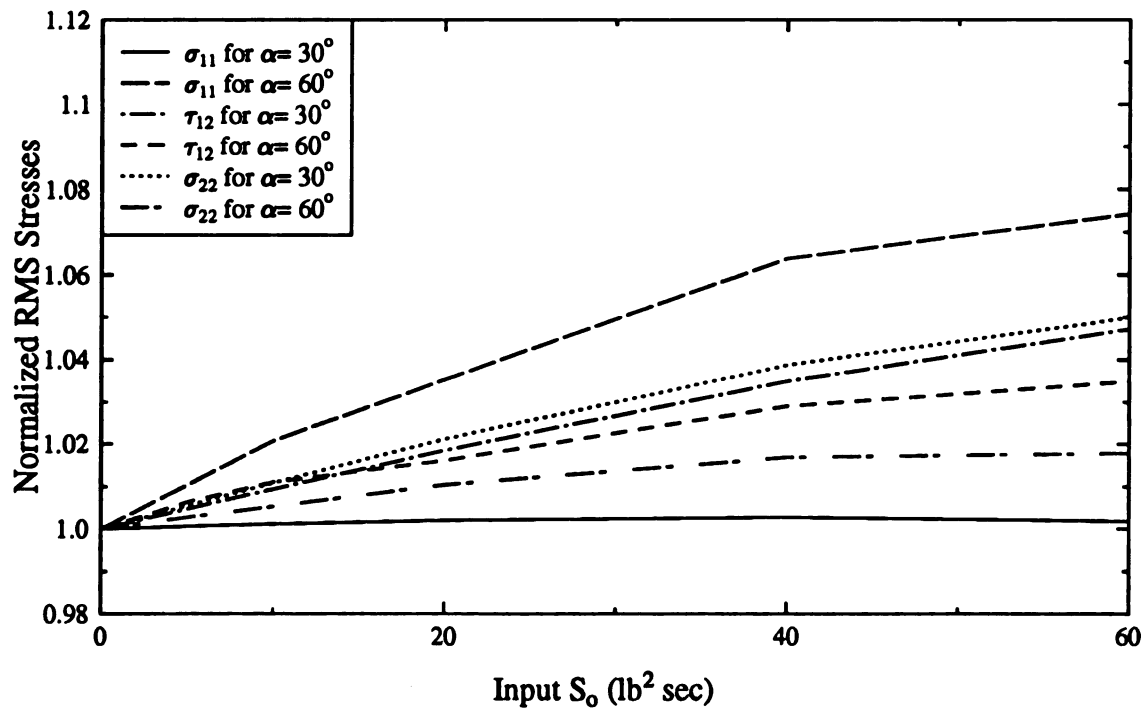


Figure 5.29 Variation of normalized r.m.s. stresses at the center of element 2 with excitation load level

Case II: Two-ply laminated plate with fiber orientation α and $-\alpha$ in top and bottom layers, respectively, as shown in Figure 5.30. The total plate thickness is the same as in Case I.

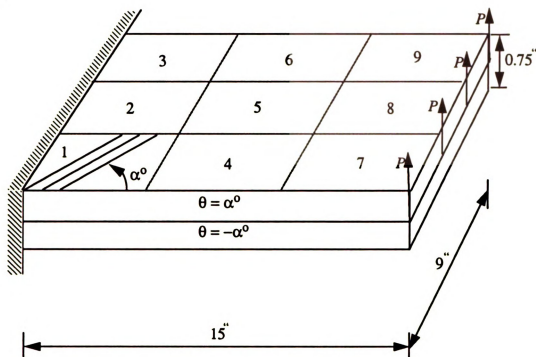


Figure 5.30 Two-ply plate with fiber orientation α

Table 5.13 lists the first five natural frequencies from linear and nonlinear analysis for the excitation level $S_0 = 80 \text{ lb}^2 \text{ sec}$. Due to the softening effect of the shear nonlinearity, the natural frequencies show a slight decrease. Note that the laminate $[30^\circ/-30^\circ]$ is stiffer than that of $[60^\circ/-60^\circ]$ as indicated by its higher natural frequencies.

Table 5.14 indicates that the number of iterations required for convergence of the $[30^\circ/-30^\circ]$ laminate are comparable to those of the $[60^\circ/-60^\circ]$ laminate. The number of iterations is approximately the same at all load levels.

Fig. 5.31 shows that the r.m.s. shear strain exceeds 0.007 at S_0 values of about $75 \text{ lb}^2 \text{ sec}$ for the $[30^\circ/-30^\circ]$ laminate and about $45 \text{ lb}^2 \text{ sec}$ for $[60^\circ/-60^\circ]$ laminates. As described earlier, for load levels in excess of these values the approximate fifth-order shear stress-strain law breaks down.

TABLE 5.13 First five natural frequencies from linear (first iteration) and nonlinear (last iteration) analysis for load level $S_0 = 80 \text{ lb}^2 \text{ sec}$

Mode	[30°/-30°]		[60°/-60°]	
	First Iteration	Last Iteration	First Iteration	Last Iteration
1	24.0 HZ	23.1 HZ	15.6 HZ	15.2 HZ
2	74.5	73.3	46.4	45.8
3	92.2	91.	86.7	85.3
4	152.5	148.2	95.0	92.7
5	215.8	212.6	103.7	101.4

TABLE 5.14 Number of iterations required for convergence

Load level, S_0 ($\text{lb}^2 \text{s}$)	No. of iterations	
	[30°/-30°]	[60°/-60°]
5	3	3
10	3	3
20	4	4
40	4	4
60	4	3
80	4	4

Fig. 5.32 shows that nonlinearity causes the r.m.s. z-displacement of the corner nodes to increase by about 6% for the [30°/-30°] laminate and about 3.5% for the [60°/-60°] laminate at S_0 values of 80 and 60 $\text{lb}^2 \text{ sec}$, respectively.

Figs. 5.33 and 5.34 show the effect of nonlinearity on the normal and shear strains and stresses. They indicate that the nonlinearity in the constitutive law significantly affects most strains and stresses.

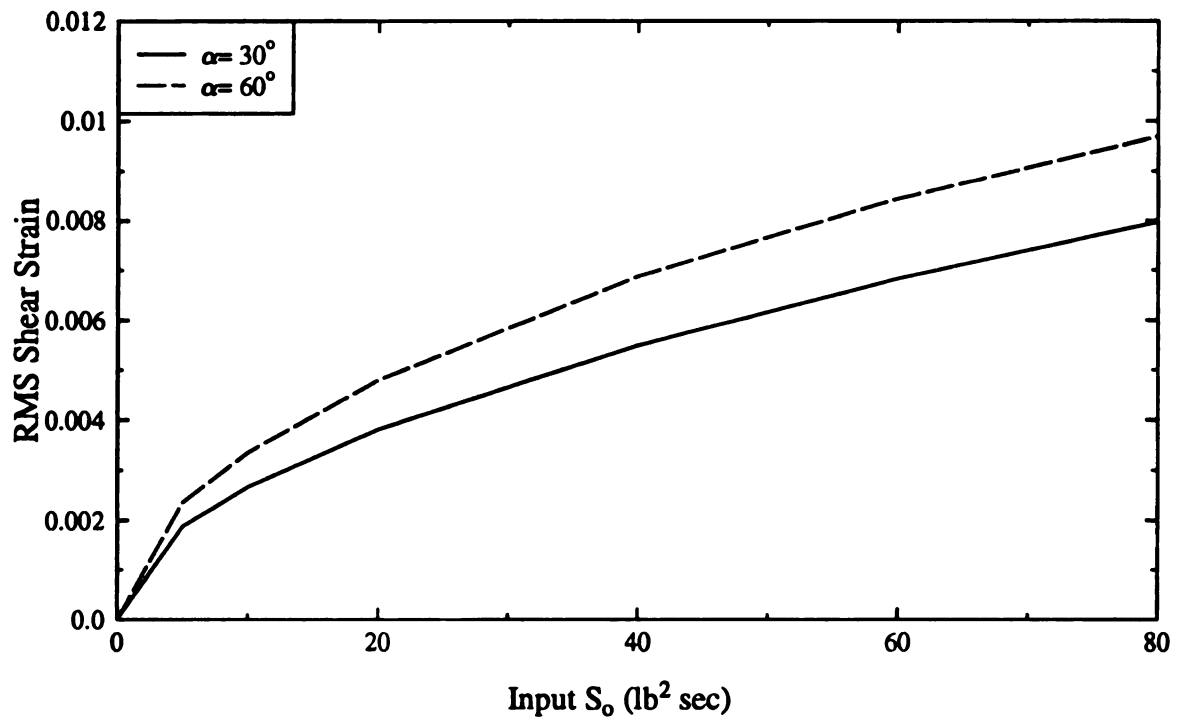


Figure 5.31 Variation of absolute r.m.s. shear strain at the center of element 2 with excitation load level

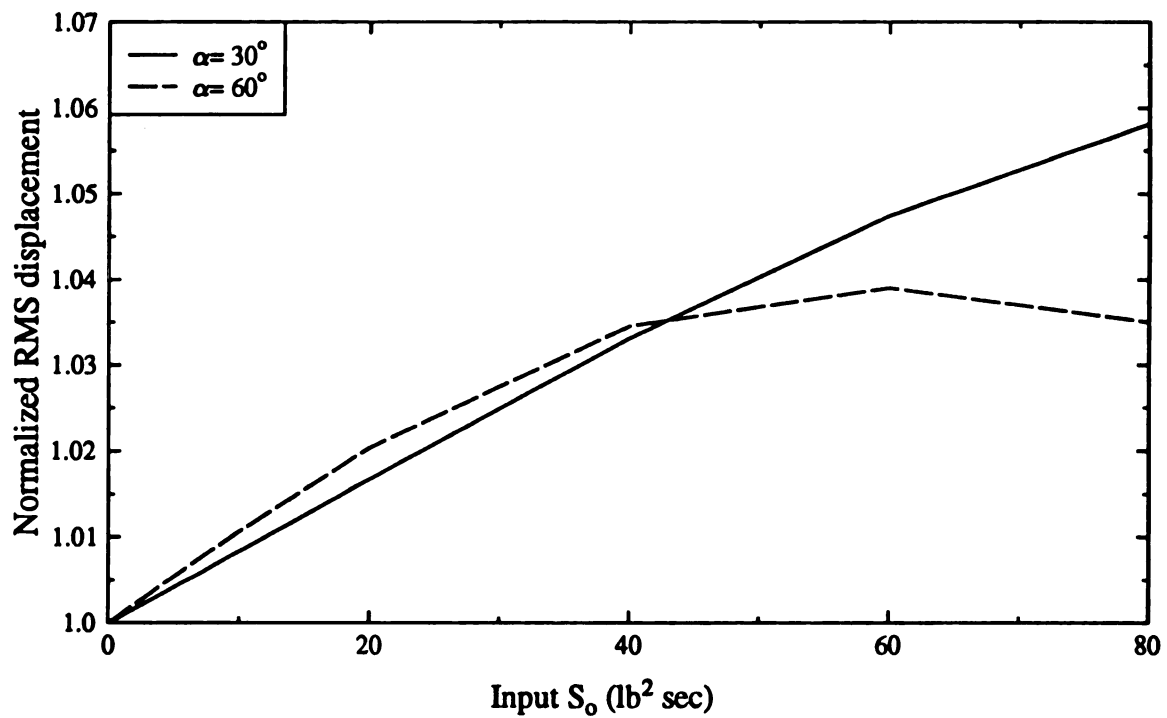


Figure 5.32 Variation of normalized r.m.s. displacement at free corner node with excitation load level

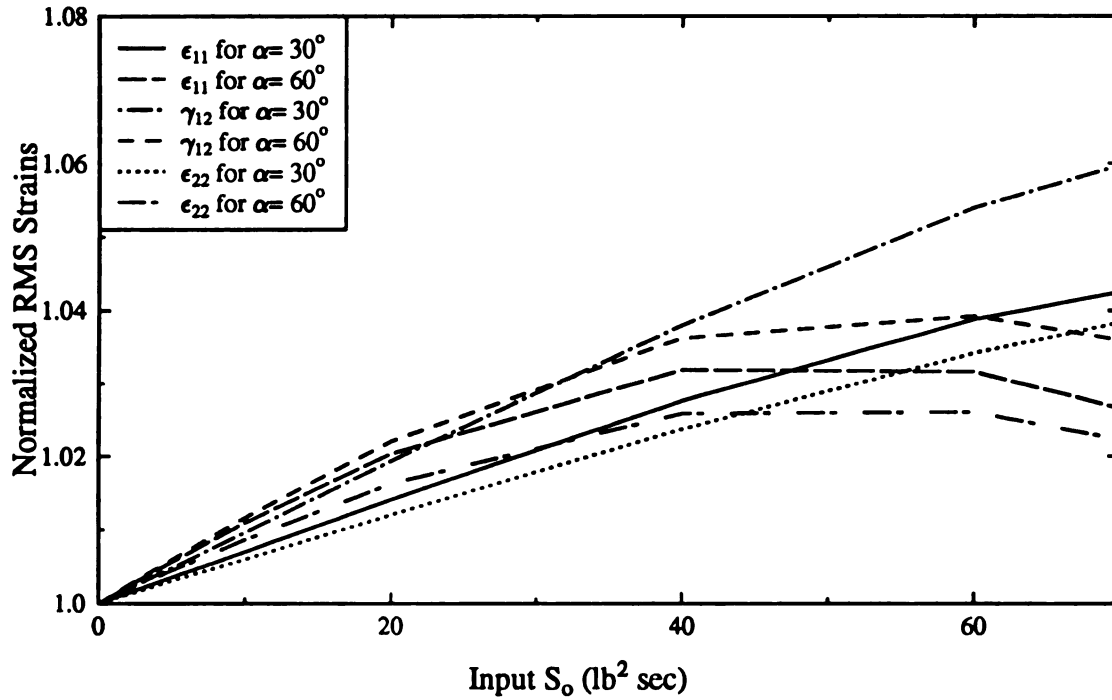


Figure 5.33 Variation of normalized r.m.s. strains at the center of element 2 with excitation load level

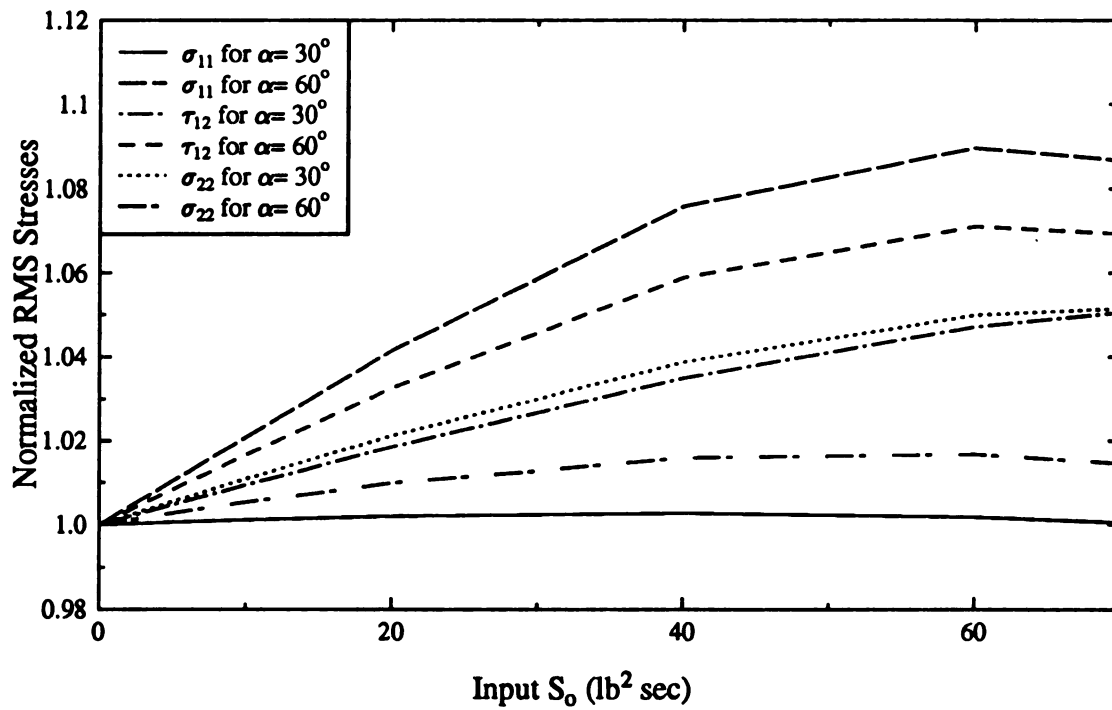


Figure 5.34 Variation of normalized r.m.s. stresses at the center of element 2 with excitation load level

Case III: Three-ply laminated plate with fiber orientation of α , 0 and $-\alpha$ in the top, middle and bottom layers, respectively The total plate thickness is identical to that used in Cases I and II.

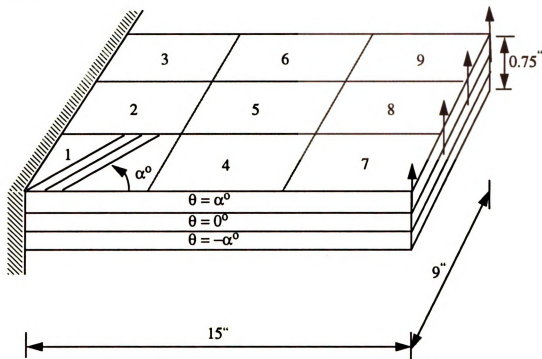


Figure 5.35 One-ply plate with fiber orientation α

Table 5.15 shows the first five undamped natural frequencies of the plate from the first and last iteration of the analysis, for the excitations level $S_0 = 80 \text{ lb}^2 \text{ sec}$. The values from the first iteration correspond to the case where nonlinearity is neglected, while the values from the last iteration show the effect of nonlinearity. Due to the softening effect of the shear nonlinearity, the natural frequencies show slight decreases. The ply arrangement with $[30^\circ/0^\circ/-30^\circ]$ is stiffer than the arrangement with $[60^\circ/0^\circ/-60^\circ]$, as indicated by the higher natural frequencies for the former case

Table 5.16 shows the number of iterations required for convergence of the root-mean-square (r.m.s) nodal displacements according to the criterion in Eq. 3.50 with $\epsilon = 10^{-3}$. The number of iterations required for convergence increases with the excitation load level

TABLE 5.15 First five natural frequencies from linear (first iteration) and nonlinear (last iteration) analysis for load level $S_0 = 80 \text{ lb}^2 \text{ sec}$

Mode	[30°/0°/-30°]		[60°/0°/-60°]	
	First Iteration	Last Iteration	First Iteration	Last Iteration
1	23.2 HZ	22.8 HZ	18.0 HZ	17.7 HZ
2	81.4	80.8	65.3	64.6
3	101.5	100.9	80.7	79.4
4	146.9	143.4	110.0	108.6
5	260.6	258.2	215.3	214.4

TABLE 5.16 Number of iterations required for convergence

Load level, S_0 ($\text{lb}^2 \text{ s}$)	No. of iterations	
	[30°/0°/-30°]	[60°/0°/-60°]
5	4	3
10	4	3
20	5	3
40	6	3
60	6	3
80	6	3

since the nonlinearity becomes more pronounced for higher loads. For any particular load level the number of iterations required for the ply arrangement with [30°/0°/-30°] is more than the corresponding number for the [60°/0°/-60°] laminate. This indicates the nonlinearity is less pronounced for [60°/0°/-60°].

The variation of the absolute shear strain in material coordinates at the center of element 2 with the excitation load level is shown in Fig. 5.36 and the responses are clearly non-linear. For any given excitation level, the shear strain for the [60°/0°/-60°] laminate is significantly less than that for the [30°/0°/-30°] laminate.

The variation of the normalized r.m.s. z-displacement of the corner nodes with the excitation spectrum level, S_0 , is shown in Fig. 5.37. The displacement is normalized dividing by the linear response (for which $[K^*] = [0]$). The figure illustrates that the proportional increase in the displacement due to nonlinearity steadily increases with the excitation level. The effect of nonlinearity is less pronounced for the $[60^\circ/0^\circ-60^\circ]$ laminate than for the $[30^\circ/0^\circ/-30^\circ]$ laminate. This is because the smaller shear strains in the former case reduce the overall level of nonlinearity.

The variation of normalized r.m.s. shear and normal strains and stresses in material coordinates at the center of element 2 with the excitation level are shown in Figs. 5.38 and 5.39. Again the normalizations have been performed by dividing by the corresponding linear responses. The nonlinearity in the constitutive law results in a significant increase in the shear and normal strains and stresses for the $[30^\circ/0^\circ/-30^\circ]$ laminate, but it does not affect the normal strains and shear strain for the $[60^\circ/0^\circ/-60^\circ]$ laminate.

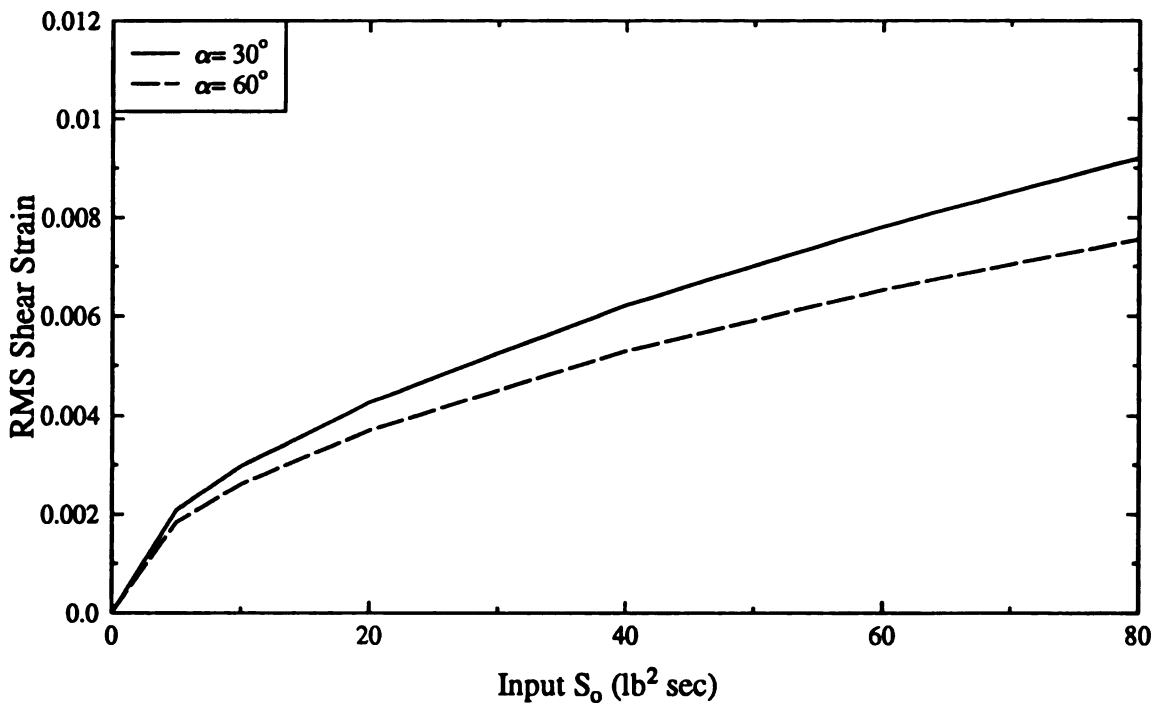


Figure 5.36 Variation of absolute r.m.s. strain at the center of element 2 with excitation load level

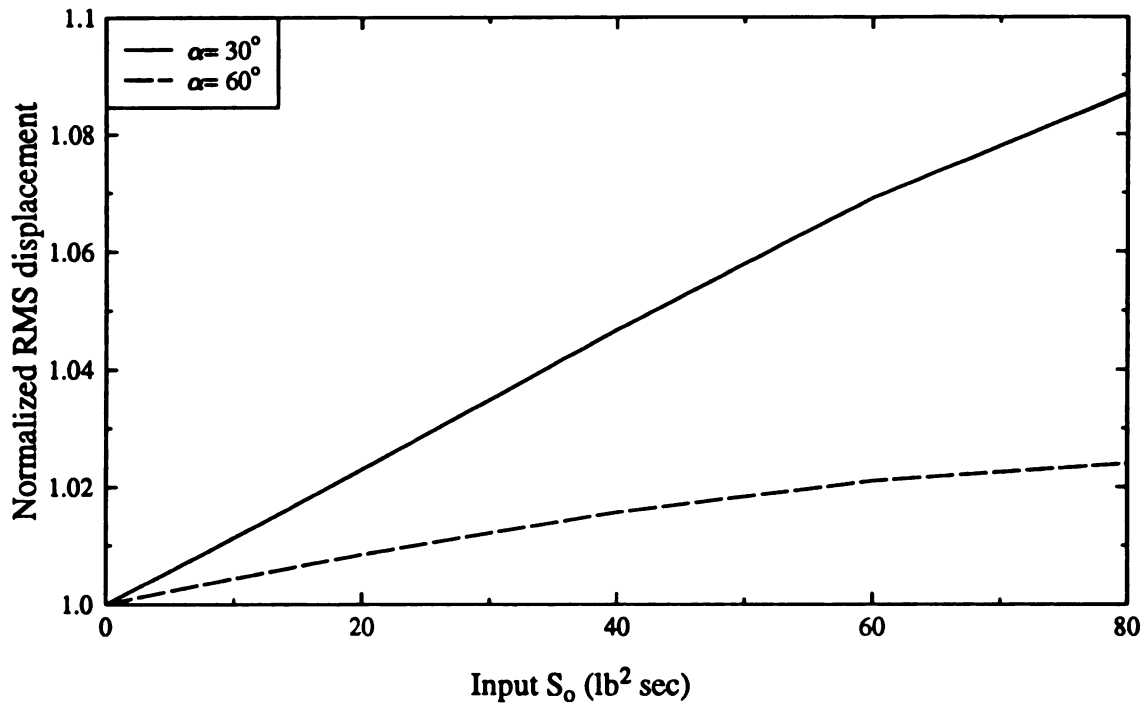


Figure 5.37 Variation of normalized r.m.s. displacement at free corner node with excitation load level

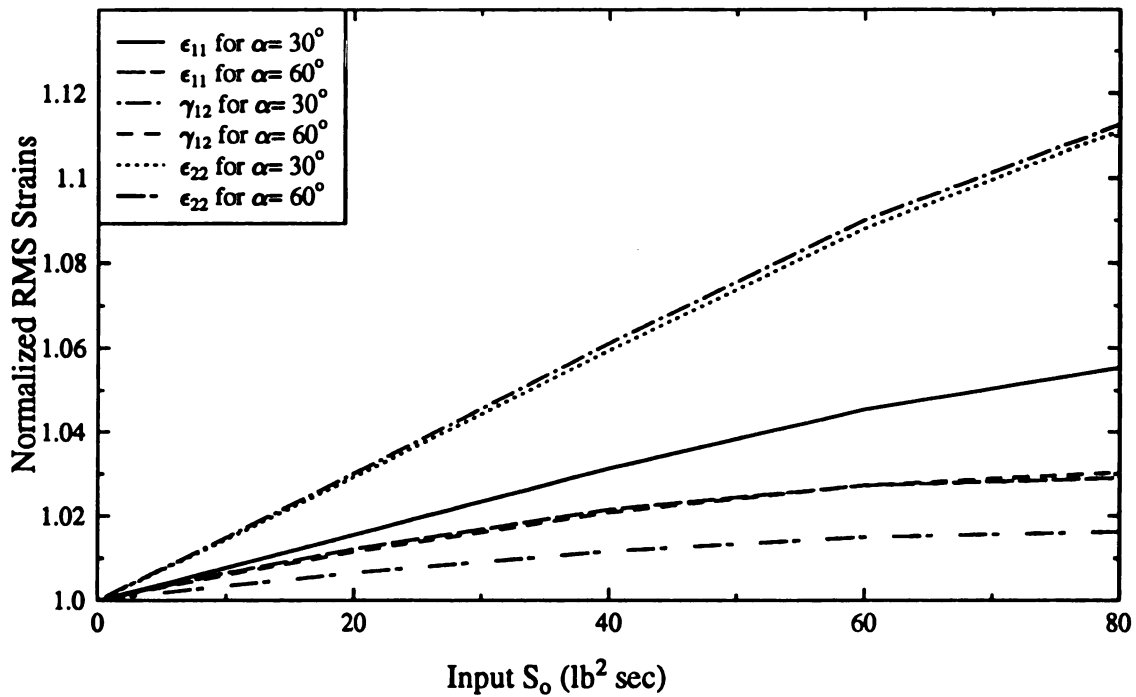


Figure 5.38 Variation of normalized r.m.s. strains at the center of element 2 with excitation load level

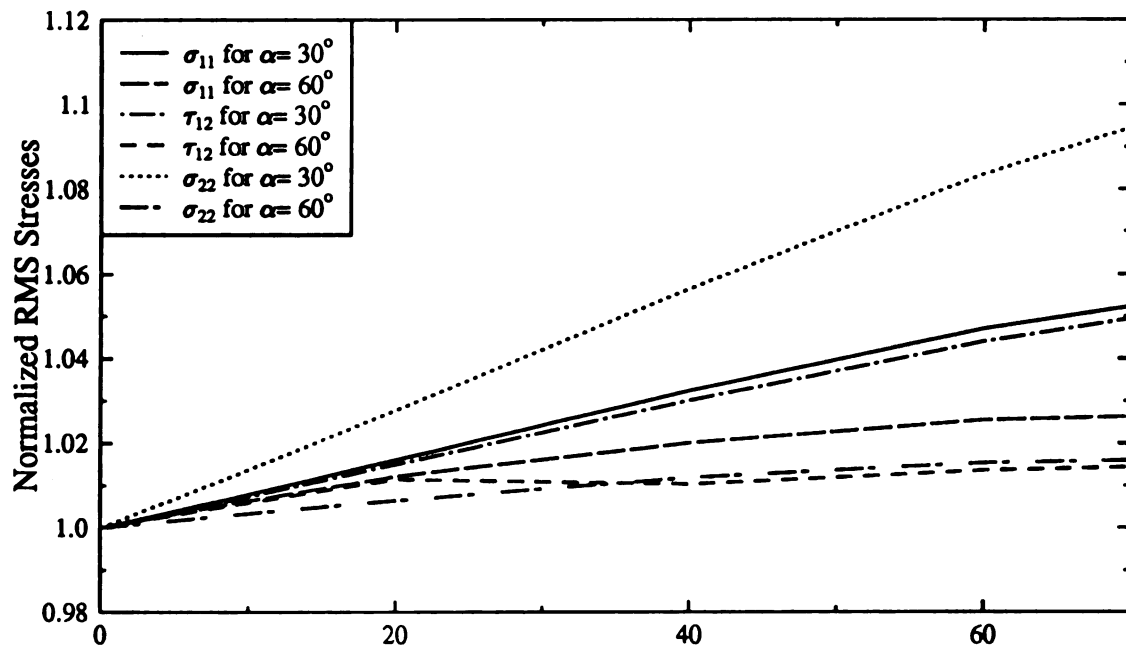


Figure 5.39 Variation of normalized r.m.s. stresses at the center of element 2 with excitation load level

in

TA



Table 5.17 provides an overall summary of the responses for which nonlinearity is important for the Narmco 5505 material.

TABLE 5.17 The significance of nonlinearity on the responses of various loading conditions

Loading	Stacking Sequence	Responses for which nonlinearity is significant		
		Low less than 5%	Moderate 5 - 10%	High more than 10%
In-plane extension	[30°]	$\sigma_{11}, \sigma_{22}, \epsilon_{11}, \epsilon_{22}$	γ_{12}, τ_{12}	u
	[60°]	$\sigma_{11}, \sigma_{22}, \epsilon_{11}, \epsilon_{22}$	γ_{12}, τ_{12}	u
	[30°/30°]	$\sigma_{11}, \sigma_{22}, \epsilon_{11}, \gamma_{12}, \tau_{12}, \epsilon_{22}, u$		
	[60°/60°]	σ_{22}, τ_{12}	γ_{12}	$\sigma_{11}, \epsilon_{11}, \epsilon_{22}, u$
	[30°/0°/60°]	$\epsilon_{11}, \epsilon_{22}, \gamma_{12}, \sigma_{11}, \sigma_{22}, \tau_{12}, u$		
	[60°/0°/60°]	$\epsilon_{11}, \epsilon_{22}, \gamma_{12}, \sigma_{11}, \sigma_{22}, \tau_{12}, u$		
In-plane shear	[30°]	$\epsilon_{11}, \epsilon_{22}, \sigma_{11}, \tau_{12}, \sigma_{22}$	v	γ_{12}
	[60°]	$\epsilon_{11}, \epsilon_{22}, \gamma_{12}, v, \sigma_{11}, \tau_{12}, \sigma_{22}$		
	[30°/0°/30°]	$\sigma_{11}, \tau_{12}, \sigma_{22}$	ϵ_{11}, v	$\epsilon_{22}, \gamma_{12}$
	[60°/0°/60°]	$\epsilon_{11}, \gamma_{12}, \sigma_{11}, \tau_{12}, \sigma_{22}$	v	ϵ_{22}
Out-of- plane	[30°]	$\epsilon_{11}, \epsilon_{22}, \gamma_{12}, w, \sigma_{11}, \tau_{12}, \sigma_{22}$		
	[60°]	$\epsilon_{22}, \sigma_{12}, \sigma_{22}$	$\gamma_{12}, w, \sigma_{11}$	ϵ_{11}
	[30°/30°]	$\epsilon_{22}, \sigma_{11}$	$\epsilon_{11}, \gamma_{12}, w, \tau_{12}, \sigma_{22}$	
	[60°/60°]	$\epsilon_{11}, \epsilon_{22}, \gamma_{12}, w, \sigma_{22}$	σ_{11}, τ_{12}	
	[30°/0°/30°]		$\sigma_{11}, \epsilon_{11}, \tau_{12}, w$	$\sigma_{22}, \epsilon_{22}, \gamma_{12}$
	[60°/0°/60°]	$\sigma_{11}, \sigma_{22}, \tau_{12}, \epsilon_{11}, \epsilon_{22}, \gamma_{12}, w$		

6. Conclusions and Recommendations

6.1 Conclusions

A general formulation for the nonlinear random vibration analysis of laminated composite plates modeled using finite elements and classical plate theory is presented. Only nonlinearity in the shear stress-strain law, which is most significant for filamentary composites, is considered. An approximate representation of the non-linear shear stress-strain law in terms of an odd-powered polynomial of arbitrary order results in a tractable formulation that is sufficiently accurate for practical purposes. The solution is performed iteratively using linear random vibration analysis during each iteration. Although classical laminate theory is often inadequate for composite laminates, it was used as a starting point in this study. An overview of the finite element discretization is presented. The plate element considered is a four noded one having 5 degrees-of-freedom per node.

The bending-extension coupling which always exists for unsymmetrical laminates was investigated. The numerical examples presented indicate that the effect of nonlinearity on the responses for any given load level depends on the ply-arrangement, and as expected becomes more significant for higher loads. The responses were computed for Narmco 5505 material, and root-mean-square displacements and strains were found to increase as much as 20% for certain ply arrangements and loads. For other composite materials with different degrees of nonlinearity, the results could be significantly different.

To realize the above mentioned objectives, a computer program was developed and implemented for the nonlinear random vibration analysis described above. Several optimization techniques were developed and used, including an efficient indexing scheme using a variation of the pascal triangle, for the computation of the covariance matrix of the nodal displacements. The multidimensional symmetry in the calculation of the covariance matrix was fully exploited to drastically reduce the actual number of computations. The formulation presented herein requires the use of a large number of nested loops. Testing for

zero entries of the strain-displacement matrices within the outer loops made it possible to skip a number of intermediate nested loops and thus eliminate a large number of unnecessary computations. While the above mentioned optimization techniques were able to greatly reduce the computational time, it may still be unacceptable for large problem. Parallel processing techniques appear to be well-suited for this type of analysis and are discussed in the next section in the context of recommendations for future work.

6.2 Recommendations for future work

The amount of computations for the nonlinear random vibration analysis presented in this work tends to increase rapidly with the increasing size of the problem. For large structures, and more general formulations involving shear deformation and interlaminar shear stresses, the calculation of the nonlinear stiffness matrix discussed in Chapter 3 is even more computation-intensive. Even with moderate size problems, the computations become excessive on currently available uniprocessor workstations. For practical analysis using finer finite element idealization, the most promising computers are supercomputers and massively parallel machines. While supercomputers can greatly speed up all vector and matrix operations, parallel computers offer great potential in the near future.

There are a number of stages in the analysis described in this work where parallel computation may be effectively employed. Some initial ideas along this front are explored.

There are three stages during each iteration in which intensive computations are required. Possibilities for parallelizing each of these stages are discussed below:

1. The use of modal analysis requires the solution of an eigenvalue problem. The eigensolutions vary only slightly from one iteration to the next, and may be computed from the old ones using the inherently parallel homotopy continuation method. The solution of the eigenproblem for the very first cycle may also be parallelized using this method (Zhang and Harichandran 1989, Chu 1984).

2. The coefficients α and β needed in the computation of the nonlinear stiffness matrix must be evaluated at each Gauss point for the numerical quadrature. Since the coefficients are estimated on an element by element basis, elements can be divided into as many groups as there are processors, and the computations for different groups of elements can be performed in parallel.
3. When a large number of modes, n , must be considered owing to their natural frequencies being in the dominant excitation frequency range, considerable time is required to compute the integrals corresponding to the $n(n + 1) / 2$ pairs of modes in order to evaluate the r.m.s. responses. Since each integral is independent, the computations can be performed in parallel.

While the techniques outlined above do provide for parallelism, they also require a fair amount of communication between processors. In step 1 the system matrices must be accessible to all processors, and in step 2 the nodal covariances for each group of elements needs to be accessible to the corresponding processors. Therefore, while the proposed schemes should be efficient for shared memory computers, they may need to be further enhanced for scalable distributed memory computers. Research and implementation is needed to address these questions.

The classical plate theory used in this study can yield significant error even for moderately thick composite laminae because transverse shear deformation is neglected. It is well known that transverse shear deformation is significant for thick plates, and this is especially true for composites since the shear moduli of polymer matrices are significantly lower than the extensional moduli. While the first-order shear theory (Reissner 1945, Mindlin 1951) is adequate for plates made of conventional materials, a higher-order shear is usually required for composite laminates (Reddy 1990, Noor and Burton 1989). Even higher-order shear theories are usually adequate only for global modeling (i.e., prediction of displacements, natural frequencies and buckling loads), and are not sufficiently accurate for stress field computations. Local layer-wise models that represent each layer as a homo-

geneous anisotropic continuum are usually required for accurate stress computations, but these often magnify the size of the problem. For random vibration analysis, both global and local models are of interest since one or the other may be applicable in a specific situation. It appears therefore that separate solution schemes using both types of models should be developed.

Composite laminates are typically used in either plate or shell configurations. The analysis using laminated shell elements is much more complicated than that using laminated plate elements, primarily because their geometry is more complicated. Although composite shells are widely used in the design of aircraft and automobile components, very little work has been done on the nonlinear random vibration analysis of elements made of composites. There is an important need to address this deficiency, and to develop suitable techniques for the random vibration analysis.

References

- Amijima, S., and Adachi, T. (1979). "Nonlinear stress-strain response of laminated composites," *Journal of Composite Materials*, 13, 206-218.
- Bathe, K.-J. (1982). *Finite Element Procedures in Engineering Analysis*, Prentice-Hall, Inc, New Jersey.
- Cederbaum, G. (1990). "Random vibrations of viscoelastic laminated plates," *Transactions of the ASME*, 57, 688-693.
- Cederbaum, G., Elishakoff, I., and Librescu, L. (1989). "Random vibrations of laminated plates modeled within the first order shear deformation theory," *Composite Structures*, 12(2), 97-111.
- Chia, C. Y. (1980). *Nonlinear Analysis of Plates*, McGraw-hill, New York.
- Chu, M.T. (1984). "A simple application of the homotopy method to symmetric eigenvalue problems," *Linear Algebra Applications*, 59, 85-90.
- Cook, R.D., Malkus, D.S, and Plesha, M. E. (1974). *Concepts and Applications of Finite Element Analysis*, John Willey & Sons, New York.
- Dietz, A. G. H. (1969). *Composite Engineering Laminates*, The MIT Press.
- Hahn, H. T. (1973). "Nonlinear behavior of laminated composites," *Journal of Composite Materials*, 7, 257-271.
- Hahn, H. T., and Tsai, S. W. (1973). "Nonlinear elastic behavior of unidirectional composite laminae," *Journal of Composite Materials*, 7, 102-118.
- Halpin, J. C. (1992). *Primer on Composite Material Analysis*, Technomic Inc.
- Harichandran, R. S. (1992). "Random vibration under propagating excitation: Closed-form solutions," *Journal of Engineering Mechanics*, ASCE, 118(3), 575-586.
- Harichandran, R. S., and Hawwari, A. (1992). "Nonlinear random vibration of filamentary composites." *Computing Systems in Engineering*, 3(1-4), 469-475.
- Huebner, K. H., and Thornton, E. A. (1982). *The Finite Element Method for Engineers*, John Willey & Sons, New York.
- Iwan, W. D., and Yang, I-Mi. (1972). "Application of statistical linearization techniques to nonlinear multi-degree-of-freedom systems," *Journal of Applied Mechanics*, 13, 545-549.
- Iwan, W. D., and Mason, A. B. (1979). "Equivalent linearization for systems subjected to non-stationary random excitation," *International Journal of Non-linear Mechanics*, 15, 71-82
- Jones, R. M. (1975). *Mechanics of Composite Materials*, McGraw-Hill, New York.
- Kant, T., Ravichandran, R. V., Pandia, B. N., and Mallikarjuna (1988). "Finite element transient dynamic analysis of isotropic and fiber reinforced composite plates using a higher-order theory," *Composite Structures*, 9(4), 319-342.
- Lo, K. H., Christensen, R. M., and Wu, E. M. (1977). A high-order theory of plate deformation. Part 1: Homogeneous plates. Part2: Laminated plates." *Journal of Applied Mechanics*, ASME, 44(4), 663-676.
- Mei, C., and Prasad, C. B. (1989). "Effects of large deflection and transverse shear on response of rectangular symmetric composite laminates subjected to acoustic excitation," *Journal of Composite Materials*, 23, 606-639.
- Melosh, R. J. (1963). "Basis of derivation of matrices for the direct stiffness method," *AIAA Jour.*,1(7), 1631-1637.

- Mindlin, R. D. (1951). "Influence of rotary inertia and shear deformation on flexural motions of isotropic elastic plates." *Journal of Applied Mechanics, ASME*, 18, 31-38.
- Nelson, R. B., and Lorch, D. R. (1974). "A refined theory for laminated orthotropic plates." *Journal of Applied Mechanics, ASME*, 4(1), 177-183.
- Noor, A. K., and Burton, W. S. (1989). "Assessment of shear deformation theories for multilayer composite plates." *Applied Mechanics Review*, 42(1), 177-183.
- Newland, D. E. (1984). *An Introduction to Random Vibrations and Spectral Analysis*, Longman, New York.
- Owen, D. R.J., and Li, Z. H. (1987). "A refined analysis of laminated plates by finite element displacement methods: I. Fundamentals and static analysis; II. Vibration and stability." *Computers & Structures*, 26(6), 907-923.
- Pagano, N. J., and Soni, S. R. (1983). "Global-local laminational model." *International Journal for Solids and Structures*, 19, 207-228.
- Paz, M. (1991). *Structural Dynamics Theory and Computation*, Van Nostrand Reinhold, New York.
- Phan, N. D., and Reddy, J. N. (1985). "Analysis of laminated composite plates using a higher-order shear deformation theory," *International Journal for Numerical Methods in Engineering*, 21, 2201-2219.
- Reddy, J. N. (1982). "Bending of laminated anisotropic shells by a shear deformable finite element," *Fiber Science and Technology*, 17,9.
- Reddy, J. N. (1984). "A simple higher-order theory for laminated composite plates." *Journal of Applied Mechanics, ASME*, 51(4), 745-752.
- Reddy, J. N. (1987). "A generalization of two-dimensional theories of laminated composite plate." *Communications in Applied Numerical Methods*, 3(1), 173-180.
- Reddy, J. N. (1990). "A review of refined theories of laminated composite plates." *Shock and Vibration Digest*, 22(7), 3-17.
- Reddy, J. N., and Chao, W. C. (1981). "Large-deflection and large-amplitude free vibrations of laminated composite-material plates," *Computers and Structures*, 313-341.
- Reissner, E. (1945). "The effect of transverse shear deformation on the bending of elastic plates." *Journal of Applied Mechanics, ASME*, 12, A69-A77.
- Roberts, J. B., and Spanos, P. D. (1986). *Random Vibration and Statistical Linearization*, Wiley, New York.
- Sandhu, R. S. (1976). "Nonlinear behavior of unidirectional and angle ply laminates," *Journal of Aircraft*, 13(2), 104-111.
- Schuessler, G. I., Shinozuka, M. (1987). *Stochastic Methods in Structural Dynamics*, Kluwer Academic Publishers, MA.
- Sheinman, I., and Grief, S. (1984). "Dynamic analysis of laminated shells of revolution," *Journal of Composite Materials*, 18, 200.
- Walz, J. E., Fulton, R. E., and Cyrus N. J. (1968). "Accuracy and convergence of finite element approximation," *Proceedings of 2nd Conference of Matrix methods in Structural Mechanics*, Wright Patterson Airforce Base, Dayton, Ohio.
- Weaver, W., and Johnston P. R. (1984). *Finite Elements for Structural Analysis*, Prentice-Hall, Inc., New Jersey.
- Wen, W. K. (1977). "Approximation techniques for random vibrations of non-linear systems," *Journal of Engineering Mechanics, ASCE*, 103, 673-687.
- Whitney, J. M., (1987). *Structural Analysis of Laminated Anisotropic Plates*, Technomic. Inc.

- Whitney, J. M., Daniel, I. M., and Pipes, R. B. (1982). *Experimental Mechanics of Fiber Reinforced Composite Materials*, Prentice-Hall, Inc., New Jersey.
- Whitney, J. M., and Sun, C. T. (1974). "A refined theory for laminated anisotropic, cylindrical shells." *Journal of Applied Mechanics*, ASME, 471-476.
- Witt, M. (1986). "Dynamic response and reliability of laminated plates to random loading," In *Refined Dynamical Theories of Beams, Plates and Shells and their Applications*, I. Elishakoff and H. Irretier (eds), Springer-Verlag, New York, 274-285.
- Witt, M., and Sobczyk, K. (1989). "Dynamic response of laminated plates to random loading," *International Journal of Solids and Structures*, 16, 231-238.
- Zhang, Y., and Harichandran, R. S. (1989). "Eigenproperties of large-scale structures by finite element partitioning and homotopy continuation," *International Journal for Numerical Methods in Engineering*, 28, 2113-3122.
- Zienkiewicz, O. C. (1977). *The Finite Element Method*, McGraw-Hill, New York.
- Zienkiewicz, O. C., and Cheung, Y. K. (1964). "The finite element method for analysis of elastic isotropic and orthotropic slabs," *Proceedings of the Institute of Civil Engineers*, 28, 471-488.

APPENDIX
PROGRAM

```

!+-----+
!! This program is to compute the non-linear random
!! vibration response of laminated composite plate.
!!
!! VAR Explanation
!! -----
!! q(3,3) Inverse of the linear compliance matrix [S]
!! T1(5,3,3) Inverse of the orthogonal rotational
!! transformation matrix [T]. T(3,3)
!! T1t(5,3,3) Inverse transpose of [T].
!! T3(5,3) Row matrix consisting of the 3rd row of [T1t].
!! Tstr(5,3,3) [T1]Diag(0,0,1)[T1t]
!! x(3) Sampling point in Gauss-Legendre Num. Integral
!! y(3) Sampling point in Gauss-Legendre Num. Integral
!! h(3) Weight in Gauss-Legendre Num. Integral
!! Iguass Order of integration.
!! ak(20,20) Elemental linear Stiffness matrix.
!! bk(80,80) Assembled linear Stiffness matrix.
!! bm(80,80) Assembled Mass matrix.
!! id(25,20) Node topography.
!! tz(5) Layer thickness.
!! angl(5) Fiber orientation (for each layer).
!! xt(3,3) [Ti] [q] [T1t]
!! ttm(60,60) Total Elemental mass matrix without support.
!! tm(60,60) Assembled mass matrix without support.
!! bb(60,60) A copy of tm.
!! ttk(60,60) Total Elemental Stiffness mat. without support.
!! sttk(60,60) Save copy of " "
!! tk(60,60) Assembled Stiffness matrix without support.
!! aa(60,60) A copy of tk.
!! w(60) Sorted Eigen Values.
!! z(60,60) Normalized Eigen vectors.
!! g(32,60) Participation factor.
!! cov(60,60) Covariance without support
!! covk(80,80) Covariance (with support)
!! cove(25,20,20) Elemental covariance matrix (per element)
!! stral(3,3) Strain in local (material) coordinates.
!! strag(3,3) Strain in global coordinates.
!! stresl(3,3) Stress in local (material) coordinates.
!! stresg(3,3) Stress in global coordinates.
!! ldof(32) Degrees of freedom to load.
!! bn2(9,3,20) B': Generalized in-plane strain-disp. mat.
!! bn3(9,3,20) B'': Generalized out-of-plane strain-disp. mat.
!! mx Number of elements per row
!! nm Number of elements per column
!! ny Number of free degrees of freedom
!! s0 Spectrum Level
!! ICElem Monitored element
!! llyrs Number of layers.
!! ldof Number of degrees of freedom (currently 5)
!! Lind Current layer (during execution)
!+-----+
!! EstCov Compute/Read elemental covariance matrix.
!! dbg Print/Hide debugging information.
!! alpha & beta (See AlfBta.f)
!! dint(60,60) (See ddmcov.f)
!+-----+
Implicit real*8 (a-h,o-z)
dimension q(3,3),T1(5,3,3),T1t(5,3,3),T3(5,3),Tstr(5,3,3)
dimension x(3),y(3),h(3)
dimension ak(20,20),bm(80,80),bk(80,80)
dimension id(25,20),tz(5),angl(5), bn2(9,3,20),bn3(9,3,20)
dimension Ts(3,3),Tm(60,60),tk(60,60),aa(60,60),bb(60,60)
dimension g(32,60),w(60)
dimension dint(60,60)
dimension cov(60,60),covk(80,80),cove(25,20,20,20)
dimension tcov(60), tcove(20)
dimension stral(3,3),strag(3,3),stresl(3,3),stresg(3,3)
dimension sksl1(25,3,20,20), sksl12(25,3,20,20)
dimension ldof(32), xt(3,3)
dimension alpha1(9,25,3), alpha2(9,25,5)
dimension beta1(9,25,2,20), beta2(9,25,4,20)
dimension sttk(60,60), ttk(60,60), ttm(60,60)
integer mx,nm,ICElem,llyrs,ldof,Iguass,Lind,ndof
logical EstCov, dbg, frstlim, Cnvrqd
external f02bjf, x02ajf, f04saf
external schz, adm3, shape2, shape3, CmatKM, tpgraph
!+-----+
external COVE.F
external readcv, Ccove, calcov, InitBN, alfBta,
InitAl, GetInp
character *32 fnam
dimension xi(60)
common /iblk/ mx,ny,nm,ICElem,llyrs,ldof,Iguass,Lind
common /coef/ xb,xc
write(*,*) 'Input paramters file name?'
read(*,*) fnam
open(unit=12,file=fnam,status='unknown')
DO I=1,60,1
tcov(I) = 0.1d-12
DO J=1,60,1
ttm(I,J) = 0.d0
sttk(I,J) = 0.d0
END DO
! J
END DO
! I
!+-----+
call GetInp(dbg,tz,angl,zeta,EstCov,id,ldof,ndof,s0)

```

```

      s133 = dsqrt(streal(3,3))
    end if
  END DO
  do nd = 1, ndof, 1
    xi(ldof(nd)) = dsqrt(cov(ldof(nd), ldof(nd)))
  end do
  ilst = ilst + 1
end if

call TstCnv(cov,tcov,iCElem,frstim,Cnvrqd)
if (Cnvrqd) then
  write(*,*) 'Cove converged.'
  CovCnv = 1
else
  write(*,*) 'CPettk '
  call CPattk(sttk,ttk)           ! Copy sttk -> ttk.
  DO Lind = 1, ilyrs, 1
    !*** Compute Alpha and Beta for the current layer (Lind).
    write(*,*) 'AlfBta for Lind= ',Lind
    call AlfBta(alpha1,alpha2,beta1,beta2,cove,bn2,bn3,T3,tz,x,y)

    !*** Compute the Non-Linear Stiffness Matrix.
    write(*,*) 'nlmstf for Lind= ',Lind
    call nlnstf(alpha1,alpha2, beta1,beta2, bn2,bn3,
               tz,T3,tstr,sksl11,sksl12,h,xb,xc)

    !*** Add the Linear and Non-Linear parts of Stiffness Matrix.
    write(*,*) 'Addstf for Lind= ',Lind
    call Addstf(kskl11, sksl12, ttk, id, a1, a2)
  END DO
  ! Lind
end if
! DO I=1,60,1
! WHILE (no convergence)
!write(12,*) 'Final Cov : '
!DO I=1,60,1
! write(12,10) (cov(I,J),J=1,60,1)
! write(12,*)
!END DO
call PrDisp(cov)
do nd = 1, ndof, 1
  xf = dsqrt(cov(ldof(nd), ldof(nd)))
  write(12,109) nd, xf / xi(ldof(nd))
  write(*,109) nd, xf / xi(ldof(nd))
end do
!****
! Compute the following for a middle element (i.e. for a 3x3,
! we compute for element # 5):

```

```

!**** Initialize global variables.
call InitAl(q,ifall,eps1,xb,xc,ro,a1,a2,x,y,h,
           bm,bk,Ts,dbg,Ti,Tit,T3,Tstr,angl)
+
call InitBN(bn2,bn3,x,y)
DO Lind = 1, ilyrs, 1

!*** Compute Elemental Mass and Stiffness Matrixes
!*** Assemble Global Mass and Stiffness Matrixes.
!*** Assemble Mif and Kff
call CmatRM(x,y,h,ro,tz,xb,xc,Xt,Ti,q,Tit,id,
           bm,bk,ak,tm,tk,angl,as,bb,bn2,bn3)
+
!*** Add the mass and stiffness to their Total mats.
call AdHMats(tm,tk,ttm,sttk)
! Lind
END DO

call CPattk(sttk,ttk) ! Copy sttk -> ttk.

if (dbg) write(*,*) 'EstCov = ',EstCov

CovCnv = 0
itnum = 0
ilst = 0
frstim = .true.
DO WHILE (CovCnv .ne. 1)
  itnum = itnum + 1
  write(*,*) 'Computing cov then cove'

  call calcov(cov,ttk,ttm,eps1,zeta,w,g,dint,ttm,ldof,ndof,s0)
  call Ccove(cov,covk,cove,tcove,frstim,id)
  if (ilst .lt. 1) then
    !write(12,*) 'Initial Cov : '
    !DO I=1,60,1
    ! write(12,10) (cov(I,J),J=1,60,1)
    ! write(12,*)
    !END DO
    !write(12,*) 'Stresses & Strains for layer (Initial)'
    DO Lind = 1, ilyrs, 1
      ! write(12,*) 'Layer: ',Lind
      call CStrs (bn2,bn3,Ti,Tit,cove,q,tz,streal,
                stresg,streal,strag)
      if (Lind .le. 1) then
        s11 = dsqrt(streal(1,1))
        s22 = dsqrt(streal(2,2))
        s33 = dsqrt(streal(3,3))
        s111 = dsqrt(streal(1,1))
        s122 = dsqrt(streal(2,2))

```

```

: 1- Covariance of the stresses in Global Coordinates: Stresg(3x3)
: 2- Covariance of the stresses in Local Coordinates: Stresl(3x3)
: 3- Covariance of the strains in Global Coordinates: Strag(3x3)
: 4- Covariance of the strains in Local Coordinates: Stral(3x3)

:write(12,*) 'Stresses & Strains for layer (Final)'
DO Lind = 1, ilyrs, 1
  write(12,*) 'Layer:',Lind
  call CStrs(bn2,bn3,Ti,Tit,cove,q,tz,stresl,atresg,stral,strag)
  if (Lind .le. 1) then
    fs11 = dsqrt(stresl(1,1))
    fs22 = dsqrt(stresl(2,2))
    fs33 = dsqrt(stresl(3,3))
    sf11 = dsqrt(stral(1,1))
    sf22 = dsqrt(stral(2,2))
    sf33 = dsqrt(stral(3,3))
  write(12,*) 'Final Stress, Layer=', Lind
  write(12,11) fs11, fs22, fs33
  write(12,*) 'Normalized Stress, Layer=', Lind
  write(12,11) fs11/sf11, fs22/sf22, fs33/sf33
  write(12,*) 'Final Strains, Layer=', Lind
  write(12,11) sf11, sf22, sf33
  write(12,*) 'Normalized Strains, Layer=', Lind
  write(12,11) sf11/sf11, sf22/sf22, sf33/sf33
  write(12,*) 'Total Iters =', itnum
  write(*,*) 'Final Stress, Layer=', Lind
  write(*,11) fs11, fs22, fs33
  write(*,*) 'Normalized Stress, Layer=', Lind
  write(*,11) fs11/sf11, fs22/sf22, fs33/sf33
  write(*,*) 'Final Strains, Layer=', Lind
  write(*,11) sf11, sf22, sf33
  write(*,*) 'Normalized Strains, Layer=', Lind
  write(*,11) sf11/sf11, sf22/sf22, sf33/sf33
  write(*,*) 'Total Iters =', itnum
  end if
END DO

9      format(///1x,A)
10     format(1x,5(e14.8,' '))
11     format(1x,3(e14.8,' '))
101    format(1x,A,e14.8)
109    format(1x,'ficov',I3,''] = ',e14.8)

STOP
END

subroutine CPettk(sttk,ttk)
implicit double precision (a-h,o-z)
dimension sttk(60,60), ttk(60,60)

DO I = 1, 60, 1
  DO J = 1, 60, 1
    ttk(I,J) = sttk(I,J)
  END DO
END DO

RETURN
END

subroutine PrDisp(cov)
implicit double precision (a-h,o-z)
dimension cov(60,60), zs(16)

write(12,*) 'Disp = '
ic = 0
do i = 3,60,5
  ic = ic + 1
  zs(ic) = dsqrt(cov(i,i)) * sign(1, cov(3,i))
  write(12,10) zs(ic)
end do

format(1x,e14.8)
END

10

subroutine GetImp(dbg,tz,angl,zeta,EstCov,id,ldof,ndof,s0)
implicit real*8 (a-h,o-z)
dimension id(25,20),tz(5),angl(5),ldof(32)
logical      dbg,EstCov
common /iblk/  mx,ny,nm,iCElem,ilyrs,idof,iguass,Lind

dbg = .false.
write(*,101) '1/0 for dbg On/Off'
read(*,*) idebug
if (idebug .eq. 1) dbg = .true.

write(*,101) 'number of layers'
read(*,*) ilyrs
DO I=1,ilyrs,1
  write(*,102) 'thickness & angle for layer',I
  read(*,*) tz(I),angl(I)
END DO

write(*,101) 'damping ratio'
read(*,*) zeta
write(*,101) 'Spectrum level'
read(*,*) s0

write(*,101) '1 if you estimate cov. mean'

```



```

: 1- Covariance of the stresses in Global Coordinates: Stresg(3x3)
: 2- Covariance of the stresses in Local Coordinates: Stral(3x3)
: 3- Covariance of the strains in Global Coordinates: Strag(3x3)
: 4- Covariance of the strains in Local Coordinates: Stral(3x3)

'write(12,*) 'Stresses & Strains for layer (Final)'
DO Lind = 1, nlyrs, 1
  write(12,*) 'Layer: ',Lind
  call CStrs(bn2,bn3,Ti,Tit,cove,q,tz,stresl,stresg,stral,strag)
  if (Lind .le. 1) then
    fs11 = dsqrt(stresl(1,1))
    fs22 = dsqrt(stresl(2,2))
    fs33 = dsqrt(stresl(3,3))
    sf11 = dsqrt(stral(1,1))
    sf22 = dsqrt(stral(2,2))
    sf33 = dsqrt(stral(3,3))
  write(12,*) 'Final Stress, Layer=', Lind
  write(12,11) fs11, fs22, fs33
  write(12,*) 'Normalized Stress, Layer=', Lind
  write(12,11) fs11/ss11, fs22/ss22, fs33/ss33
  write(12,*) 'Final Strains, Layer=', Lind
  write(12,11) sf11, sf22, sf33
  write(12,*) 'Normalized Strains, Layer=', Lind
  write(12,11) sf11/ss11, sf22/ss22, sf33/ss33
  write(12,*) 'Total Iters =', itnum

  write(*,*) 'Final Stress, Layer=', Lind
  write(*,11) fs11, fs22, fs33
  write(*,*) 'Normalized Stress, Layer=', Lind
  write(*,11) fs11/ss11, fs22/ss22, fs33/ss33
  write(*,*) 'Final Strains, Layer=', Lind
  write(*,11) sf11, sf22, sf33
  write(*,*) 'Normalized Strains, Layer=', Lind
  write(*,11) sf11/ss11, sf22/ss22, sf33/ss33
  write(*,*) 'Total Iters =', itnum
  end if
END DO

9  format(///1x,A)
10 format(1x,5(e14.8,' '))
11 format(1x,3(e14.8,' '))
101 format(1x,A,e14.8)
109 format(1x,'fcov',I3,'') = '.e14.8)

STOP
END

subroutine CPettk(sttk,ttk)
implicit double precision (a-h,o-z)
dimension sttk(60,60), ttk(60,60)

DO I = 1, 60, 1
  DO J = 1, 60, 1
    ttk(I,J) = sttk(I,J)
  END DO
END DO

RETURN
END

subroutine PrDisp(cov)
implicit double precision (a-h,o-z)
dimension cov(60,60), zs(16)

write(12,*) 'Disp = '
ic = 0
do i = 3,60,5
  ic = ic + 1
  zs(ic) = dsqrt(cov(i,i)) * sign(1, cov(3,i))
  write(12,10) zs(ic)
end do

format(1x,e14.8)
END

subroutine GetInp(dbg,tz,angl,zeta,EstCov,id,ldof,ndof,s0)
implicit real*8 (a-h,o-z)
dimension id(25,20),tz(5),angl(5),ldof(32)
logical dbg,EstCov
common /iblk/ mx,ny,nm,icElem,ilyrs,idof,iguass,Lind

dbg = .false.
write(*,101) '1/0 for dbg On/Off'
read(*,*) idebug
if (idebug .eq. 1) dbg = .true.

write(*,101) 'number of layers'
read(*,*) ilyrs
DO I=1,ilyrs,1
  write(*,102) 'thickness & angle for layer',I
  read(*,*) tz(I),angl(I)
END DO

write(*,101) 'damping ratio'
read(*,*) zeta
write(*,101) 'Spectrum level'
read(*,*) s0

write(*,101) '1 if you estimate cov. mean'

```



```

Tit(I,1,1) = (dcos(angl(I)))**2
Tit(I,1,2) = (dsin(angl(I)))**2
Tit(I,1,3) = (dsin(angl(I)) * dcos(angl(I)))
Tit(I,2,1) = (dsin(angl(I)))**2
Tit(I,2,2) = (dcos(angl(I)))**2
Tit(I,2,3) = -dsin(angl(I)) * dcos(angl(I))
Tit(I,3,1) = -2.d0 * dsin(angl(I)) * dcos(angl(I))
Tit(I,3,2) = 2.d0 * dsin(angl(I)) * dcos(angl(I))
Tit(I,3,3) = (dcos(angl(I)))**2 - (dsin(angl(I)))**2

T3 (I,1) = Tit(I,3,1)
T3 (I,2) = Tit(I,3,2)
T3 (I,3) = Tit(I,3,3)

Tstr(I,1,1) = Ti(I,1,3) * Tit(I,3,1)
Tstr(I,1,2) = Ti(I,1,3) * Tit(I,3,2)
Tstr(I,1,3) = Ti(I,1,3) * Tit(I,3,3)
Tstr(I,2,1) = Ti(I,2,3) * Tit(I,3,1)
Tstr(I,2,2) = Ti(I,2,3) * Tit(I,3,2)
Tstr(I,2,3) = Ti(I,2,3) * Tit(I,3,3)
Tstr(I,3,1) = Ti(I,3,3) * Tit(I,3,1)
Tstr(I,3,2) = Ti(I,3,3) * Tit(I,3,2)
Tstr(I,3,3) = Ti(I,3,3) * Tit(I,3,3)

END DO

RETURN
END

function shape2(i,j,x,y)
implicit real*8 (a-h,o-z)
common /coef/ xb,xc

shape2 = 0.0
if ((i .eq. 1 .and. j .eq. 1) .or. (i .eq. 2 .and. j .eq. 2)) then
  shape2 = (1-x)*(1-y)
else if ((i .eq. 1 .and. j .eq. 6) .or. (i .eq. 2 .and. j .eq. 7)) then
  shape2 = (1+x)*(1-y)
else if ((i .eq. 1 .and. j .eq. 11) .or. (i .eq. 2 .and. j .eq. 12)) then
  shape2 = (1+x)*(1+y)
else if ((i .eq. 1 .and. j .eq. 16) .or. (i .eq. 2 .and. j .eq. 17)) then
  shape2 = (1-x)*(1+y)
end if
shape2 = shape2 / 4.0

return
end

function shape3(i,j,x,y)
implicit real*8 (a-h,o-z)
common /coef/ xb,xc

shape3 = 0.0
if (i .eq. 1) then
  if (j .eq. 3) then
    shape3 = (1-x)*(1-y)*(2-x-y-x**2-y**2)
  else if (j .eq. 8) then
    shape3 = (1+x)*(1-y)*(2+x-y-x**2-y**2)
  else if (j .eq. 13) then
    shape3 = (1+x)*(1+y)*(2+x-y-x**2-y**2)
  else if (j .eq. 18) then
    shape3 = (1-x)*(1+y)*(2-x-y-x**2-y**2)
  end if
else if (i .eq. 2) then
  if (j .eq. 4) then
    shape3 = xc * (1-x) * (1+y) * (1-y)**2
  else if (j .eq. 9) then
    shape3 = xc * (1+x) * (1+y) * (1-y)**2
  else if (j .eq. 14) then
    shape3 = -xc * (1+x) * (1-y) * (1+y)**2
  else if (j .eq. 19) then
    shape3 = -xc * (1-x) * (1-y) * (1+y)**2
  end if
else
  if (j .eq. 5) then
    shape3 = -xb * (1+x) * (1-y) * (1-x)**2
  else if (j .eq. 10) then
    shape3 = xb * (1-x) * (1-y) * (1+x)**2
  else if (j .eq. 15) then
    shape3 = xb * (1-x) * (1+y) * (1+x)**2
  else if (j .eq. 20) then
    shape3 = -xb * (1+x) * (1+y) * (1-x)**2
  end if
shape3 = shape3 / 8.0

return
end

C*****
C C Function to compute the Strain Displacement Matrix for
C C In-Plane actions.
C C*****

```



```

      sch3 = (4 - 3*x**2 - 3*y**2) / (xb*xc)
    else if (j .eq. 4) then
      sch3 = (1-y) * (1+3*y) / xb
    else if (j .eq. 5) then
      sch3 = -(1-x) * (1+3*x) / xc
    else if (j .eq. 8) then
      sch3 = -(4 - 3*x**2 - 3*y**2) / (xb*xc)
    else if (j .eq. 9) then
      sch3 = -(1-y) * (1+3*y) / xb
    else if (j .eq. 10) then
      sch3 = -(1+x) * (1-3*x) / xc
    else if (j .eq. 13) then
      sch3 = (4 - 3*x**2 - 3*y**2) / (xb*xc)
    else if (j .eq. 14) then
      sch3 = -(1+y) * (1-3*y) / xb
    else if (j .eq. 15) then
      sch3 = (1+x) * (1-3*x) / xc
    else if (j .eq. 18) then
      sch3 = -(4 - 3*x**2 - 3*y**2) / (xb*xc)
    else if (j .eq. 19) then
      sch3 = (1+y) * (1-3*y) / xb
    else if (j .eq. 20) then
      sch3 = (1-x) * (1+3*x) / xc
    end if
  end if
  sch3 = sch3 / 4.0
return
end

subroutine Tprgraph(id)
dimension id(25,20)
common /blk/  mx,ny,nm,icElem,llyrs,llyrs,idof,iguass,Lind
  ilim = 4 * idof
  ic=0
  imx = mx
  iny = ny
  do i=1,imx
    do j=1,iny
      ic = ic+1
      do ii=1,idof
        id(ic, ii) = ((i-1)*(iny+1)+(j-1))*idof+ii
        id(ic,1*idof+ii) = ( i *(iny+1)+(j-1))*idof+ii
        id(ic,2*idof+ii) = id(ic,1*idof+ii) + idof
        id(ic,3*idof+ii) = id(ic, ii) + idof
      enddo
    enddo
  enddo
enddo

```

```

enddo
enddo
return
end
subroutine GetZks(tz,zk,zkml)
implicit real*8 (a-h,o-z)
dimension tz(5)
common /blk/  mx,ny,nm,icElem,llyrs,idof,iguass,Lind
  rmid = llyrs / 2.0
  lmid = rmid + 0.5
  loff = MOD(llyrs, 2)
  if (loff .eq. 1 .and. lind .eq. lmid) then
    zkml = -tz(lmid) / 2.0
    zk = tz(lmid) / 2.0
  return
  else if (lind .ie. lmid) then
    isig = -1
  else
    isig = 1
  end if
  if (Lind .ie. Rmid) then
    ib = Lind
    ie = lmid - loff
  else
    ib = lmid + 1
    ie = Lind - 1
  end if
  zkml = 0.0
  zk = 0.0
  DO I = ib, ie, 1
    zkml = zkml + tz(I)
    zk = zk + tz(I)
  END DO
  zk = zk + isig * tz(Lind)
  if (loff .eq. 1) then
    tz2 = tz(lmid) / 2.0
    zkml = zkml + tz2
    zk = zk + tz2
  end if
  zkml = zkml * isig
  zk = zk * isig
RETURN
END

```

```

complex*16 function denom (ip, np, p)
-----
c Compute denominator of residue and partial fraction terms for p(ip)
c On input: ip = pole for which the denominator is required
c          np = total number of poles
c          p = complex*16 array of poles
-----
complex*16 p(np)

denom = dcmplx (1.d0, 0.d0)
do i = 1, ip-1
  denom = denom*(p(ip)-p(i))
end do
do i = ip+1, np
  denom = denom*(p(ip)-p(i))
end do
return
end

complex*16 function blint1 (m, p, w1, w2)
-----
c Computes the integral of w**m/(w-p) from w1 to w2 using a closed-form
c finite sum
c On input: m = integer >= 0
c          p = complex pole
c          d = delay term in complex exponential
c          w1, w2 = lower and upper limits of integration
-----
implicit real*8 (a-h,o-z)
complex*16 p

blint1 = p**m*log((w2-p)/(w1-p))
do k = 1, m
  blint1 = blint1 + (p**(m-k)*(w2**k-w1**k))/k
end do
return
end

complex*16 function blint2 (m, p, d, w1, w2)
-----
c Computes the integral of w**m*exp(idw)/(w-p) from w1 to w2 using a
c closed-form finite sum
c On input: m = integer >= 0
c          p = complex pole
c          d = delay term in complex exponential
c          w1, w2 = lower and upper limits of integration

```

```

real*8 function wn (wj, zj, wk, zk, d, m)
-----
c Uses contour integration to compute the closed-form integral of
c Re [w**m * conjg(Hj(w)) * Hk(w) * exp(idw)], which is the
c dynamic displacement modal covariance to white noise excitation
c when m is 0 or 2. When m is 1 or 3, it calls BLWN with w1=0 and
c w2=100*max(wj,wk).
c On input: wj, wk = circular natural frequencies of modes j and k
c          zj, zk = damping ratios for modes j and k
c          d = propagation time delay
c          m = spectral moment that is required >= 0
c Calls: BLWN when m is 1 or 3
-----
implicit real*8 (a-h,o-z)
complex*16 i, p(4), denom
parameter (pi=3.1415926535897932, i=(0.d0,1.d0))

c Damped frequencies

wjd = wj*sqrt(1-zj*zj)
wkd = wk*sqrt(1-zk*zk)

c Poles

p(1) = dcmplx (wjd, -zj*wj)
p(2) = dcmplx (-wjd, -zj*wj)
p(3) = dcmplx (wk, zk*wk)
p(4) = dcmplx (-wk, zk*wk)

c Residues and closed form result

if (m .eq. 0 .or. m .eq. 2) then
  if (d .ge. 0) then
    wn = -pi * dimag(p(3))*m*exp(i*d*p(3))/denom(3,4,p)
    + p(4)*m*exp(i*d*p(4))/denom(4,4,p)
  else
    wn = pi * dimag(p(1))*m*exp(i*d*p(1))/denom(1,4,p)
    + p(2)*m*exp(i*d*p(2))/denom(2,4,p)
  end if
else
  w1 = 0
  w2 = 100*max(wj,wk)
  wn = blwnd (wj, zj, wk, zk, d, w1, w2, m)
end if
return
end

```

```

c-----
c      real*8 function wj, zj, wk, zk, d, m)
c-----
c Uses contour integration to compute the closed-form integral of
c  $\text{Re} [w^*m \cdot \text{conj}(H_j(w)) \cdot H_k(w) \cdot \exp(i\omega t)]$ , which is the
c dynamic displacement modal covariance to white noise excitation
c when m is 0 or 2. When m is 1 or 3, it calls BLMN with w1=0 and
c  $w2=100 \cdot \max(wj, wk)$ .
c On input:  wj, wk = circular natural frequencies of modes j and k
c           zj, zk = damping ratios for modes j and k
c           d = propagation time delay
c           m = spectral moment that is required >= 0
c Calls:    BLMN when m is 1 or 3
c-----
implicit real*8 (a-h,o-z)
complex*16 i, p(4), denom
parameter (pi=3.1415926535897932, i=(0.d0,1.d0))

c Damped frequencies
wjd = wj*sqrt(1-zj*zj)
wkd = wk*sqrt(1-zk*zk)

c Poles
p(1) = dcmplx (wjd, -zj*wj)
p(2) = dcmplx (-wjd, -zj*wj)
p(3) = dcmplx (wkd, zk*wk)
p(4) = dcmplx (-wkd, zk*wk)

c Residues and closed form result
if (m .eq. 0 .or. m .eq. 2) then
  if (d .ge. 0) then
    wn = -pi * dimag(p(3))*m*exp(i*d*p(3))/denom(3,4,p)
    & + p(4)*m*exp(i*d*p(4))/denom(4,4,p)
  else
    wn = pi * dimag(p(1))*m*exp(i*d*p(1))/denom(1,4,p)
    & + p(2)*m*exp(i*d*p(2))/denom(2,4,p)
  end if
else
  w1 = 0
  w2 = 100*max(wj,wk)
  wn = blwnd (wj, zj, wk, zk, d, w1, w2, m)
end if
return
end

```

```

c-----
c      complex*16 function denom (ip, np, p)
c-----
c Compute denominator of residue and partial fraction terms for p(ip)
c On input:  ip = pole for which the denominator is required
c           np = total number of poles
c           p = complex*16 array of poles
c-----
complex*16 p(np)

denom = dcmplx (1.d0, 0.d0)
do i = 1, ip-1
  denom = denom*(p(ip)-p(i))
end do
do i = ip+1, np
  denom = denom*(p(ip)-p(i))
end do
return
end

c-----
c      complex*16 function blint1 (m, p, w1, w2)
c-----
c Computes the integral of  $w^*m/(w-p)$  from w1 to w2 using a closed-form
c finite sum
c On input:  m = integer >= 0
c           p = complex pole
c           d = delay term in complex exponential
c           w1, w2 = lower and upper limits of integration
c-----
implicit real*8 (a-h,o-z)
complex*16 p

blint1 = p**m*log((w2-p)/(w1-p))
do k = 1, m
  blint1 = blint1 + (p**(m-k)*(w2**k-w1**k))/k
end do
return
end

c-----
c      complex*16 function blint2 (m, p, d, w1, w2)
c-----
c Computes the integral of  $w^*m \cdot \exp(i\omega t)/(w-p)$  from w1 to w2 using a
c closed-form finite sum
c On input:  m = integer >= 0
c           p = complex pole
c           d = delay term in complex exponential
c           w1, w2 = lower and upper limits of integration

```

```

c-----
implicit real*8 (a-h,o-z)
complex*16 i, p, blint3
complex arg1, arg2, ei2ml
intrinsic cmplx
parameter (i=(0.d0,1.d0))

arg1 = cmplx(i*d*(w1-p))
arg2 = cmplx(i*d*(w2-p))
blint2 = p**m*exp(i*p*d)*ei2ml(arg1,arg2)
do j = 1, m
  n = m - j
  blint2 = blint2 + p**(j-1) * blint3(n,d,w1,w2)
end do
return
end

complex*16 function blint3 (n, d, w1, w2)
c-----
c Computes the integral of w**n*exp(i*d*w) from w1 to w2 using a
c closed-form finite sum
c On input:  n = integer >= 0
c           d = non-zero delay term in complex exponential
c           w1, w2 = limits of integration
c-----
implicit real*8 (a-h,o-z)
complex*16 i
parameter (pi2=1.570796326794897, i=(0.d0,1.d0))

blint3 = dcmplx(0.d0, 0.d0)
nfac = 1
do k = 0, n-1
  blint3 = blint3 + nfac/d**(k+1)*(w2**(n-k)*exp(i*d*w2+k*pi2))
  nfac = nfac*(n-k)
end do

c To avoid 0**0 error when w1=0, do the last term outside the loop
if (w1 .ne. 0) then
  blint3 = blint3 + nfac/d**(n+1)*(exp(i*d*w2+n*pi2))
else
  blint3 = blint3 + nfac/d**(n+1)*exp(i*d*w2+n*pi2)
end if

blint3 = -i*blint3
return
end

c-----
implicit real*8 (a-h,o-z)
complex*16 p, blint4
complex arg1, arg2, ei2ml
parameter (i=(0.d0,1.d0))

arg1 = cmplx(i*d*(w1-p))
arg2 = cmplx(i*d*(w2-p))
blint5 = exp(i*p*d)*ei2ml(arg1,arg2)/p**n
do k = 1, n
  blint5 = blint5 + exp(-i*(k-1)*pi2)*d**(k-1)/p**(n-k+1)
  ei2ml(k-1,cmplx(-i*d*w1),cmplx(-i*d*w2))
end do
return
end

complex function ei2ml (arg1, arg2)
c-----
c Computes Ei(arg2) - Ei(arg1), taking care of the 2*pi*i jump across
c the branch cut along the positive real axis
c On input:  arg1, arg2 = complex*8 arguments
c-----
complex*16 function blint4 (n, p, w1, w2)
c-----
c Computes the integral of 1/w**n/(w-p) from w1 to w2 using a
c closed-form finite sum
c On input:  n = integer >= 1
c           p = complex pole
c           w1, w2 = lower and upper limits of integration > 0
c-----
implicit real*8 (a-h,o-z)
complex*16 p
blint4 = log(w1*(w2-p)/w2/(w1-p))/p**n
do k = 1, n-1
  blint4 = blint4 + (1/w2**(n-k) - 1/w1**(n-k))/(n-k)/p**k
end do
return
end

complex*16 function blint5 (n, p, d, w1, w2)
c-----
c Computes the integral of exp(i*d*w)/w**n/(w-p) from w1 to w2 using a
c closed-form finite sum
c On input:  n = integer >= 1
c           p = complex pole
c           d = non-zero delay term in complex exponential
c           w1, w2 = lower and upper limits of integration > 0
c Calls:  cexpli from nawcplib.a library
c-----
implicit real*8 (a-h,o-z)
complex*16 p, i
complex arg1, arg2, ei2ml, gn2ml
parameter (pi2=1.570796326794897, i=(0.d0,1.d0))

arg1 = cmplx(i*d*(w1-p))
arg2 = cmplx(i*d*(w2-p))
blint5 = exp(i*p*d)*ei2ml(arg1,arg2)/p**n
do k = 1, n
  blint5 = blint5 + exp(-i*(k-1)*pi2)*d**(k-1)/p**(n-k+1)
  ei2ml(k-1,cmplx(-i*d*w1),cmplx(-i*d*w2))
end do
return
end

complex function ei2ml (arg1, arg2)
c-----
c Computes Ei(arg2) - Ei(arg1), taking care of the 2*pi*i jump across
c the branch cut along the positive real axis
c On input:  arg1, arg2 = complex*8 arguments
c-----

```

```

c Calls:      cexpli from newclib.a library
-----
complex arg1, arg2, cexpli, ei1, ei2, i
parameter (tpi=6.283185307179587, i=(0..1.))

call cexpli(0, arg1, ei1)
call cexpli(0, arg2, ei2)
ei2m1 = ei2 - ei1

c If arg1 is in 4th quadrant and arg2 is in 1st quadrant, add 2*pi*i
c to be on the correct branch for Ei(arg2).

if (real(arg1).gt. 0 .and. real(arg2).gt. 0 .and.
& aimag(arg1)*aimag(arg2).lt. 0) then
  ei2m1 = ei2 - ei1 + sign(1,aimag(arg2))*tpi*i
end if
return
end

complex function gn2m1 (n, x1, x2)
-----
c Computes [gamma(-n,x2) - gamma(-n,x1)]
c On input:  n = integer >= 0
             x1, x2 = complex arguments
c Calls:    cexpli from newclib.a library
-----
complex x1, x2, ei2m1, sum1, sum2

sum1 = cmplx(0.,0.)
sum2 = cmplx(0.,0.)
lfac = 1
do l = 0, n-1
  sum1 = sum1 + lfac/x1**(l+1)
  sum2 = sum2 + lfac/x2**(l+1)
  lfac = -lfac*(l+1)
end do
gn2m1 = -(ei2m1*(-x1,-x2) + exp(-x2)*sum2 - exp(-x1)*sum1)/lfac
return
end

subroutine InitBN(bn2,bn3,x,y)
implicit real*8 (a-h,o-z)
dimension   bn2(9,3,20),bn3(9,3,20),x(3),y(3)
common /ibik/  mx,ny,mm,ICElem,ilyrs,idof,iguass,Lind
write(*,*) 'Init bn'
ic = 0
DO Ix = 1, iguass, 1

```

```

DO Iy = 1, iguass, 1
  ic = ic + 1
  DO K = 1, 3, 1
    DO J = 1, 20, 1
      bn2(ic,K,J) = schm2(K,J,x(Ix),y(Iy))
      bn3(ic,K,J) = schm3(K,J,x(Ix),y(Iy))
    END DO
  END DO
END DO
RETURN
END

```

```

!*** Add the assembled mass and stiffness for each layer.
subroutine AdMats(tm,tk,ttm,ttk)
implicit real*8 (a-h,o-z)
dimension tm(60,60),tk(60,60),ttm(60,60),ttk(60,60)

```

```

DO I = 1, 60, 1
  DO J = 1, 60, 1
    ttm(I,J) = ttm(I,J) + tm(I,J)
    ttk(I,J) = ttk(I,J) + tk(I,J)
  END DO
END DO

```

```

RETURN
END

```

```

C****
C      Compute Stiffness and Mass matrices for each element and
C      then assembling them.
C****

```

```

subroutine CmatKM(x,y,h,ro,tz,xb,xc,Xt,Ti,q,Tit,
  id,bm,bk,ak,tm,tk,angl,sa,bb,bn2,bn3)
implicit real*8 (a-h,o-z)
dimension   q(3,3),x(3),y(3),h(3)
            ak(20,20),bm(80,80),bk(80,80)
            tm(60,60),tk(60,60),Ti(5,3,3),Tit(5,3,3)
            xc(3,3),angl(5),tz(5),id(25,20)
            sa(60,60), bb(60,60)
            bn2(9,3,20),bn3(9,3,20)
            am1(20,20),am2(20,20),am3(20,20),am4(20,20)
            am(20,20),tak(20,20)

```




```

119      format (1x,5 (d14.8, ' '))
      do I=1,nm,1
      do J=1,nm,1
      aa(I,J) = tk(I,J)
      bb(I,J) = tm(I,J)
      end do
      end do
      RETURN
      END
      !-----
      ! 1- Computes Eigen values
      ! 2- Sorts Eigen values.
      ! 3- Compute Eigen vectros.
      ! 4- Load selected degrees of freedom
      ! 5- Compute dint.
      ! 6- Compute covariance: cov(80,80)
      !-----
      subroutine calcov(cov,aa,bb,epsi,zeta,w,g,dint,tm,ldof,ndof,a0)
      implicit real*8 (a-h,o-z)
      dimension cov(60,60),aa(60,60),bb(60,60)
      dimension g(32,60),w(60),dint(60,60),tm(60,60)
      dimension ldof(32)
      dimension wk(60),c(60),z(60,60)
      dimension alfr(60),alfr(60),beta(60),iter(60)
      dimension taa(60,60),tbb(60,60)
      logical matz
      common /iblk/ mx,ny,nm,icelem,ilyrs,idof,iguass,Lind
      DO I=1,60,1
      DO J=1,60,1
      taa(I,J) = aa(I,J)
      tbb(I,J) = bb(I,J)
      z (I,J) = 0.d0
      END DO
      alfr(I) = 0.d0
      alfi(I) = 0.d0
      beta(I) = 0.d0
      iter(I) = 0
      END DO
      write(*,*) 'Computing Eigen values'

```

```

100      DO Ix = 1, iguass, 1
      DO Iy = 1, iguass, 1
      ic = ic + 1
      tak(I,J) = tak(I,J) + (h(Ix) * h(Iy)) *
      * ( emp1(ic,I,J)*(zk - zkml) +
      * emp2(ic,I,J)*(zk**2 - zkml**2)/2.0 +
      * emp3(ic,I,J)*(zk**2 - zkml**2)/2.0 +
      * emp4(ic,I,J)*(zk**3 - zkml**3)/3.0 )
      END DO
      END DO
      ak(I,J) = ak(I,J) + tak(I,J) * xb * xc
      END DO
      END DO
      format (1x,5 (d14.8, ' '))
      write(*,*) 'Assemble Mass and Stiffness'
      C
      C**** Assembling the Mass and Stiffness matrices of the whole system
      C
      110      format (//1x,A, ' : /1x,30 ('-''))
      101      format (1x,10(16))
      ic = 0
      DO I = 1, mx, 1
      DO J = 1, ny, 1
      ic = ic + 1
      DO K = 1, 20, 1
      DO L = 1, 20, 1
      ik = id(ic,K)
      il = id(ic,L)
      bm(ik,il) = bm(ik,il) + am(K,L)
      bk(ik,il) = bk(ik,il) + ak(K,L)
      END DO
      END DO
      END DO
      END DO
      END DO
      109      format (1x,80(d8.2, ' '))
      write(*,*) 'Assemble Kff and Mff'
      C
      C**** Assembling the Kff, Mff
      C
      iofs = (ny+1) * idof
      DO I = 1, nm, 1
      DO J = 1, nm, 1
      tk(I,J) = bk(iofs+I,iofs+J)
      tm(I,J) = bm(iofs+I,iofs+J)
      END DO
      END DO

```

```

c**** Compute Eigen values
c****
      matz = .true.

      call f02bjf(nm,taa,nm,tbb,nm,eps1,alfr,alfr,beta,matz,z,
      *
      nm,iter,ifail)
      write(12,*) 'The ifail from f02bjf ',ifail
      do I=1,nm,1
        w(I) = alfr(I) / beta(I)
      end do

      Sorting of Eigen values
c****
c****
      do I=1,nm-1,1
        do M=I,nm,1
          if (w(I) .gt. w(M)) then
            temp = w(I)
            w(I) = w(M)
            w(M) = temp
          do J=I,nm,1
            wk(J) = z(J,M)
            z(J,M) = z(J,I)
            z(J,I) = wk(J)
          end do
        end if
      end do

      Output Eigen values
c****
c****
      write(12,*)
      write(12,*) 'Sorted Eigen values:'
      do I=1,nm,1
        write(12,*) w(I), dsqrt(w(I))
        w(I) = dsqrt(w(I))
      end do

      Normalization of Eigen vectors
c****
c****
      do K=1,nm,1
        ec = 0.d0
        do I=1,nm,1
          do J=1,nm,1
            ec = ec + z(I,K) * tm(I,J) * z(J,K)
          end do
        end do
        c(K) = dsqrt(ec)
        do I=1,nm,1
          z(I,K) = z(I,K) / c(K)
        end do
      end do

      end do
      call dumb(tm,z)

      write(*,*) 'Loading nodes....'
      do I=1,ndof,1
        do L=1,nm,1
          g(I,L) = z(ldof(I),L)
        end do
      end do

      write(*,*) 'The Integration Matrix:'
      ii=0
      do I=1,60,1
        do J=1,60,1
          dint(I,J) = s0 * wn(w(I), zeta, w(J), zeta, 0.d0, 0)
        end do
      end do

      write(*,*) 'The diagonal elements of the covariance matrix'
      do I1=1,60,1
        cov(I1,J1) = 0.d0
        do I2=1,60,1
          do J2=1,60,1
            ztmp = 0.d0
            do I3=1,ndof,1
              do J3=1,ndof,1
                ztmp = ztmp + g(I3,I2) * g(J3,J2)
              end do
            end do
            cov(I1,J1) = cov(I1,J1) + ztmp * z(I1,I2) * z(J1,J2) * dint(I2,J2)
          end do
        end do
        write(*,*) cov(I1,I1)
      end do

      RETURN

      format(1x,5(d8.2,' '))
      format(1x,5(d14.8,' '))
      format(/x,18(1x,d8.2))
      format(1x,'DOF(',13,') = '$)

      END

      ||-----||
      || 1- Compute covariance without support: covk(60,60)
      || 2- Compute elemental covariance matrix for 'ICElem'

```

```

!|-----
subroutine Ccove(cov,covk,cove,tcoved,frstim,id)
implicit real*8 (a-h,o-z)
logical frstim
dimension cov(60,60),covk(80,80),cove(25,20,20),id(25,20)
dimension /iblk/ mx,ny,nm,icElem,iLyrs,idof,iguass,Lind
common /iblk/ mx,ny,nm,icElem,iLyrs,idof,iguass,Lind
if (.not. frstim) then
DO I = 1, 20, 1
tcoved(I) = cove(icElem,I,I)
END DO
end if
write(*,*) 'Init covk'
do I=1,(ny+1)*5*(mx+1), 1
do J=1,(ny+1)*5*(mx+1), 1
covk(I,J)=0.d0
end do
end do
write(*,*) 'Compute covk'
is=1
do I=(ny+1)*5+1, ((ny+1)*5)*(mx+1), 1
iq = 1
do J=(ny+1)*5+1, ((ny+1)*5)*(mx+1), 1
covk(I,J) = cov(is,iq)
iq=iq+1
end do
is=is+1
end do
write(*,*) 'Compute cove'
ic=0
do I=1,mx,1
do J=1,ny,1
ic=ic+1
do K=1,20,1
cove(ic,K,M) = covk(id(ic,K),id(ic,M))
end do
end do
end do
format(1x,5(d8.2,' '))
RETURN
END

```

```

subroutine TstCnv(cov,tcov,icElem,frstim,Cnvrqd)
implicit double precision (a-h,o-z)
dimension cov(60,60), tcov(60)
logical frstim, Cnvrqd
Cnvrqd = .false.
if (frstim) then
frstim = .false.
write(*,*) 'first time => Cnvrqd = ',Cnvrqd
RETURN
end if
sum = 0.d0
osum = 0.d0
DO I = 1, 20, 1
sum = sum + (cov(I,I) - tcov(I))**2
osum = osum + tcov(I)**2
END DO
sum = sqrt(sum)
osum = sqrt(osum)
if (sum / osum .lt. 1.d-3) then
Cnvrqd = .true.
else
DO I=1,60,1
tcov(I) = cov(I,I)
END DO
end if
write(12,*)
write(12,*)
write(12,*) 'Convergence test:'
write(12,*) 'sum/osum = ',sum,' / ',osum,' = ',sum/osum
write(12,*)
RETURN
END
subroutine dumb(fMM,eigvct)
implicit real*8 (a-h,o-z)
dimension fMM(60,60), eigvct(60,60), r(60,60), s(60,60)
do i=1,60,1
do j=1,60,1
r(i,j) = 0.d0
do k=1,60,1
r(i,j) = r(i,j) + eigvct(k,i) * fMM(k,j)
end do
end do
do i=1,60,1
do j=1,60,1
s(i,j) = 0.d0

```



```

171 format(1x,5(d14.8,))
111 format(1x,20I5)
END

C***** [Ke*] = [Ke*] + [Ke*] + [Ke*]
C***** sksti1(1) Ke* for i = 1
C***** sksti2(1) Ke* for i = 2
C***** sksti1(2) Ke* for i = 1
C***** sksti2(2) Ke* for i = 2
C***** sksti1(3) Ke* for i = 1
C***** sksti2(3) Ke* for i = 2

SUBROUTINE ninetf(alfal,alfaz,betal,beta2,bn2,bn3,
* tz,T3,Tstr,sksti1,sksti2,h,xb,xc)
IMPLICIT REAL*8 (a-h,o-z)
dimension bn2(9,3,20), bn3(9,3,20), T3(5,3), Tstr(5,3,3)
dimension res11(3,20), sksti2(25,3,20,20), h(3)
dimension alfa1(9,25,3), alfa2(9,25,5), betal(9,25,2,20)
dimension beta2(9,25,4,20), tz(5)

dimension A1(3,20,20), A12(3,20,20), z1(5)
dimension selfq(3), self2q(3)
dimension res11(3,20), res211(3,20), res212(3,20), res212(3,20)
dimension tksti1(9,3,20,20), tksti2(9,3,20,20)
common /iblk/ mx,ny,nm,icElem,ilyrs,idof,iguass,Lind

call GetZks(tz,sk,zkm1)

DO ielem=1,25,1
DO I=1,3,1
DO J=1,20,1
DO K=1,20,1
sksti1(ielem,I,J,K) = 0.d0
sksti2(ielem,I,J,K) = 0.d0
END DO
END DO
END DO

!*** For all elements (mx X ny) DO
DO ielem=1,mx*ny,1
ic = 0
DO Ix = 1, iguass, 1 ! Gauss points integration.
DO Iy = 1, iguass, 1
ic = ic + 1
DO I=1,3,1
DO J=1,20,1
DO K=1,20,1
A11(I,J,K) = 0.d0
A12(I,J,K) = 0.d0
END DO
END DO
END DO

!***
DO L = 0, 3, 1 ! SUM( Beta(L) [T3] (B' (...) + B'' (...)) ), i=2
DO I = 1, 20, 1
DO J = 1, 20, 1
A11(Iq,I,J) = A11(Iq,I,J) + beta1(ic,ielem,L+1,I) *
(T3(Lind,1)*(bn2(ic,1,J)*z1(L+1)+bn3(ic,1,J)*z1(L+2)) +
T3(Lind,2)*(bn2(ic,2,J)*z1(L+1)+bn3(ic,2,J)*z1(L+2)) +
T3(Lind,3)*(bn2(ic,3,J)*z1(L+1)+bn3(ic,3,J)*z1(L+2)))
END DO
END DO

DO L = 0, 2, 1
DO I = 1, 20, 1
DO J = 1, 20, 1
A12(Iq,I,J) = A12(Iq,I,J) + beta2(ic,ielem,L+1,I) *
(T3(Lind,1)*(bn2(ic,1,J)*z1(L+1)+bn3(ic,1,J)*z1(L+2)) +
T3(Lind,2)*(bn2(ic,2,J)*z1(L+1)+bn3(ic,2,J)*z1(L+2)) +
T3(Lind,3)*(bn2(ic,3,J)*z1(L+1)+bn3(ic,3,J)*z1(L+2)))
END DO
END DO

DO L = 0, 3, 1 ! SUM( Beta(L) [T3] (B' (...) + B'' (...)) ), i=2
DO I = 1, 20, 1
DO J = 1, 20, 1
A11(Iq,I,J) = A11(Iq,I,J) + beta1(ic,ielem,L+1,I) *
(T3(Lind,1)*(bn2(ic,1,J)*z1(L+1)+bn3(ic,1,J)*z1(L+2)) +
T3(Lind,2)*(bn2(ic,2,J)*z1(L+1)+bn3(ic,2,J)*z1(L+2)) +
T3(Lind,3)*(bn2(ic,3,J)*z1(L+1)+bn3(ic,3,J)*z1(L+2)))
END DO
END DO

DO L = 0, 2, 1
DO I = 1, 20, 1
DO J = 1, 20, 1
A12(Iq,I,J) = A12(Iq,I,J) + beta2(ic,ielem,L+1,I) *
(T3(Lind,1)*(bn2(ic,1,J)*z1(L+1)+bn3(ic,1,J)*z1(L+2)) +
T3(Lind,2)*(bn2(ic,2,J)*z1(L+1)+bn3(ic,2,J)*z1(L+2)) +
T3(Lind,3)*(bn2(ic,3,J)*z1(L+1)+bn3(ic,3,J)*z1(L+2)))
END DO
END DO

DO I = 1, 20, 1
DO J = 1, 20, 1
A12(Iq,I,J) = 4 * A12(Iq,I,J) ! Compute [A1], i=2
A11(Iq,I,J) = 2 * A11(Iq,I,J) ! Compute [A1], i=1
END DO
A12(Iq,I,I) = A12(Iq,I,I)+self2q(Iq) ! Compute [A1], i=2
A11(Iq,I,I) = A11(Iq,I,I)+self1q(Iq) ! Compute [A1], i=1
END DO

END DO ! iq

```



```

1113 kolbut = 0
      : Compute K*.
      DO I = 1, 3, 1
      DO J = 1, 20, 1
      tres1 = 0.d0
      tres2 = 0.d0
      DO K = 1, 20, 1
      tres1 = tres1+bn2(ic,I,K) * A11(1,K,J) !R1= [B'] [A1], i=1
      tres2 = tres2+bn2(ic,I,K) * A12(1,K,J) !R2= [B'] [A1], i=2
      END DO
      res11(I,J) = tres1
      res12(I,J) = tres2
      END DO
      END DO
      DO I = 1, 3, 1
      DO J = 1, 20, 1
      res211(I,J) = (Tstr(Lind,I,1) * res11(1,J) + !R1= [T*] [R1], i=1
      Tstr(Lind,I,2) * res11(2,J) +
      Tstr(Lind,I,3) * res11(3,J))
      res212(I,J) = (Tstr(Lind,I,1) * res12(1,J) + !R2= [T*] [R2], i=2
      Tstr(Lind,I,2) * res12(2,J) +
      Tstr(Lind,I,3) * res12(3,J))
      END DO
      END DO
      DO I = 1, 20, 1
      DO J = 1, 20, 1
      tkst11(ic,2,I,J) = ! [K*1] = [B'] [R1]
      (bn3(ic,1,I) * res211(1,J) +
      bn3(ic,2,I) * res211(2,J) +
      bn3(ic,3,I) * res211(3,J))
      tkst12(ic,2,I,J) = ! [K*2] = [B'] [R2]
      (bn3(ic,1,I) * res212(1,J) +
      bn3(ic,2,I) * res212(2,J) +
      bn3(ic,3,I) * res212(3,J))
      END DO
      END DO
      DO I = 1, 3, 1
      DO J = 1, 20, 1
      tres1 = 0.d0
      tres2 = 0.d0
      DO K = 1, 20, 1
      tres1 = tres1+bn3(ic,I,K) * A11(2,K,J) !R1= [B'] [A1], i=1
      tres2 = tres2+bn3(ic,I,K) * A12(2,K,J) !R2= [B'] [A1], i=2
      END DO
      res11(I,J) = tres1
      res12(I,J) = tres2
      END DO
      END DO
      DO I = 1, 3, 1
      DO J = 1, 20, 1
      res211(I,J) = (Tstr(Lind,I,1) * res11(1,J) + !R1= [T*] [R1], i=1
      Tstr(Lind,I,2) * res11(2,J) +
      Tstr(Lind,I,3) * res11(3,J))
      res212(I,J) = (Tstr(Lind,I,1) * res12(1,J) + !R2= [T*] [R2], i=2
      Tstr(Lind,I,2) * res12(2,J) +
      Tstr(Lind,I,3) * res12(3,J))
      END DO
      END DO
      DO I = 1, 20, 1
      DO J = 1, 20, 1
      tkst11(ic,1,I,J) = ! [K*1] = [B'] [c [R1]
      (bn2(ic,1,I) * res211(1,J) +
      bn2(ic,2,I) * res211(2,J) +
      bn2(ic,3,I) * res211(3,J))
      tkst12(ic,1,I,J) = ! [K*2] = [B'] [c [R2]
      (bn2(ic,1,I) * res212(1,J) +
      bn2(ic,2,I) * res212(2,J) +
      bn2(ic,3,I) * res212(3,J))
      END DO
      END DO
      : Compute K** = ([B'] [T*] [B'] + [B'] [T*] [B']) [A2]
      DO I = 1, 3, 1
      DO J = 1, 20, 1
      tres1 = 0.d0
      tres2 = 0.d0
      DO K = 1, 20, 1
      tres1 = tres1+bn2(ic,I,K) * A11(2,K,J) !R1= [B'] [A1], i=1
      tres2 = tres2+bn2(ic,I,K) * A12(2,K,J) !R2= [B'] [A1], i=2
      END DO
      res11(I,J) = tres1

```



```

END DO
END DO

do I=1,80,1
  do j=1,80,1
    bk(i,j) = 0.d0
  end do
end do

ic = 0
DO I = 1, mx, 1
  DO J = 1, ny, 1
    ic = ic + 1
  DO K = 1, 20, 1
    DO L = 1, 20, 1
      ik = id(ic,K)
      il = id(ic,L)
      bk(ik,il) = bk(ik,il) + tkstr(ic,K,L)
    END DO
  END DO
END DO

iofs = (ny+1) * idof
DO I = 1, nm, 1
  DO J = 1, nm, 1
    tck(I,J) = tck(I,J) + bk(iofs+I,iofs+J)
  END DO
END DO

format(///1x,A)
format(1x,5(d14.8, ' '))

END

SUBROUTINE CStrs(bn2,bn3,Ti,Tit,cove,q,tz,stres1,stresg,stral,strag)
IMPLICIT double precision (a-h,o-z)
dimension bn2(9,3,20), bn3(9,3,20), Ti(5,3,3), Tit(5,3,3)
dimension cove(25,20,20), q(3,3), tz(5)
dimension stres1(3,3), stresg(3,3), stral(3,3), strag(3,3)
common /iblk/ mx,ny,nm,ICElem,ilyrs,idof,iguass,Lind
dimension bb(3,20), bt(20,3), bc(3,20), tb(3,3)

call GetZKa(tz,zk,zkml)

if (zk .le. 0.0) then
  zz = zkml
else
  zz = zk

```

```
end if
```

```
DO I = 1, 3, 1
  DO J = 1, 20, 1
    bb(I,J) = sdm2(I,J,0.0,d0) + zz * sdm3(I,J,0.0,d0,0.0,d0)
  END DO
END DO
```

```
C Computation of strain in local coordinates.
```

```
DO I = 1, 3, 1
  DO J = 1, 20, 1
    bc(I,J) = 0.d0
  DO K = 1, 20, 1
    bc(I,J) = bc(I,J) + bb(I,K)*cove(ICElem,K,J)
  END DO
END DO
```

```
DO I = 1, 20, 1
  DO J = 1, 3, 1
    bt(I,J) = bb(1,I)*Ti(Lind,1,J) +
    + bb(2,I)*Ti(Lind,2,J) +
    + bb(3,I)*Ti(Lind,3,J)
  END DO
END DO
```

```
DO I = 1, 3, 1
  DO J = 1, 3, 1
    tb(I,J) = 0.d0
  DO K = 1, 20, 1
    tb(I,J) = tb(I,J) + bc(I,K) * bt(K,J)
  END DO
END DO
```

```
DO I = 1, 3, 1
  DO J = 1, 3, 1
    stral(I,J) = Tit(Lind,I,1) * tb(1,J) +
    + Tit(Lind,I,2) * tb(2,J) +
    + Tit(Lind,I,3) * tb(3,J)
  END DO
END DO
```

```
C Computation of strain in global coordinates
```

```
DO I = 1, 3, 1
  DO J = 1, 3, 1
    strag(I,J) = 0.d0
  DO K = 1, 20, 1
    strag(I,J) = strag(I,J) + bc(I,K)*bb(J,K)
  END DO
END DO
```



```

END DO
C
C      Computation of stress in local coordinates
C      (The normal stresses are considered to be linear, the shear stress
C      is considered to be non-linear).
C
C      Compute the normal stresses for given location: Zk, x, y
DO I = 1, 3, 1
  DO J = 1, 3, 1
    stral(I,J) = 0.d0
  END DO
END DO
DO I = 1, 2, 1
  DO J = 1, 2, 1
    tb(I,J) = stral(I,1)*q(J,1) + stral(I,2)*q(J,2)
  END DO
END DO
DO I = 1, 2, 1
  DO J = 1, 2, 1
    stral(I,J) = q(I,1)*tb(1,J) + q(I,2)*tb(2,J)
  END DO
END DO
C
C      Compute the shear stresses for a given element
sigs = stral(3,3)
tstres = q(3,3)**2 * sigs +
+      2*q(3,3) * (3*a1*sigs**2 + 15*a2*sigs**3) +
+      a1*a1*15*sigs**3 + 2*a1*a2*105*sigs**4 +
+      a2*a2*945*sigs**5
stral(3,3) = sqrt(tstres)
C
C      Computation of stress for global coordinates.
DO I = 1, 3, 1
  DO J = 1, 3, 1
    tb(I,J) = stral(I,1)*Tfit(Lind,1,J) +
+      stral(I,2)*Tit(Lind,2,J) +
+      stral(I,3)*Tfit(Lind,3,J)
  END DO
END DO
DO I = 1, 3, 1
  DO J = 1, 3, 1
    streg(I,J) = Ti(Lind,I,1)*tb(1,J) +
+      Ti(Lind,I,2)*tb(2,J) +
+      Ti(Lind,I,3)*tb(3,J)
  END DO
END DO
write(12,*) 'Local strain'
write(12,10) ((stral(i,j),j=1,3),i=1,3)
write(12,*) 'Local stress'

```

```

write(12,10) ((stresl(i,j),j=1,3),i=1,3)

```

```

return
format(x,3(d18.12,' '))
END

```

10

MICHIGAN STATE UNIV. LIBRARIES



31293010191967